



QEX

\$5

March/April 2008
www.arrl.org

A Forum for Communications Experimenters

Issue No. 247



W8NUE and **N2APB** describe the NUE-PSK digital modem. Operate PSK-31 *anywhere* without a computer!

ARRL The national association for
AMATEUR RADIO

225 Main Street
Newington, CT USA 06111-1494

TOKYO HY-POWER

HL-450B

HF 400W Linear Amplifier

Another Fine
NEW PRODUCT
from
**TOKYO
HY-POWER!**

**New High Power for your
Mobile, RV and more!**



Micro-processor Based Technology!

The HL-450B has a built-in auto band-select function. It uses a newly developed micro-processor based technology, and works a smooth automatic operation when driven by RF from the radio in either SSB or CW mode. In addition, manual band setting is possible as well. It is designed to be "user friendly".

- Since the HL-450B is compatible with our optional external remote controller (HRC-60), operation is possible from remote locations, if plugged into the socket at the rear panel.
- The HL-450B is equipped with a hard-key terminal to allow precise send / receive switching with the radio. Built-in ALC circuit helps suppress excessive output and avoid the signal distortion.
- The HL-450B has various protection circuits such as for high antenna SWR, over drive, over current, etc. When any abnormal condition is detected, operation is automatically shut down.
- The large analog power meter is easy to read and the output can always be monitored.

Built-in functions

1. Send / receive switching terminal (hard key)
2. Protection circuit (antenna SWR, over-current, over-voltage, over-drive, over-temperature, band mis-set)
3. Output power meter
4. ALC terminal
5. External controller (HRC-60, optional) terminal.

Specifications

Freq. Band:

All HF amateur bands of 3.5 - 28MHz

Operation Mode:

SSB, CW, FM

Output:

SSB (PEP) / CW 400W max.
350W typ., 300W min.

RF Input

50W

DC Power Supply

DC 13.8V 60A max.

Input / Output

50 ohms

Final Transistor

THP - 120 x 4

Cooling System

Forced-air cooling

Input / Output Connector

UHF (SO-239)

Accessories

DC power cord (red / black pair) 6' x1,
Coaxial jumper cable: 2' x1,
Stand-by cable (with RCA plug) 4' x1,
Spare fuses: 30A x4, Instruction manual,
warranty card

Dimensions

8.7 x 3.5 x 13 inches (WxHxD)

Weight

Approx. 11lbs.

Option

External remote controller - HRC-60
Matching DC power supply - HP-450
(Light weight switching mode, 13.8V 60A)

TOKYO HY-POWER

TOKYO HY-POWER LABS., INC. - USA
487 East Main Street, Suite 163
Mount Kisco, NY 10549
Phone: 914-602-1400
e-mail: thpusa@mac.com

TOKYO HY-POWER LABS., INC. - JAPAN
1-1 Hatanaka 3chome, Niiza Seitama 352-0012
Phone: +81 (48) 481-1211 FAX: +81 (48) 479-6949
e-mail: info@thp.co.jp
Web: <http://www.thp.co.jp>



Exclusively from Ham Radio Outlet!

www.hamradio.com

Western US/Canada 1-800-854-6046	Southeast 1-800-444-7927	Northeast 1-800-644-4476
Mountain/Central 1-800-444-9476	Mid-Atlantic 1-800-444-4799	New England/Eastern Canada 1-800-444-0047



QEX (ISSN: 0886-8093) is published bimonthly in January, March, May, July, September, and November by the American Radio Relay League, 225 Main Street, Newington, CT 06111-1494. Periodicals postage paid at Hartford, CT and at additional mailing offices.

POSTMASTER: Send address changes to: QEX, 225 Main St, Newington, CT 06111-1494 Issue No 247

Harold Kramer, WJ1B
Publisher

Larry Wolfgang, WR1B
Editor

Lori Weinberg, KB1EIB
Assistant Editor

L. B. Cebik, W4RNL
Zack Lau, W1VT
Ray Mack, W5IFS
Contributing Editors

Production Department

Steve Ford, WB8IMY
Publications Manager
Michelle Bloom, WB1ENT
Production Supervisor
Sue Fagan, KB1OKW
Graphic Design Supervisor

Devon Neal, KB1NSR
Technical Illustrator

Advertising Information Contact:

Janet L. Rocco, W1JLR
Business Services
860-594-0203 – Direct
800-243-7768 – ARRL
860-594-4285 – Fax

Circulation Department

Cathy Stepina, QEX Circulation
Offices

225 Main St, Newington, CT 06111-1494 USA
Telephone: 860-594-0200
Fax: 860-594-0259 (24 hour direct line)
e-mail: qex@arrl.org

Subscription rate for 6 issues:

In the US: ARRL Member \$24,
nonmember \$36;

US by First Class Mail:

ARRL member \$37, nonmember \$49;

Elsewhere by Surface Mail (4-8 week delivery):

ARRL member \$31, nonmember \$43;

Canada by Airmail: ARRL member \$40,
nonmember \$52;

Elsewhere by Airmail: ARRL member \$59,
nonmember \$71.

Members are asked to include their membership control number or a label from their QST when applying.

In order to ensure prompt delivery, we ask that you periodically check the address information on your mailing label. If you find any inaccuracies, please contact the Circulation Department immediately. Thank you for your assistance.



Copyright ©2008 by the American Radio Relay League Inc. For permission to quote or reprint material from QEX or any ARRL publication, send a written request including the issue date (or book title), article, page numbers and a description of where you intend to use the reprinted material. Send the request to the office of the Publications Manager (permission@arrl.org).

March/April 2008

About the Cover

Milt Cram, W8NUE, and George Heron, N2APB describe the design and construction details of their NUE-PSK digital modem. Portable PSK-31 — Now you can operate anywhere, without a computer.



In This Issue

Features

3 NUE-PSK Digital Modem
By Milt Cram, W8NUE and George Heron, N2APB

15 The Star-10 Transceiver—Part 2
By Cornell Drentea, KW7CD

46 Carbon Composition, Carbon Film and Metal Oxide Oxide Film Resistors
By Jack R. Smith, K8ZOA

Columns

58 Antenna Options
By L.B. Cebik, W4RNL

62 Upcoming Conferences

61 In the Next Issue of QEX

63 Letters to the Editor

Index of Advertisers

American Radio Relay League:.....	Cover III
Atomic Time:.....	64
Down East Microwave Inc:.....	14
Kenwood Communications:.....	Cover IV
National RF, Inc:	41
Nemal Electronics International, Inc:.....	62
RF Parts	61, 63
Teri Software:.....	62
Tokyo Hy-Power Labs, Inc:	Cover II
Tucson Amateur Packet Radio:	57

The American Radio Relay League



The American Radio Relay League, Inc. is a noncommercial association of radio amateurs, organized for the promotion of interest in Amateur Radio communication and experimentation, for the establishment of networks to provide communications in the event of disasters or other emergencies, for the advancement of the radio art and of the public welfare, for the representation of the radio amateur in legislative matters, and for the maintenance of fraternalism and a high standard of conduct.

ARRL is an incorporated association without capital stock chartered under the laws of the state of Connecticut, and is an exempt organization under Section 501(c)(3) of the Internal Revenue Code of 1986. Its affairs are governed by a Board of Directors, whose voting members are elected every three years by the general membership. The officers are elected or appointed by the Directors. The League is noncommercial, and no one who could gain financially from the shaping of its affairs is eligible for membership on its Board.

"Of, by, and for the radio amateur," ARRL numbers within its ranks the vast majority of active amateurs in the nation and has a proud history of achievement as the standard-bearer in amateur affairs.

A *bona fide* interest in Amateur Radio is the only essential qualification of membership; an Amateur Radio license is not a prerequisite, although full voting membership is granted only to licensed amateurs in the US.

Membership inquiries and general correspondence should be addressed to the administrative headquarters:

ARRL
225 Main Street
Newington, CT 06111 USA
Telephone: 860-594-0200
FAX: 860-594-0259 (24-hour direct line)

Officers

President: JOEL HARRISON, W5ZN
528 Miller Rd, Judsonia, AR 72081

Chief Executive Officer: DAVID SUMNER, K1ZZ

The purpose of *QEX* is to:

- 1) provide a medium for the exchange of ideas and information among Amateur Radio experimenters,
- 2) document advanced technical work in the Amateur Radio field, and
- 3) support efforts to advance the state of the Amateur Radio art.

All correspondence concerning *QEX* should be addressed to the American Radio Relay League, 225 Main Street, Newington, CT 06111 USA. Envelopes containing manuscripts and letters for publication in *QEX* should be marked Editor, *QEX*.

Both theoretical and practical technical articles are welcomed. Manuscripts should be submitted in word-processor format, if possible. We can redraw any figures as long as their content is clear. Photos should be glossy, color or black-and-white prints of at least the size they are to appear in *QEX* or high-resolution digital images (300 dots per inch or higher at the printed size). Further information for authors can be found on the Web at www.arrl.org/qex/ or by e-mail to qex@arrl.org.

Any opinions expressed in *QEX* are those of the authors, not necessarily those of the Editor or the League. While we strive to ensure all material is technically correct, authors are expected to defend their own assertions. Products mentioned are included for your information only; no endorsement is implied. Readers are cautioned to verify the availability of products before sending money to vendors.

Larry Wolfgang, WR1B

lwolfgang@arrl.org

Empirical Outlook

In the last couple of issues I've mentioned my goal of encouraging readers to write articles for *QEX*. This includes finding new authors, as well as getting previous authors to share more of their work. I've been talking with quite a few readers and even some potential authors who don't presently read *QEX*. One theme seems to keep coming up. Many experimenters and builders just don't like writing about their work! Some people have told me that this may be a trait being taught in engineering schools. Actually, I doubt that is true, but I could believe that schools aren't really teaching *how* to write.

When I was a high school student oh so many years ago, and then as a physics major in college, my science teachers and college professors seemed to think it was important to write a fairly detailed summary/report about any laboratory experiment we carried out in class. Perhaps that is why, when I was teaching high school physics, I also placed quite a bit of emphasis on writing clear reports.

I have never really considered myself to be a writer, although after more than 26 years as an ARRL technical editor, I have written quite a bit of material. I will even admit to enjoying an opportunity to put fingers to keyboard, although sometimes it can be quite challenging to clearly express my ideas. (For those of you wondering what I'm talking about right now, I rest my case.)

How should you go about writing a *QEX* article? Well, to start, I'll bet that virtually every experimenter and engineer keeps some type of notebook, with at least some sketchy notes about circuits tried, what worked and what didn't, as well as a schematic of the final working circuit. Those notes should form the basis of an article. If your notes don't serve as a good reminder of what you've done, then keep better notes the next time you start a project! Keep track of what you have done, how you reached milestones along the way, and how you solved various problems.

I seem to be talking only about construction-type articles at this point, but that isn't true. You might want to write a theoretical discussion or explain some technical point to our readers. A good starting point would still be to make some notes about the issues you want to discuss, the background reference information you want to review or the theoretical viewpoint you want to present. An outline format can be very helpful in organizing your thoughts.

Your manuscript doesn't have to be in impeccable English. The important thing is to provide us with an article that is technically correct and complete, with all relevant information. Now I'll admit that I prefer articles written in something close to proper English, but part of my job as Editor is to ensure that we follow most of the rules of grammar, and that the article flows in a manner that I hope makes it enjoyable to read. One technique that many authors find helpful is to ask someone else to read the article and give them some feedback. Another good technique can be to read the article out loud. If it doesn't sound right, it probably isn't.

You may have noticed that photos and figures in *QEX* articles are all called Figures, and that we refer to them in numerical order in the text. It would be very unusual to begin with a reference to Figure 10, then Figure 4, and so on in a rather random order. If that is the way your text flows, then perhaps you should consider either reorganizing the text topics or renumbering the Figures. The same comments apply to Notes or Footnotes in an article. The first reference to a Note is always in numerical order. It is okay to refer back to an earlier Note later in the article, of course.

Can you organize your material that way? Then you can write a *QEX* article! It really is just about that simple. There are more guidelines to writing an article and preparing a manuscript on the *QEX* Web site, www.arrl.org/qex. That "Author's Guide" always needs some updates, but it will give you some good general ideas. Of course we prefer to receive article manuscripts electronically. If the article is too large to e-mail to us, you can put it on a CD and send that through the mail.

Some authors seem to believe that writing an article includes formatting the text in a "camera ready" form. I suspect that some potential authors may even be put off by the thought of trying to present an article that looks like the pages of *QEX*. Unfortunately, when an article is submitted with the text formatted in special ways, and graphics elements are embedded into the manuscript file, it creates more work for everyone, including the author. Our professional typesetting software (*Adobe InDesign*) needs separate text and graphics files. Our Graphics artists take virtually every drawing submitted for an article, and create a new drawing in the format and using the standard drawing symbols used in all ARRL publications. In other words, we can't use the formatted files.

We use Microsoft *Word* to prepare a manuscript file. This is a text file, with no graphics. Tables and Figure captions are included at the end of the file, or could be separate files. We can probably work from any word processing program you are using. If not, we may ask you to convert the file to rich text format (.rtf). Even if you have never written an article for publication, give it a try. You may find that you have a real knack for writing, and even come to enjoy it!

NUE-PSK Digital Modem

Enables PSK31 field operation... without using a PC!

PSK31 is one of the latest communications modes to capture the interest of hams worldwide. Its inherent ability to dig out low, nearly inaudible signals is ideally suited for low power, QRP, enthusiasts. The PSK31 digital modem engine, however, requires intense digital signal processing (DSP) that is only commonly available in PC sound cards. Thus, the PSK operator desiring portability for field operation is locked into using a laptop computer as a controller, which results in a cumbersome station. But there's hope!

This article presents the design and construction of a stand-alone, battery-operated digital modem using a Microchip dsPIC microcontroller. The project includes a graphic display for transmit and receive text data, as well as a band spectrum and tuning indicator. Using GPL open source software, the modem can be homebrewed for less than \$80. When coupled with an SSB-capable transceiver or with a popular PSK-xx transceiver board from Small Wonder Labs, you too can have an effective portable PSK31 station.

Background

PSK31 was introduced in 1998 to the ham technical community at large in RSGB's *RadCom* magazine.¹ Hams could get on the air with this digital mode using a dedicated (expensive) DSP card, a crude DOS control program for entering/displaying messages, and interface cables for connection to the station SSB transceiver. Later, a brilliant PC program was developed (*DigiPan*) that used a panoramic graphical display to show all signals occurring within a band segment, and print received messages on the PC screen.² This was an astonishing improvement in the user interface for PSK31! Later in 2001, Dave Benson, K1SWL, designed a single board PSK31 transceiver kit (PSK-20) that required no physical tuning, and when used with *DigiPan* running on a PC, it made a quite compact PSK31 station.³

Even with these clever hardware and software designs, however, there *still* was

¹Notes appear on page 14.



room for improvement. The sound card in a laptop or PC is still needed for the intense demodulation requirements of the PSK algorithm. If you were to use a modern laptop for that computing power, taking an expensive and delicate computer into the field is a hair-raising experience. It is difficult to see the subtle spectral lines or the screen text data when viewing a laptop LCD display in the bright sunlight of a mountaintop QSO. Then, only *if* your laptop battery lasts long enough to enjoy the fun of operating PSK out in the open, and *if* you can see the laptop display in the bright sunlight, and *if* you feel like lugging that expensive laptop out into the harsh elements, you could indeed operate PSK31 in the field — but what an ordeal!

PSK MODULATION-DEMULATION OVERVIEW

We will not go into great depth concerning the theory and operation of PSK. In this paper we'll first overview the PSK31 encoding scheme, followed by the more demanding decoding scheme.

Note that while the NUE-PSK project focuses on the generation and decoding of PSK31, it is generally known that PSK31 is merely one of many modulation techniques within the "phase shift keying" family of communication techniques. PSK31 operates at 31.25 bits/second, while other speeds may

be achieved using slight algorithmic variations. PSK is perhaps more accurately termed BPSK, for bi-phase shift keying, whereby two distinct phase states separated by 180° are used to convey the information. Four states may also be encoded/decoded, as is done with QPSK (quad-phase shift keying), in order to provide higher speeds and the ability for better error correction methods.

We will primarily describe the topic of PSK31, yet understand that some of these other modes can also be achieved with the same hardware and software used in NUE-PSK.

Modulation (PSK31 Encoding)

The PSK31 modulation algorithm is quite straightforward and could even be implemented on a conventional PIC-like device (one without a DSP core). This was done in several projects over the years within the QRP community; see, for example, the PSK31 Beacon project from the NJQRP Club.

Summary of the encoding steps:

1) Varicode encoding of the input text character stream coming from the keyboard to create an optimized bit-representation of the text;

2) BPSK serialization of the Varicode character to create the proper sequence of phase changes in the waveform based on the bits in the Varicode;

3) Form the wave shape from the com-

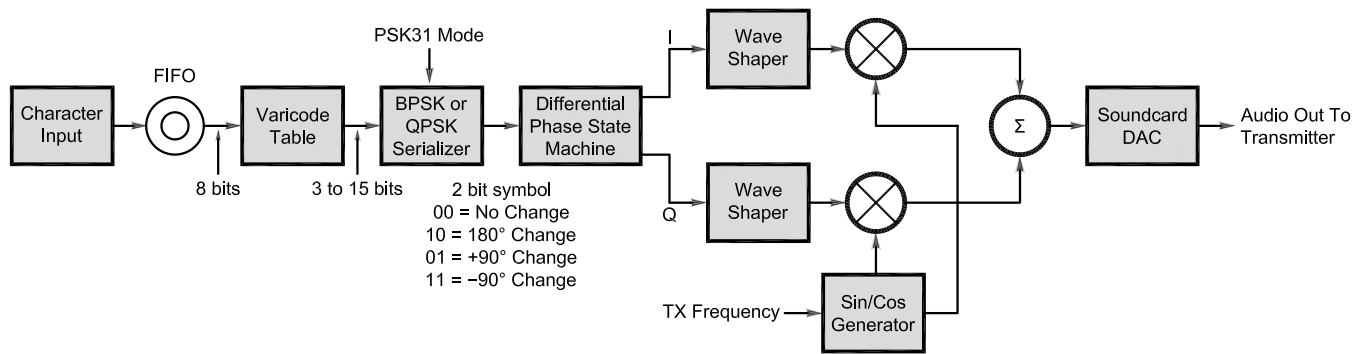


Figure 1 — PSK modulation block diagram.

bination of phase changes coming from the serializer, being careful to reduce the power level to zero when the 90° phase changes occur, thus reducing the bandwidth of the transmitted PSK signal.

These steps are all performed by a dsPIC processor, per the functional block diagram shown in Figure 1. As ASCII characters are produced by a keyboard, they are first converted to Varicode encoded characters using a lookup table. A string of binary bits, the length of which is variable (hence “Varicode”), is generated from the table. The strings of bits are then used to drive a differential phase state machine, which uses predefined tables to modulate the amplitude of the quadrature outputs (sine and cosine waveforms) of a numerically-controlled oscillator (NCO). The sine and cosine codes are derived from a lookup table to produce the NCO carrier.

The two quadrature oscillator signals are multiplied by amplitude functions, as determined by the phase state machine, and the resulting channels of data are added to produce a digital version of either a BPSK or QPSK signal. Although a simpler scheme could be used for BPSK alone, this method has the advantage that it can also generate QPSK. This digital stream of data is then sent to a digital to analog converter (DAC) to produce an audio carrier with BPSK/QPSK modulation. The output of the DAC is sent to the transceiver audio input for conversion to RF.

Demodulation (PSK Decoding)

Whereas the encoding process described above is pretty straightforward, the PSK decoding algorithm is significantly more complex and computationally demanding. This may be why there have been so few homebrew standalone PSK demodulator projects in the ham community. The PC sound card is clearly the easiest way to provide the intense DSP processing needed for decoding PSK; hence PC-based PSK31 programs abound.

This is where the stand-alone (PC-less) NUE-PSK project excels — it is able to independently handle the complex PSK decoding algorithm in real time, thus providing the first truly portable digital modem for hobby use.

Follow Figure 2, the PSK demodulation block diagram, as we walk through the decoding steps.

Summary of the decoding steps:

1) Receiver audio is sampled at 8 kHz, creating a digital floating point representation of the audio stream.

2) Data is fed into a 512 point Fast Fourier Transform (FFT) for display, tuning and visual signal monitoring purposes.

3) The audio floating point data stream is converted to a baseband signal centered on the operating frequency. The NCO generates sine and cosine signals and multiplies them with the audio stream to produce I (in phase) and Q (quadrature phase) data streams.

4) The I and Q data streams are decimated by 16 to reduce the sample rate to 16 times the signal BW. The final sampling rate then is $8000 / 16 = 500$ Hz. [In digital-signal-processing speak, to decimate a signal by some number, n , you keep every n th sample, throwing away all of the other samples.—Ed.]

5) A 65-tap “matched bit” finite impulse response (FIR) filter is applied to produce a magnitude response for best signal to noise ratio (SNR) for data extraction, and to minimize inter-symbol interference (ISI) presented in the signal path and in the receive filter.

6) AFC is performed to lock on the incoming signal frequency by using another FIR with $BW = 31.25$ Hz.

7) AGC is accomplished by computing the average signal magnitude from the I and Q data streams. Infinite impulse response (IIR) filters are selected to provide either slow decay or fast attack settings.

8) Frequency error detection is done by scanning the FFT data within the capture range while looking for the nearest peak. Also, a wide range AFC algorithm is per-

formed by calculating the slope and moving the NCO to place the peak at the center.

9) Symbol synchronization is done by finding the center of each symbol in order to sample at the optimum time. There are 16 samples per symbol at 500 Hz intervals, so each sample energy is IIR-filtered and stored in an array. The array elements with the most energy are selected as the center of the data symbol at each symbol period of 32 ms.

10) Squelching is done by taking the histogram of incoming signals and considering the spread (difference angle, or arctangent of Q / I between each sample) around 0° and 180° as a measure of signal quality. The narrower the spread, the stronger and more coherent the signal.

11) Symbol decoding is the last step, whereby we convert the I and Q signals back to two possible symbols by using the difference angle ($<90^\circ = 1, >90^\circ = 0$). The resultant symbols are shifted into a register until the inter-character mark (2 or more zeros) is found. The shift register is then used as an index into a reverse Varicode table containing the originally transmitted characters.

These eleven algorithm steps can be followed in the block diagram of the demodulation process.

The Path to a Design

After operating with the limitations of using a laptop in the field, we decided that we wanted a PSK station that did not require the use of a PC in any form. We wanted something that would be very portable and compatible with QRP operations, providing many hours of operation from batteries. The project described in this article is a result of this desire — but it took a little time for advancing technology to pave the road.

The initial efforts to develop a “portable PSK” controller began about eight years ago with a reproduction of the original G3PLX approach described in *RadCom*, but with a more current DSP card providing the horse-

power for the PSK31 engine. The design also included a novel Morse user interface and tight coupling to the PSK-20 transceiver. The project was documented in the QRP literature and was presented at ham conferences, but ultimately it was too complex and fragile for wide-scale use.⁴ See Figure 3.

The next approach we considered was

based on the use of low power DDS (direct digital synthesis) chips for generating audio tones with the proper phase modulation. A multiplying DAC was used for modulating and shaping the amplitude of the tones, and a microcontroller was used to demodulate the PSK and display the resulting characters. Analog filters were used for filtering the

PSK signal ahead of digital processing in the microcontroller. The analog filters, however, proved to be too bulky and difficult to design when trying to use standard-value components. Such filters also cannot provide the same level of performance as can be obtained with digital filters. Eventually this approach was also abandoned.

Table 1
NUE-PSK Digital Modem Parts List

<i>Designator</i>	<i>QTY</i>	<i>Description</i>	<i>Source</i>	<i>P/N</i>
C1, C2, C3, C7, C9, C11				
C13, C17, C18, C19, C21				
C22, C23, C24, C25	15	Capacitor, 0.1 μ F, 1206 SMT	Digi-Key	PCC1883CT-ND
C4, C5, C9, C10, C12, C17	6	Capacitor, 1 μ F, 16 V, SMT	Digi-Key	PCE3045CT-ND
C6	1	Capacitor, 10 μ F, 25 V, SMT	Digi-Key	PCE3118TR-ND
C15, C16	2	Capacitor, 20 pF, 1206 SMT	Digi-Key	311-1153-1-ND
D1, D2, D3	0	Diode, Schottky 1N5817, DO-41	Digi-Key	1N5817DICT-ND
D4, D5	2	Diode, Schottky MA2SE01, SMT	Digi-Key	MA2SE0100LCT-ND
ENC-1	1	Rotary encoder	Mouser	688-EC12E2420802
J1	1	Coaxial dc power connector, 2.1 mm	Mouser	163-5004-E
J2	1	6-pin Mini-DIN	Mouser	161-2206
J3	1	8-pin Mini-DIN	Mouser	161-2208
J4	1	Pinheader, female, 1 \times 2	Mouser	517-870-01-03
J5	1	IC socket, 16-pin DIP	Mouser	575-199316
J6, J7	2	9 V battery clip	All Electronics	BST-3
LCD	1	LCD, CFAG12864, 128 \times 64, graphics	Crystalfontz	CFAG12864BTFHV
P1	1	Pinheader, 1 \times 2, 0.1"	Mouser	517-834-01-36
P3	1	Pinheader, 2 \times 3, 0.1"	Mouser	517-834-01-36
P4	1	Pinheader, 1 \times 4, 90°	Mouser	517-5111TG
P5	1	Pinheader, 1 \times 2, 0.1", 90°	Mouser	517-5111TG
P8	1	8-pin Mini-DIN plug	Mouser	171-2608
PB1	1	Pushbutton, DPST, momentary	New ark	19C6398
PB1-cap	1	Pushbutton cap	New ark	18M6492
Piezo	1	Piezo buzzer	Digi-Key	433-1023-ND
Q1, Q2, Q3	3	Transistor, NFET, 2N7000	Digi-Key	497-3110-ND
R1, R2, R9, R12	4	Resistor, 1 k Ω , 1206 SMT	Digi-Key	RHM1.00KFCT-ND
R4	1	Resistor, 10 k Ω , 1206 SMT, 1%	Mouser	71-CRCW1206-10K
R7, R8, R10, R11	4	Resistor, 10 k Ω , 1206 SMT	Digi-Key	311-10KECT-ND
R13	1	Mini-potentiometer, 1 k Ω	Mouser	317-2080F-1K
R3	1	Resistor, 47 Ω , 1/2 W axial	Mouser	293-47-RC
R14	1	Trim pot, 10 k Ω	Mouser	652-3306W-1-103
R15, R16	2	Resistor, 6.8 k Ω , 1206 SMT	Digi-Key	311-6.8KECT-ND
R5	1	Resistor, 2.0 k Ω , 1206 SMT, 1%	Mouser	71-CRCW1206-2K
S1	1	Switch, SPDT, slide, PCB mount, 90°	Digi-Key	EG1917-ND
SH-1	1	Pinheader, 1 \times 2 shunt	Mouser	517-951-00
U1	1	IC, Microchip DSC, 64-pin QFP, dsPIC33FJ128MC706	Mouser	579-33FJ128MC706IPT
U2, U3	2	IC, Octal Level Shifting Buffer, TXB0108 (TSSOP-20)	Mouser	595-TB0108PWR
U4	1	IC, Microchip EEPROM, 24AA256 (8SOIC)	Digi-Key	24AA256-I/SN-ND
U5	1	IC, Freescale microcontroller, MC68HC908QY4, 16-DIP	Digi-Key	MC68HC908QY4VPE-ND
U6	1	IC, Dual-DAC, MCP4922, 14SOIC	Digi-Key	MCP4922-E/SL-ND
U7	1	IC, Programmable Gain Amplifier, MCP6S21, 8SOIC	Digi-Key	MCP6S21-I/SN-ND
U8	1	IC, Op Amp, MCP601, 8SOIC	Digi-Key	MCP601-I/SN-ND
U9	1	Voltage regulator, 5 V switching, PT78ST105H, 5 V	Digi-Key	PT78ST105H-ND
U10	1	Voltage regulator, 3.3 V, LP2950 (TO-92)	Digi-Key	LP2950CZ-3.3-ND
X1	1	Crystal, 10 MHz, 20 pF (FOXSLF/100-20)	Digi-Key	631-1101-ND
W1	1	Flex cable assembly, 1 \times 20	Newark	FSN-21A-20
Hardware	1	Cable assembly, 3-wire (battery clips)		
	8	Machine screw, pan slotted, #2-56 \times 0.25"	Mouser	5721-440-1/4-SS
	8	Machine screw, pan slotted, #4-40 \times 0.25"	Mouser	5721-256-1/4-SS
	4	Spacer, hex tapped, #2, 0.375" (LCD)		
	4	Spacer, nylon, hex tapped, 4-40 \times 0.25" (PCB)	Mouser	561-L4.25
	1	Knob	Mouser	506-PKG50B1/4

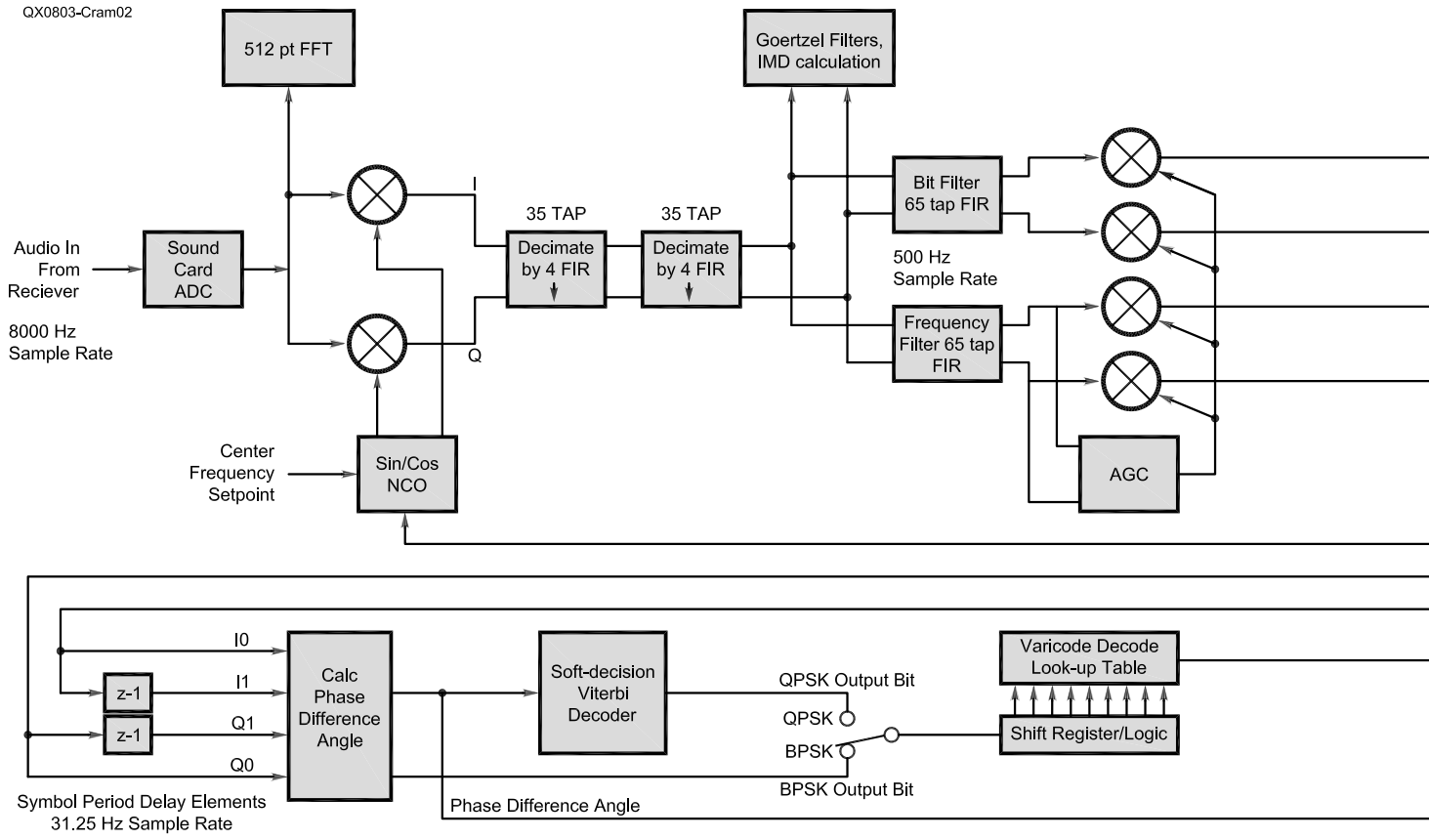


Figure 2 — PSK demodulation block diagram.

Success At Last

The approach that ultimately proved workable in every regard was one in which all processing is accomplished within a single microcontroller — one that is capable of performing the digital signal processing “number crunching” as well as handling all control chores. The newly-released dsPIC33 microcontroller from Microchip is a delightfully powerful combination of a conventional control processor with a DSP core for intense digital signal processing.⁵ Available in a small package with lots of I/O for controlling peripherals, this was just what the doctor ordered.

It was perhaps fortuitous that others in our QRP clubs were having similar fantasies at about the same time. K5JHF was exploring the dsPIC chip family and decided they would make a good basis for a number of projects of interest to the group. He kick-started things with the design of a dsPIC33 project board, including such peripherals as a programmable gain amplifier (PGA), digital to analog converter (DAC), EEPROM memory, liquid crystal display (LCD), a quadrature rotary encoder and interfaces

for a programmer and a keyboard. This was enough to give birth to what we now call the NUE-PSK digital modem.

NUE-PSK Hardware Overview

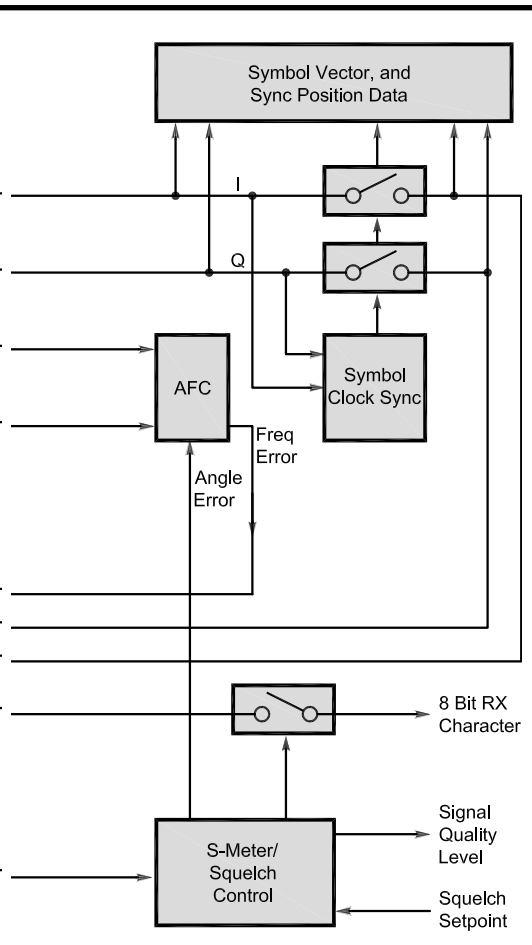
As illustrated in the schematic diagram of Figure 4, U1 — a dsPIC33F is at the heart of the project design. This highly-integrated

dsPIC33F device employs a powerful 16-bit architecture that seamlessly integrates the control features of a Microcontroller (MCU) with the computational capabilities of a DSP IC. The resulting functionality is ideal for applications that rely on high-speed, repetitive computations, as well as control — just perfect for our PSK31 digital modem project! Table 1 is the complete parts list for the NUE-PSK modem.

The dsPIC33F central processing unit (CPU) has extensive mathematical processing capability with its DSP engine, dual 40-bit accumulators, hardware support for division operations, barrel shifter, 17 × 17 multiplier, large array of 16-bit working registers and a wide variety of data addressing modes. Flexible and deterministic interrupt handling, coupled with a powerful array of peripherals, renders the dsPIC33F devices suitable for control applications. Reliable, field programmable flash program memory ensures scalability of applications that use the dsPIC33F family of devices. The specific device we used contains 128 KB of program flash memory, 16 KB of RAM, nine 16-bit timers, 16 general-purpose I/O pins, a pulse



Figure 3 — We built this portable PSK unit around 2000. It was too complex and expensive, with separate boards for DSP and control processing. It did include a novel CW user interface.



width modulation port, a port designed for reading quadrature encoders, two 16-channel ADCs, two UARTS, two SPI ports, two I2C ports, and comes in a 64-pin quad surface mount flat pack package. Whew, this sure is a powerful chip.

The initial prototype used the dsPIC to capture and decode signals from the PS2 Keyboard. This worked fine, except that on rare occasions, the dsPIC appeared to reset itself. This had the unfortunate effect of losing current operating information such as the frequency, call sign, and other. After reviewing all information regarding the PS2 keyboard, we didn't like the way we were capturing scan codes from the keyboard. Data was being sent synchronously from the keyboard to the dsPIC, using a clock of only roughly known frequency (~10-20 kHz). Each clock pulse caused an interrupt in the dsPIC, which then sampled the data stream. With the keyboard protocol, selected by IBM many years ago, each scan code is sent using 11 clock pulses. In addition, each keystroke press and release results in three or more scan codes being generated. Consequently, each keystroke generated a minimum of 33 interrupts.

Buying or Building Your Own NUE-PSK

Assembled and tested NUE-PSK modems can be purchased from the American QRP Club at www.amqrp.org/kits/nue-psk31/. The cost is \$199 for US and Canadian shipment; \$219 for overseas orders. Accessories are also available. You can order online, or send a check or money order payable to the American QRP Club c/o George Heron, 2419 Feather Mae Ct, Forest Hill, MD 21050. Full and partial kit versions will be available later this year. Check the American QRP Club Web page for the latest updates.

If you prefer to source your own parts and build from scratch, see Figure 1. The NUE-PSK software is available for free downloading on the NUE-PSK Web page.

Whether you decide to homebrew the modem, or perhaps get the partial kit and assemble it yourself, don't be afraid of soldering the surface mount ICs used in this project. Here's a technique that works great even for the 64-pin dsPIC chip. Using a magnifying lamp, position the IC on the pads and tack solder two corner leads to hold the package in place. Liberally solder all the leads to the pads without any concern for shorts between the leads. Next, use some desoldering braid (like SolderWick) to remove all excess solder along the rows of leads. Don't worry about overheating the IC package — it's tough. After all that excess solder is sucked up, you're left with the cleanest looking connections that could ever be achieved by hand soldering!

Apparently too much time was being wasted just processing keyboard interrupts, and that was the likely cause for the occasional dsPIC resets. To solve this problem, we decided to use another small microcontroller to do most of the work handling the keyboard data. This second microcontroller, U5 (Freescale 68MC908QY4) simply responds to the clock from the keyboard and gathers the bits received into a complete scan code (11 interrupts). Once a scan code is completed, the 'QY4 generates a strobe pulse to the dsPIC. Again, an interrupt in the dsPIC causes the dsPIC to capture an entire scan code on a set of port pins, and place it in a buffer, or merely sets a flag if the scan code is not a usable character. The ultimate effect of this division of responsibilities is that the dsPIC now responds to only 1/11th of the number of keyboard interrupts that were present in the first attempt.

Two LCD displays were initially chosen for the PSK interface. A character LCD was used for displaying received decoded text and as a monitor for text being placed in the transmit queue. Text is displayed when in transmit and as macros are being played back. The cursor changed from steady to flashing when in transmit. Setup Menus were also displayed on the text display. A 144 x 32 pixel graphics LCD was then used to display the FFT-generated spectrum of the audio passband. The lowest six rows of the display were used for the tuning cursor. Since a 512-point FFT is used with an 8 kHz sampling rate, we have 256 points for a 4 kHz passband. We chose to display only the frequency range from 500 Hz to 2500 Hz, using 128 columns of the display. (The last 16 of the 144 horizontal pixels in each row were not used.) The data and control lines for each display were buff-

ered by level translators U2 and U3, required to match the voltage levels between the 3.3 V dsPIC and the 5 V displays.

Since our original prototypes were built, we decided that we could possibly save some cost and simplify packaging by using a single graphics display for both text and spectral display. A 128 x 64 pixel display was chosen. The display drivers were combined into one, and modified to handle display of text buffers and an FFT of the input signal (spectral display), along with a "cursor" for tuning. Text is displayed on the bottom half of the display, using 5 x 8 pixel characters with 4 lines of display. The top 32 pixels are used for the spectral display, and the tuning cursor. In addition, the display incorporates a backlight that can be turned on or off by means of either a hot key or from a menu selection. FET transistor Q2 buffers the control line going to the backlight pin on the LCD.

The EEPROM, U4 (24AA256), provides local storage for the macro and user-set variables entered during modem operation. This memory device is controlled by one of the I2C ports on the dsPIC.

A computer-adjustable gain stage, the programmable gain amplifier (U7, MCP6S21), brings the low level audio input stream coming from the SSB receiver to the analog-to-digital converter on the MCU. Amplifier U8 (MCP601) presents precisely one-half the Vdd voltage to the ac reference input of U7.

Processed digital transmit audio tones are converted to a continuous analog stream by D-to-A converter U6 (MCP4922). The audio level control R4 sets the appropriate modulation level to the input of the SSB transmitter, which is generally a one-time setting for the transmitter being used. To produce a bipolar ac signal, a numeric constant equal to one

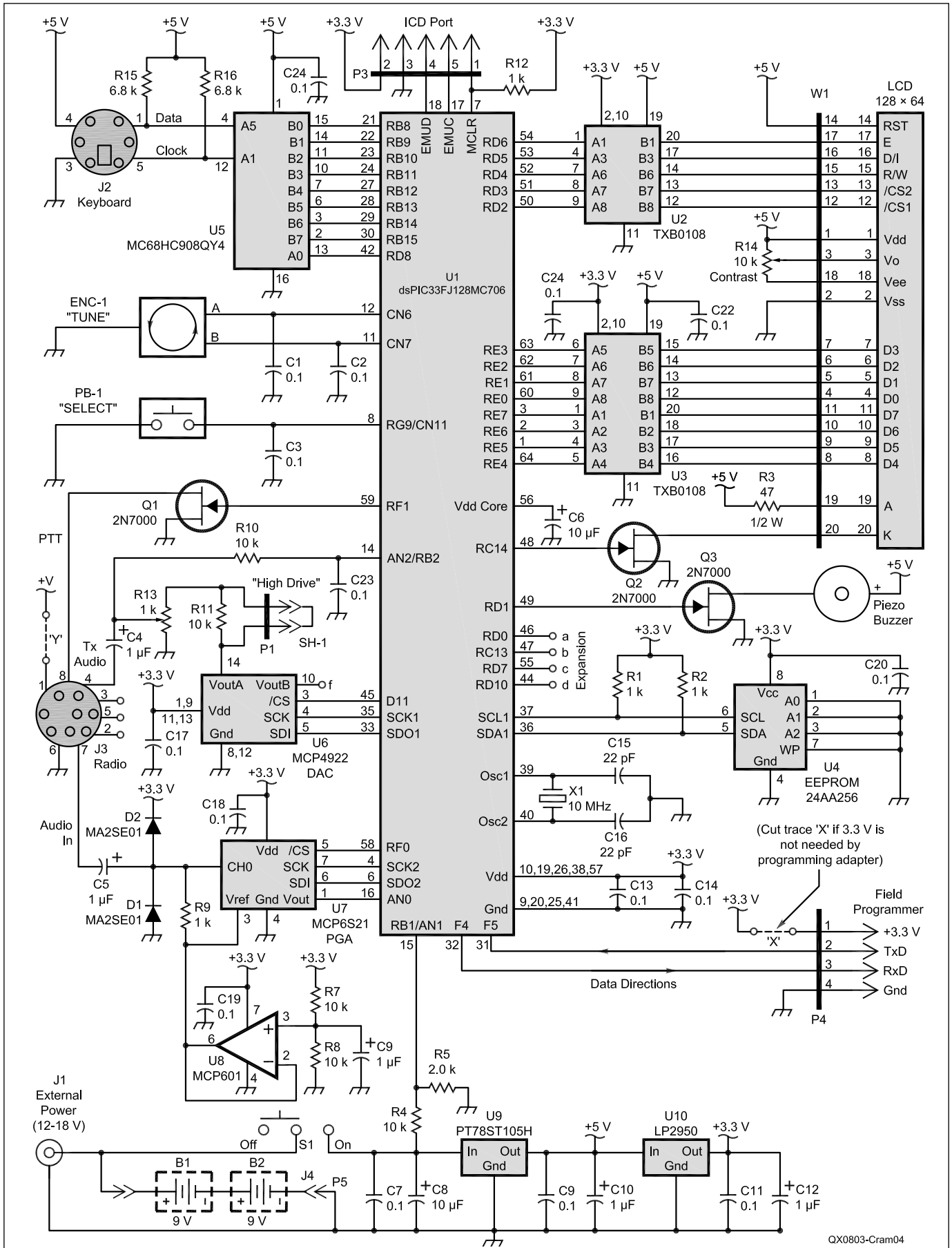


Figure 4 — The NUE-PSK schematic diagram.

half of the full scale output is added to the data stream generated by the dsPIC. Since the output is capacitively coupled, the dc term represented by the half scale constant is removed. The full analog signal is presented to the audio level control, however, and one of the dsPIC ADC inputs is used to measure the dc voltage on the wiper of the level control. This allows the dsPIC to determine the position of the wiper and display that information on the LCD, as desired (a menu option). This facilitates setup with different rigs, once the correct setting is determined for each rig. The wiper of the control is ac coupled to the rig audio input.

FET transistor Q1 (2N7000) buffers the push-to-talk (PTT) control line sent to the transceiver, used to put the radio into transmit mode.

A piezo buzzer is provided to deliver audible feedback for Tuning, menu selection and for future features. FET transistor Q3 buffers the control line to the buzzer.

The audio input, output and PTT control lines are brought off the pc board using an 8-pin mini-DIN connector, J3. This approach minimizes the number of connectors and cables normally used to connect a digital mode controller to an HF rig, as sometimes these cables can get mixed up and messy at the operating station. Further, when the NUE-PSK modem is used with a dedicated HF rig – say a Yaesu FT-817/857/897 or a

PSK-20 transceiver card — the other end of the cable may also be consolidated to a single multi-pin plug, providing a neat and elegant interconnect with the radio.

For the design of the power supply, we chose to use a switching regulator (U9) instead of the more conventional 7805 linear regulator to get 5 V on the board. This solution requires a lower operating current from the supply because of the greater efficiency

achieved by the switching “buck” regulator. A linear regulator merely dissipates the power difference between input and output in the form of heat. Thus, even though the dsPIC draws approximately 100 mA, the modem now only requires about 60 mA from the supply during normal operation, and portable power is easily provided by conventional alkaline batteries. Figure 7 shows the current requirement as a function of supply voltage.

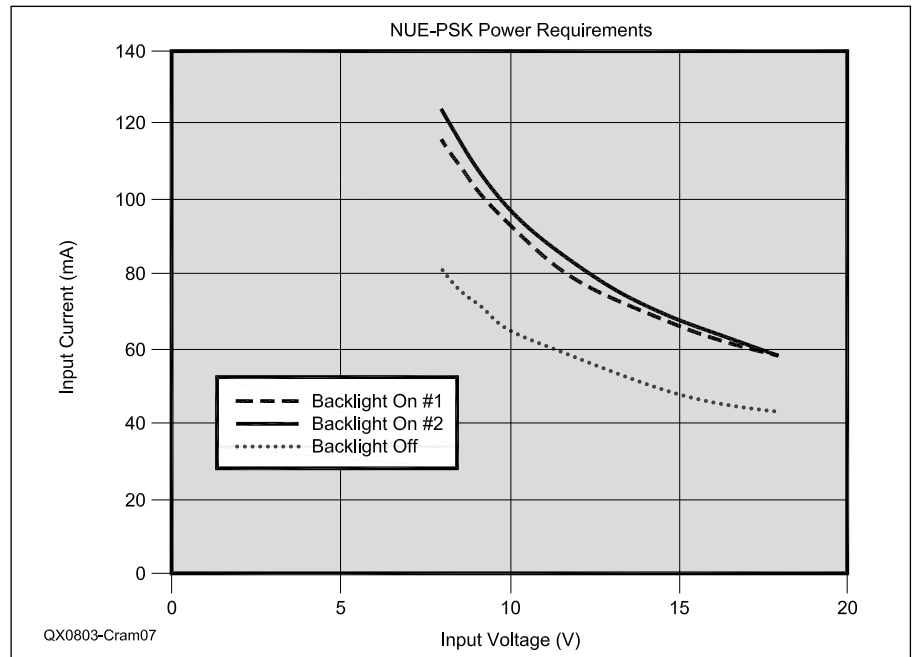


Figure 7 — Power requirements for the NUE-PSK modem. Measurements illustrate the dramatic benefits of using the switching “buck” regulator. Regulator efficiency increases as higher supply voltages are used. The top curves show the input current requirement when running with the display backlight on, while the lower curve shows 15 mA less current when the backlight is off.



Figure 5 — The two-LCD Prototype used a graphic LCD for the spectrum display (top) and a character LCD for receive and transmit text characters (bottom).

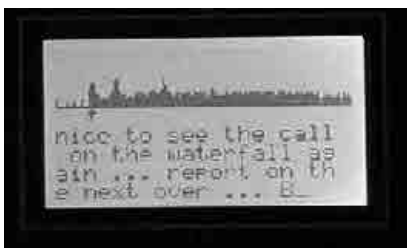


Figure 6 — The newer single graphic LCD shows both spectrum and receive or transmit characters. The backlight affords great night time visibility and costs only 20 mA in additional current demand.

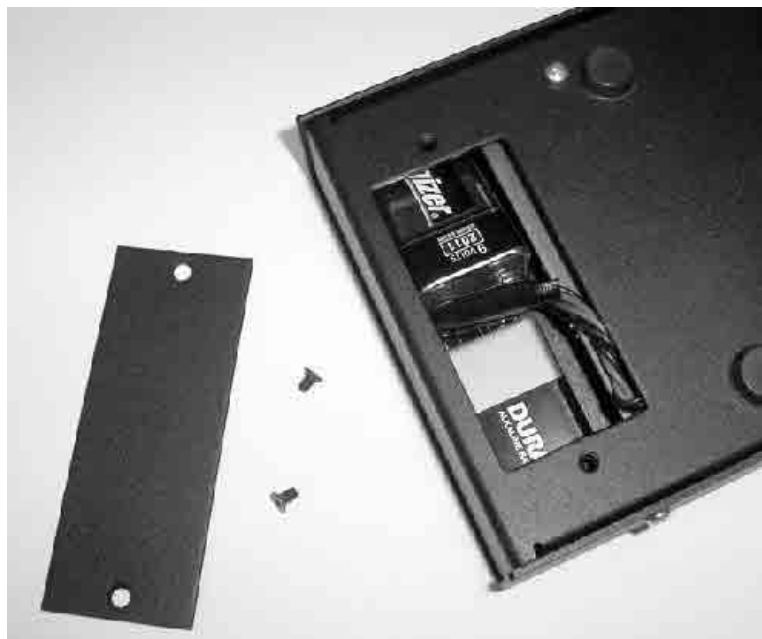


Figure 8 — The two 9 V alkaline batteries nestle tightly against the circuit board in the case compartment. When installed, the screw-on cover holds them firmly in place.

A small drawback of using the switching regulator is that a 9 V minimum input is required to maintain regulation; so battery operation is achieved by using two standard 9 V batteries in series to provide a nominal 18 V input to the modem. See Figure 8. Of course the digital modem may instead be externally powered by applying 12 V through J1. When external power is applied, the internal battery connector should be disconnected, or the batteries should be removed.

The NUE-PSK project is assembled using a single 4 × 5 inch pc board — quite an improvement over the Portable PSK projects done previously, as well as over the prototype hardware for this current design. The pc board holds all components — the LCD, rotary encoder, power connector and radio interface connectors — and may be assembled into your favorite homebrewed enclosure, or in the clam shell aluminum enclosure made available when the kit is purchased from the American QRP club.⁶ This enclosure also has a conveniently-accessed compartment on the back side that houses the 9 V batteries. See Figure 9.

Hardware Evolution

Before ending up with a neat and compact circuit board, the NUE-PSK design started out as a rather large and sprawling prototype hardware layout. This is normally the case with complex projects, because it allows the designers to try out different approaches and components, while also allowing them to easily monitor and debug the design.

The prototype design was built using a proto-board purchased at Fry's Electronics. It has plated-through holes on 0.1 inch centers to facilitate mounting through-hole components. The surface mount dsPIC microcontroller is mounted on a "Schmart-Board," also obtained from Fry's.⁷ This particular board is designed to permit attaching 32 to 100 pin SMT devices, and has 0.65 mm lead separation (pitch). Schmart Boards are available in several pitches and pin count configurations to accommodate prototyping of a range of SMT controllers. Header pins and sockets are used to connect the board to the main prototype board. Point-to-point circuit connections were accomplished using 30-gauge Kynar wire, and a hand-stripping tool was used to strip the ends prior to soldering to the socket/connector pins. Thus the prototype was rather easily assembled and the result was relatively solid when complete.

Development Tools and Getting Started in Software

While Microchip is well-known in the ham community, few of us had experience using this new family of PIC chips.



Figure 9 — This photo shows the NUE-PSK assembly. A 4 × 5 inch circuit board fits neatly into the enclosure, holding all components. (Individual wires are shown connecting the display in this prototype unit.) The battery "door" in the back of the case is visible along the left edge of the photo. Two 9 V batteries fit into the space between the circuit board and the case.

Microchip apparently foresaw this situation and they have provided an amazing number of application notes, specifications and guidance for designers to use in quickly coming up to speed.

Further, even the best chip on earth would be crippled without a good set of software development tools; but Microchip again came to the rescue with a C compiler and an extensive DSP library that proved invaluable to us in developing the project. Both of these were available for free, so what more could we ask!

To program the dsPIC, we discovered that the inexpensive (~\$25) PICkit2 programmer from Microchip is entirely adequate for the job. In-circuit debugging is not readily achieved with the free versions of the tools, but we seemed to do alright regardless.

The final essential aspect in enabling this project was a design reference for the PSK31 modem algorithm, provided by Moe Wheatley, AE4JY. His *PSKcore* documentation and C++ source code was professionally done and placed into the public domain, so it was available for our use.⁸ We concluded that it would be a straightforward conversion to C language so we could use our free compiler and have it work on the dsPIC33, and we relied heavily on it.

Software Overview

Although Wheatley's code was written in C++, and was developed for use on a PC, it was not too difficult to convert it for compilation under C, for which there is a free compiler from Microchip. As part of our QRP group project, John Fisher, K5JHF, provided much of the initial software for the project. His code includes most of the initialization code, a keyboard handler, a basic LCD driver, I2C and SPI drivers, an interface for EEPROM storage, and ADC and DAC interfaces. Milt, W8NUE, developed the remaining code fairly easily, even though his

programming experience has been mostly in BASIC and Visual Basic, with some FORTRAN.

PSK31 Decoder Processing

The receiver audio from an SSB transceiver is supplied to the NUE-PSK circuits. Before processing by the dsPIC, it is passed to the PGA, whose gain is controlled by the dsPIC via a serial peripheral interface (SPI) connection. The output of the PGA is then sampled by an internal 12-bit ADC on the dsPIC.

Timer 1 of the dsPIC provides all of the critical timing. The timer is set for interrupts every 125 microseconds, corresponding to a sample rate of 8000 samples per second. In receive (demodulation), ADC samples are captured into a 2048 word buffer. Once the buffer is half full, a flag is set to inform the system that data is available for processing. Only half of the buffer is processed at a time. This ping-pong buffering technique allows continuous data processing to be accomplished while the other half is being filled in real time.

The "main" routine of the program is an endless loop in which a number of flags are tested and, if found to be set when queried, they are used to trigger execution of various functions. For example, if the ProcPSK flag is checked and found to be set, a block of data is then processed. Each sample in the buffer is multiplied by a quadrature NCO, producing I and Q signals. Each of these is then passed two times through 35-tap decimate-by-4 FIR filters. This provides I and Q signals that are now sampled at 500 samples per second. (If in PSK63 mode, the second filter bank will decimate-by-2, providing 1000 samples per second.) While the block of 1024 samples is being processed, the second half of the buffer is being filled with new samples under control of the Timer 1 interrupts. Processing then ping-pongs between the two halves of the buffer. Using this technique we never



Figure 10 — NUE-PSK Prototype System. Clockwise from upper right: NUE-PSK displays and prototype hardware, standard PS2 keyboard, FT-817 transceiver, and power supply.

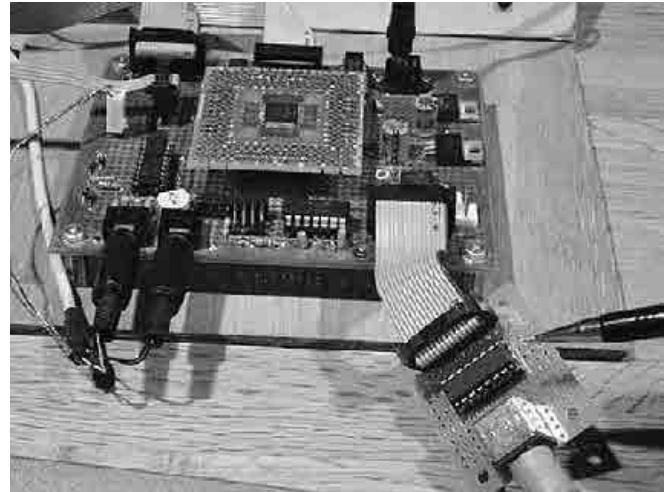


Figure 11 — This close-up of the NUE-PSK prototype shows the multiple cabling and programmer connection (lower right), which allows convenient access to the electronics during design shake down.

write new data to the part of the buffer that is being processed.

The next step is to split each of the I and Q channels into two paths. One is for the processing of the bits and one path is for processing of frequency data, producing four channels of data. Each of these channels is filtered by a 65-tap FIR. The I and Q bit channels should be optimized to minimize intersymbol interference, while the I and Q frequency channels should be optimized for fast response of the automatic frequency control (AFC) loop. All of the FIR filters have responses as specified by AE4JY. Instead of using the *PSKcore* filtering code, we are using FIR filters from the Microchip DSP library, as these software filters are designed to take into account the special hardware features of the dsPIC. The results can be shown to be the same, however. That is, they have identical frequency responses.

The bit channels are processed as described in the *PSKcore* specification to determine the proper time for determination of the phase changes that are employed in PSK. Since the bit rate of PSK31 is 31.25 Hz, each bit extends for 32 milliseconds in time. We have a sample rate of 500 Hz at this stage of processing, so there are 16 samples for each bit. The point in time for proper synchronization of the phase detection process is based on an analysis of the average energy in each of the 16 samples when averaged over several bits. Without going into the mathematical details, suffice it to say that the maximum energy always occurs at the boundary between successive bits. This fact is used to establish synchronization in the bit detector.

We used the free *WinFIRDesigner* software, with parameters obtained from the AE4JY code to calculate the FIR filter

coefficients. As noted above, the frequency responses obtained with these coefficients are identical to those published by AE4JY.

A processing block takes the four filtered signals, and proceeds to:

- 1) obtain a digital AGC control;
- 2) calculate frequency errors;
- 3) correct the numerically controlled local oscillator;
- 4) determine bit boundaries;
- 5) determine whether a 1 or a 0 is being received;
- 6) collect the decoded 1s and 0s into a Varicode pattern;
- 7) convert the Varicode pattern into ASCII characters; and finally
- 8) display the resulting characters.

The *PSKcore* routines were used to perform AGC, bit synchronization, character decoding, and so on. In addition, we added code that will perform a 512 point FFT on the samples (8 kHz sampling rate) that are provided to the FIR filters. The processed FFT is then converted to magnitude, and then to a logarithmic scale. The 500-to-2500 Hz portion of the spectrum is displayed on the upper half of a 128 × 64 pixel graphics LCD. This display is essential for tuning. More about this later.

The final demodulator processing output is a decoded ASCII character. These decoded characters are displayed on the lower half of the 128 × 64 graphics display, as four lines of 20 characters each. The display driver includes a line buffer so that once a line of characters is filled, it is scrolled up and new characters are inserted at the beginning of the second line. This approach was chosen so that printed characters remain fixed for easy reading, as opposed to all characters being in constant motion (scrolled horizontally) once a line is filled.

PSK31 Encoder Processing

As mentioned earlier, the encoding process is considerably less-intense as compared to the decoder operations. ASCII characters are accepted from the keyboard, converted to Varicode characters, and the binary string represented by the Varicode is used to modulate the phase and amplitude of an audio carrier — the PSK audio signal.

Although *PSKcore* code creates a block of data to be sent to the PC soundcard, we chose to generate a single sample of output signal for each and every 125 microsecond timer interrupt. This minimizes data memory requirements. The method of generating the desired phase and amplitude modulation is that developed by AE4JY with the exception that the tables used reside in program memory instead of data memory. The use of these tables eliminates the time-consuming calculation of sine and cosine signal components. The choice of placing these tables in program memory was made because we had plenty of program memory with the dsPIC, but not a lot of spare data memory. The calculated data samples are then scaled for output to a 12-bit DAC. The DAC output, after capacitive coupling, is then routed to the audio input of an SSB transceiver.

As each interrupt occurs, the code steps through the tables, providing modulation values for the I and Q signals, resulting in either BPSK or QPSK modulation. The modulated I and Q signals are added together prior to the DAC.

Using the NUE-PSK Digital Modem

Install two standard 9 V alkaline batteries in the battery compartment, or connect a 9 to 18 V dc supply to the coaxial power connector (2.1 mm) on the right end of the modem.

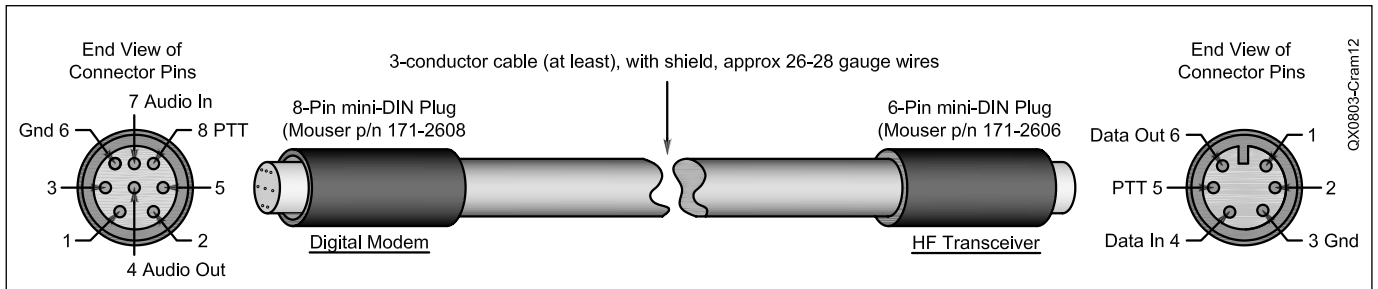


Figure 12 — Connections between NUE-PSK digital modem and a typical HF transceiver. (The wiring diagram shows the connections for a Yaesu FT-817 radio.)

Signal Connections

Install a connector, or connectors, to the end of the cable that has an 8-pin mini-DIN connector. Most modern HF rigs have a mini-DIN Data or AUX connector, which provides for PTT, fixed level audio from the receiver (independent of the volume control on the rig), and a line-level (approx 100 mV RMS) audio input to the transmitter. On the Yaesu FT-817/857/897 this connector is a 6-pin mini-DIN. On many Kenwood HF rigs there are 6-pin and 13 pin mini-DIN connectors that may be used. See Figure 12 for wiring details.

Keyboard

The modem requires an AT/PS2 style keyboard for character entry. The keyboard also provides for entry and playback of macros. Use the 6-pin mini-DIN connector on the end of the modem to connect to the keyboard.

Operation

Once you have the cable between the modem and the rig connected, keyboard attached, and power available, you are ready to operate PSK. But first, some additional setup may also be desired, as described next.

Turn on the modem. If the cable between the rig and modem is wired correctly, you should see evidence of signals and/or noise on the top half of the display (the spectrum area). Tune your rig to one of the PSK sub-bands. These are typically 70 to 74 kHz above the lower band edge on 40 and 20 meters. If there is PSK activity on the band, you should see peaks on the graphic display. The horizontal location of the peaks corresponds to the audio frequency of each signal relative to the tuned frequency of the rig. For example, if the rig is tuned to 14070 kHz, the display shows audio frequencies from 500 Hz to 2500 Hz, or actual RF frequencies from 14070.5 to 14072.5 kHz.

Now for the fun — tuning! Turn the encoder clockwise, or counterclockwise, to move the cursor to a higher, or lower frequency. (The cursor is the small triangular icon just below the spectrum display.) The audio frequency is displayed when turning the encoder. Try to align the cursor with one

of the peaks on the display. Don't worry if it is not exactly aligned. Once close to the peak, stop turning the encoder. The modem now attempts to "lock" onto the signal and fine-tune the frequency if needed. If the modem is able to lock onto a PSK signal, it will very shortly begin decoding the signal, and then display characters on the screen. The time it takes for decoded characters to appear depends on the ability of the modem to estimate the center frequency of the incoming signal, and the signal to noise ratio. Tuning can also be done with the arrow keys on the keyboard. The right and left arrow keys provide finer tuning, while the up and down arrow keys provide faster tuning. The tuning rate of the encoder on the modem can also be selected from a menu setting. Note: When tuning in receive mode, the spectral display is frozen—this is intentional.

Now, on to set-up for transmission. Connect your rig to a dummy load.

Since PSK signals generated by the modem contain simultaneous multiple frequencies (over a very narrow bandwidth), it is imperative that the audio output from the modem not overdrive the input to the rig, or very poor signal quality will result. To facilitate setting the audio drive to the rig, a potentiometer on the modem may be used to adjust the level. In addition, the modem includes provision for "measuring" the position of the potentiometer, so that it can be

easily reset to the same setting in the future. More on this later.

We have found that the best way to set up for PSK operation is to initially set the transceiver for normal SSB operation, including whatever power setting you usually employ. For example, if you have a 100 W PEP rig, set it up for 100 W on SSB.

Switch to Digital mode (if your rig provides that option, otherwise retain the SSB mode).

Then press F8 on the keyboard. This places the modem in the TUNE state, which is denoted by "TUNE" at the top left of the display. The modem is now generating a continuous tone, which is fed to the audio input of the rig. The PTT signal from the modem should also cause the transceiver to switch to transmit. At this point, the potentiometer on the modem (just to the right of the display) can be adjusted to set the power level of the transceiver. A transmit power of 15 to 40% of the rig's rated power is recommended. (In other words, 15 to 40 W with a 100 W rig). Keeping the power at this level does two things. First, it minimizes distortion due to clipping. Second, it avoids excessive heating in the rig finals, since PSK is a 100% duty cycle mode. A power meter is very handy for making this setting. Once the potentiometer has been set, press F8 again to return to receive mode.

You should now be ready for transmitting PSK.

Pressing F12 will place the modem in transmit mode, but with a PSK idle tone being generated (unlike the CW tone in TUNE). If you are ready to give it a try, press F12. At this point, anything that you type on the keyboard will be converted into Varicode characters and transmitted using PSK modulation. Pressing F12 again, will toggle back to receive. When in transmit mode, "TX" will appear at the top left of the display.

Macros

If you want to set up macros (pre-recorded strings of characters for subsequent playback) before proceeding, now is a good time to do it.

For those already familiar with PSK operations, macro setup is very similar to many of



Figure 13 — A USB-to-TTL interface adapter from SparkFun will allow your computer USB port to connect to the modem for programming updates to the software.

the popular PSK programs. There are a few differences though. Some of the typing will be “blind” — not all of the input characters will be echoed to the display.

Before you begin to operate, you should record your call sign in the modem’s EEPROM. While in receive mode, type your call sign and then press Ctrl+M.

Macro recording is initiated by pressing Ctrl plus the function key that you want to be associated with your macro. For example, to use F1 for calling CQ, press Ctrl + F1. Then begin typing “cq cq cq de.” Now enter Alt+M, press the space bar, enter Alt+M again, press the space bar again, enter Alt+M again, press the space bar, enter “K” and finally enter Ctrl+Q. (Omit the quotes during the typing). Now press F9 to store the macro. When this macro is played during transmission, by pressing function key F1, it will call CQ three times followed by your call sign 3 times, followed by “K,” and then the modem will revert to receive. In this procedure, entering Alt+M informs the modem that you want to insert your call sign into the transmit buffer. Entering Ctrl+Q, inserts a special character, which the modem recognizes as “quit transmitting and revert to receive.” Each macro can contain up to 255 characters.

You can also record the “other station’s” call sign in RAM (not in nonvolatile EEPROM) by pressing Ctrl+T after first typing their call sign on the keyboard. To insert the other station’s call sign into a macro, simply use Alt+T in the macro. Then, when you play the macro, the other station’s call sign will be inserted into the macro. This way, whenever you enter a new call sign using Ctrl+T, you do not need to re-record the macro to use the new call sign.

Menus

Configuration of the modem is done through a menu system. For example, you can select between PSK, QPSK, and QPSK reversed. You can also change the software squelch setting, the gain of the programmable gain amplifier (PGA), turn CW Identification on or off, turn the display backlight on or off, change the tuning “increment,” monitor battery voltage, or monitor the setting of the TX audio potentiometer. Other items may be added to the menu at a later time.

The menu system has two means of access. If you wish to access the menus using the keyboard, simply press F10 on the keyboard. Next enter a number on the keyboard corresponding to the submenu that you wish to access. Once this selection is made, choices for the submenu will be displayed. Another numeric entry will denote your selection. With the keyboard menu system, entering the submenu choice on the keyboard will cause an exit from the configuration menu.

The second method of menu access is

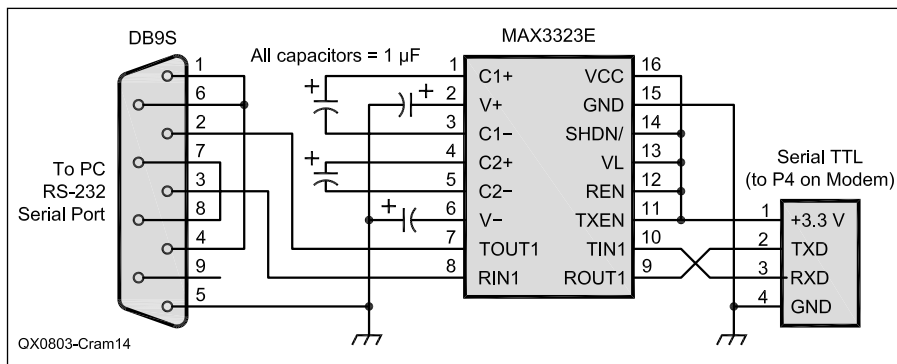


Figure 14 — This schematic diagram shows an easy-to-build RS-232 interface that you can use between your computer serial port and the serial TTL input on the NUE-PSK modem.

through the “Select” button on the menu and the rotary encoder. Pressing and holding the Select button for more than ½ second will activate the menu system. When initially activated, the display will show “Configure” on one line, followed by “Exit” on the line below. If you wish to abort configuration, simply tap the Select button at this time. If, on the other hand, you wish to configure one of the modem settings, simply rotate the encoder clockwise, or counter clockwise, to cycle through the top level menu selection. Once you see an item that you wish to change, tap the Select button again. This will then allow you to cycle through a list of choices (again by rotating the encoder). When the choice you wish to make appears on the display, tap the Select button again. This will record your choice, and the menu will revert to the top level, showing “Exit” as the default choice. You can now make additional changes, or tap the Select button again to exit the Configuration menu.

Hot Keys

A number of “Hot Keys” have been defined for use with the modem:

F1 to F7: Play Macros.

Ctrl-Fn: Record Macros — Enter keystrokes. When finished, Press F9.

Alt-Fn: Delete Macro associated with Fn.

F8: Toggle TUNE mode. May be accessed only in RX or TX (Not in Setup, or Macro Recording).

F11: Display the first few bytes stored in EEPROM.

F12: Toggle between RX and TX (again, not in Setup or Macro Recording).

F10: Display the main Setup Screen. (Accessible only in RX mode).

#: A numeric selection from the Main Menu, selects a submenu, which is then displayed. Another numeric selection activates your selected parameter.

Ctrl-M: Save keyboard entries into a fixed location in EEPROM (for recording “my call sign,” for use in Macros).

Ctrl-T: Save keyboard entries into a RAM location (for recording “their call sign” — also for use in Macros).

Alt-M: Insert “my call sign” into a Macro.

Alt-T: Insert “their call sign” into a Macro.

Ctrl-F: Save the current frequency into EEPROM so that it can be restored at the next power-up.

Alt-F: Retrieve the saved frequency and make it the current frequency.

Ctrl-Tab: Display the current (audio) frequency.

Ctrl-A: Enable AFC.

Alt-A: Disable AFC.

PgUp: Increase PGA gain.

PgDn: Decrease PGA gain.

Ctrl-L: Clears the text area of the LCD.

Ctrl-K: Clears the keyboard buffer (while receiving, keystrokes are not displayed — this allows clearing the buffer, so that call signs may be entered, or re-entered in case you think that you have entered the wrong call sign).

Ctrl-B: Clears the internal buffers.

Ctrl-Q: Inserts a TX-OFF control character in the TX buffer, or Macro.

Ctrl-O: Toggles the display backlight on and off.

Here is a useful combination of macros:

F1: CQ

F2: Call “them” twice w/ toggle

F3: Call “them” once w/o toggle

F4: BTU

F5: 73

F6: Brag File

F7: Test message

For your personal macros, choose whatever you want. You can create ones for contesting, or just for casual rag-chewing.

Updating the Modem with Newer Features

Increasingly today, microcontroller projects have an ability to be “field updated” with new features and software updates

made available by the designers. So, instead of needing to send your instrument back for reprogramming to get these new capabilities and bug fixes, you can simply download the latest-and-greatest software from the Internet and send it to the target hardware. The device automatically updates its internal memory with the new program. What a great way to keep your project completely up to date with the latest features!

We have incorporated this field updating capability into the NUE-PSK Digital Modem. You just need to connect your PC serial port to the modem using a simple adapter, and send it the new software obtained from the NUE-PSK Web site whenever new capabilities are made available.

We designed a TTL serial port into the modem, accessible via a 4-pin connector, P4, located inside the battery compartment. By connecting your computer's USB port to an inexpensive USB-to-TTL adapter such as the CP2102 from SparkFun and plugging the CP2101 (or equivalent) into P4, the modem's "Load Software" menu selection will initiate the bootload sequence to "burn" the new software into the modem's controller.⁹ Then, once you power-cycle the modem, you'll be running the latest software release containing, for example, a new digital mode, some new I/O capabilities, and so on. This is really quite a convenient and powerful capability for the project.

Possible Future Enhancements

Updating the graphics LCD to display current spectral information consumes a considerable fraction of the total processing time. If all LCD display routines were to be off-loaded to a small microcontroller, there would be more time available for processing faster digital modes, such as PSK63.

Additional dynamic range would be possible if an external ADC, with 16 to 24 bits, were to be employed. The Austin QRP group is currently evaluating ADCs and Codecs that might be used in this application.

The next logical step in the evolution of portable amateur radio digital communication is decreased size and increased portability. We envision someday — perhaps sooner rather than later — having a completely integrated, handheld digital modem and low-power transceiver.

Conclusions

"On-Air" experience with the NUE-PSK Digital Modems has clearly demonstrated the effectiveness of the design, and its suitability for portable digital-mode operations, with an attractive, compact, low-power package. It is also a testament to the wonderful design skills of Moe Wheatley and his *PSKcore* software engineer, as well as to how evolving technology

continuously improves our options in amateur radio.

We very much enjoyed collaborating on the design of this project with several members of our QRP clubs. We are confident that you will enjoy the flexibility and power offered with the NUE-PSK Digital Modem when used on your bench or out under the stars.

Notes

¹Peter Martinez, G3PLX, "PSK31: A New Radio-Teletype Mode", *RadCom*, Dec 1998 and Jan 1999. (Reprinted in *QEX*, Jul/Aug 1999, pp 3-9).

²DigiPan software, v1.2 is available at members.home.com/hteller/digipan. DigiPan stands for "Digital Panoramic Tuning" and brings the ease and simplicity of panoramic reception and transmission to PSK31 operation. DigiPan provides a panoramic display of the frequency spectrum in the form of an active dial scale extending the full width of the computer screen. Depending upon the transceiver IF bandwidth, it is possible to "see" as many as 40 to 80 PSK31 stations at one time. DigiPan was developed as freeware by Howard (Skip) Teller, KH6TY/4 and Nick Fedoseev, UT2UZ.

³PSK-20 Transceiver Kit for PSK31, Small Wonder Labs, Dave Benson, K1SWL (ex-NN1G). E-mail: dave@smallwonderlabs.com, Web site: www.smallwonderlabs.com

⁴George Heron, N2APB, "Portable PSK" project www.njqrp.org/portablepsk

⁵Microchip: www.microchip.com. Technical documentation for the entire line of Microchip microcontrollers is available. The MPLAB Integrated Development Environment, and Student Edition C compiler are available for free download.

⁶The AmQRP Club is selling the NUE-PSK Digital Modem for \$199 (US & Canada) or \$219 (DX) as a fully assembled and tested unit. (Price includes shipping. CA residents please add 8.25% sales tax.) Kits will be offered later this year. To order, write a check/MO payable to "AmQRP Club" in US funds, and send to "The American QRP Club, 2419 Feather Mae Ct, Forest Hill, MD 21050 USA". Payment also accepted through PayPal to amqrpkits@amqrp.org. See the NUE-PSK project page for all details, including source code (www.amqrp.org/kits/nue-psk). We expect to offer full kits (all parts plus housing) and partial kits (PCB and preprogrammed microcontrollers) later in the year.

⁷SchmartBoards: www.schmartboard.com See part 202-0011-01 (32-100 pin QFP, 0.5 mm).

⁸Moe Wheatley, AE4JY, "PSKCore", www.qsl.net/ae4jy/. For his source code, download [PSKCoresrc.zip](http://www.qsl.net/ae4jy/PSKCoresrc.zip). For the full technical specification, download "PSKCore Interface Specification and Technical Description Ver 1.40"

⁹USB "Breakout Board" Interface, SparkFun CP2102, www.sparkfun.com/commerce/product_info.php?products_id=198

Other Useful PSK31 Technology References:

Don Urbytes, W8LGV, "A PSK31 Tuning Aid," *QST*, Dec 1999, pp 35-37.

Steve Ford, WB8IMY, "PSK31 — Has RTTY's Replacement Arrived?," *QST*, May 1999, pp 41-44.

Steve Ford, WB8IMY, "PSK31 2000," *QST* May, 2000, p 42.

Howard "Skip" Teller, KH6TY, and Dave Benson, NN1G, "A Panoramic Transceiving System for PSK31," *QST*, June 2000, pp 31-37.

Dave Benson, K1SWL (ex-NN1G), "The NJ Warbler — a PSK-80 Single Board Transceiver for PSK31," *QRP Homebrewer*, Summer 2000, pp 15-21.

Johan Forrer, KC7WW, "Using the Motorola DSP56002EVM for Amateur Radio DSP Projects," *QEX*, Aug 1995, pp 14-20.

ARRL Web site collection of PSK31 articles, links, literature and products: www.arrl.org/tis/info/psk31.html

The "Official" Homepage of PSK31 is at aintel.bi.edu.es/psk31.html

Milt Cram, W8NUE, was first licensed in 1953 as W8NUE and has held several calls (minus the "N") with an Amateur Extra class license. He is a longtime homebrewer and member of the Austin QRP Club, enjoying operating low power and the digital modes on HF. Milt holds BEE, MS and PhD degrees in electrical engineering from Georgia Tech and comes from a family of hams (dad, Ernie, W8JKX (SK), great uncle, Oz, WIJUU (SK), and son, Marc KC5RWZ). Milt is now retired, after serving many years in electronic design and management.

George Heron, N2APB, has been a software developer and technology manager in the north-eastern US for more than 30 years, working in later years in the field of information security. He is the chief scientist for McAfee, helping to develop new security products and technologies to protect home and corporate users. A ham since 1968, he is an avid homebrewer in RF and digital circuits, with a special interest in DSP and microcontroller applications to QRP, and has co-developed the Micro908 Antenna Analyzer. He leads the New Jersey QRP and the American QRP clubs, and has previously edited/published QRP Homebrewer magazine and Homebrewer Magazine.



Down East Microwave Inc.

We are your #1 source for 50MHz to 10GHz components, kits and assemblies for all your amateur radio and Satellite projects.

Transverters & Down Converters, Linear power amplifiers, Low Noise preamps, coaxial components, hybrid power modules, relays, GaAsFET, PHEMT's, & FET's, MMIC's, mixers, chip components, and other hard to find items for small signal and low noise applications.

We can interface our transverters with most radios.

Please call, write or see our web site www.downeastmicrowave.com for our Catalog, detailed Product descriptions and interfacing details.

Down East Microwave Inc.
19519 78th Terrace
Live Oak, FL 32060 USA
Tel. (386) 364-5529

The *Star-10* Transceiver — Part 2

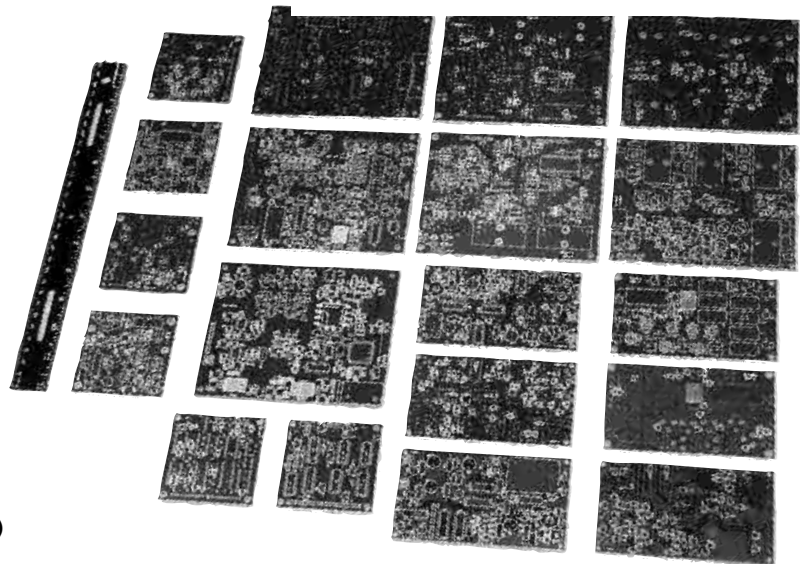
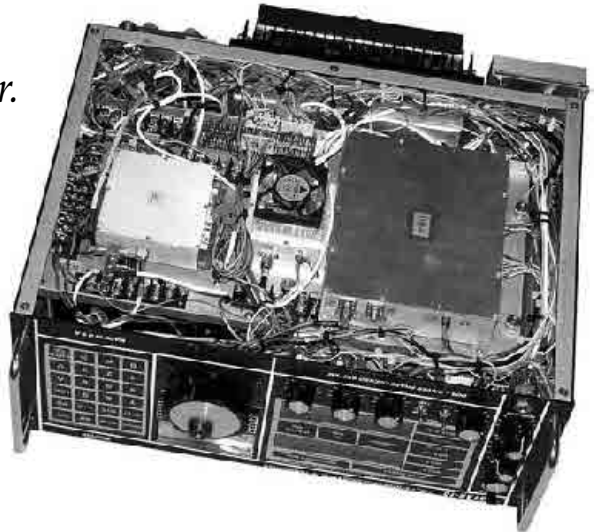
In Part 2 of this series we will look at some of the circuits used in this high-performance transceiver.

Mission — The *Star-10* transceiver has been a unique research experience into understanding what can be done from the laws-of-physics point of view in receiver and transceiver dynamic range performance. This research has been performed over a period of five years with parts, technologies and packaging means available to me at the time. The transceiver has been implemented with some unique parts that may no longer be available. The *Star-10* development has been a purely scientific endeavor intended primarily to understand what could be done to achieve ultimate receiver performance. Although the results have been outstanding, slightly better results may be possible using newer technologies and parts. The *Star-10* project was not intended as a commercial product. Its duplication is probably not economically feasible.

Introduction

In Part 1 of this series, I presented a system design criteria for a modern double conversion transceiver, namely the *Star-10*. The primary goal of this design was to produce a continuous HF coverage system with consistent high dynamic range receiver performance over the entire frequency range of 1.8 MHz to 30 MHz. I wanted to build a radio that rivals the performance of today's top-of-the-line equipment. The focus was how to design a no-compromise broadband radio, obtaining superior performance without resorting to a channelized, amateur-band-only design. The accent was put on good image and spurious rejection, using an up convert/down convert design, ample

Visible from the left are the FSYNTH assembly (left side panel), the IF75BC assembly (top left), the automatically switched half-octave receiver band-pass and transmitter high power, low-pass filter bank assembly, and the DFCB command and control assembly and keypad mounted on the back of the front panel. Front panel, side panels, top and bottom are removable allowing access to the assemblies.



(A)



(B)

Figure 6 — Part A shows the double-sided, plated-through-hole PC boards developed for the *Star-10* transceiver ready for assembly. Part B shows several of the completed assemblies for the *Star-10* transceiver. Starting from top left, PDAF (product detector/audio); IF9RX (receiver second IF); IF9TX (transmitter first IF); PLXO / MRU (phase locked crystal oscillator / master reference unit); IF75BC (bilateral front end converter), and FSYNTH / FRU (frequency synthesizer / frequency reference unit). For functionality of these blocks, refer to Figure 2 in Part 1 of the article, in the Nov/Dec 2007 issue of *QEX*.

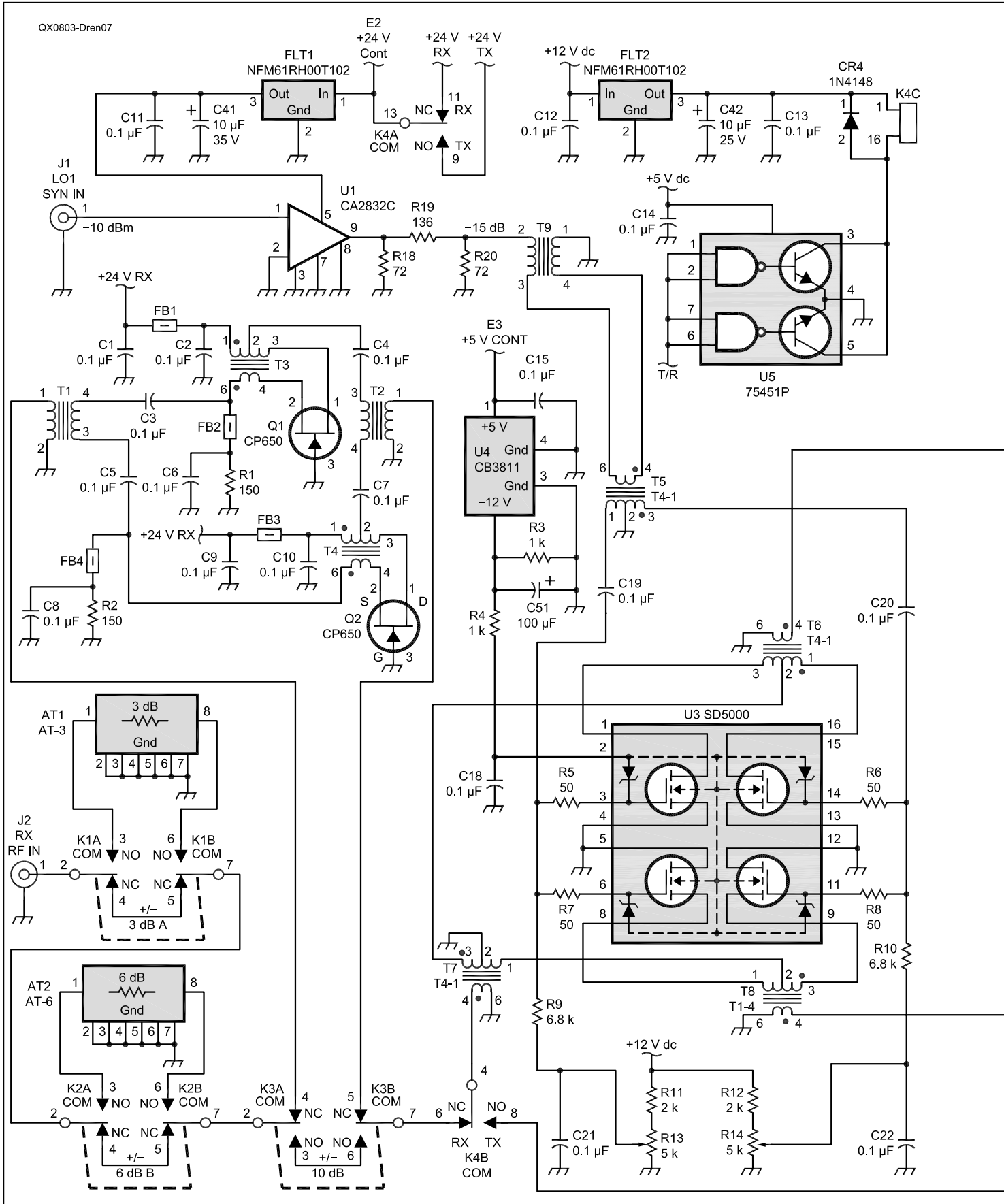
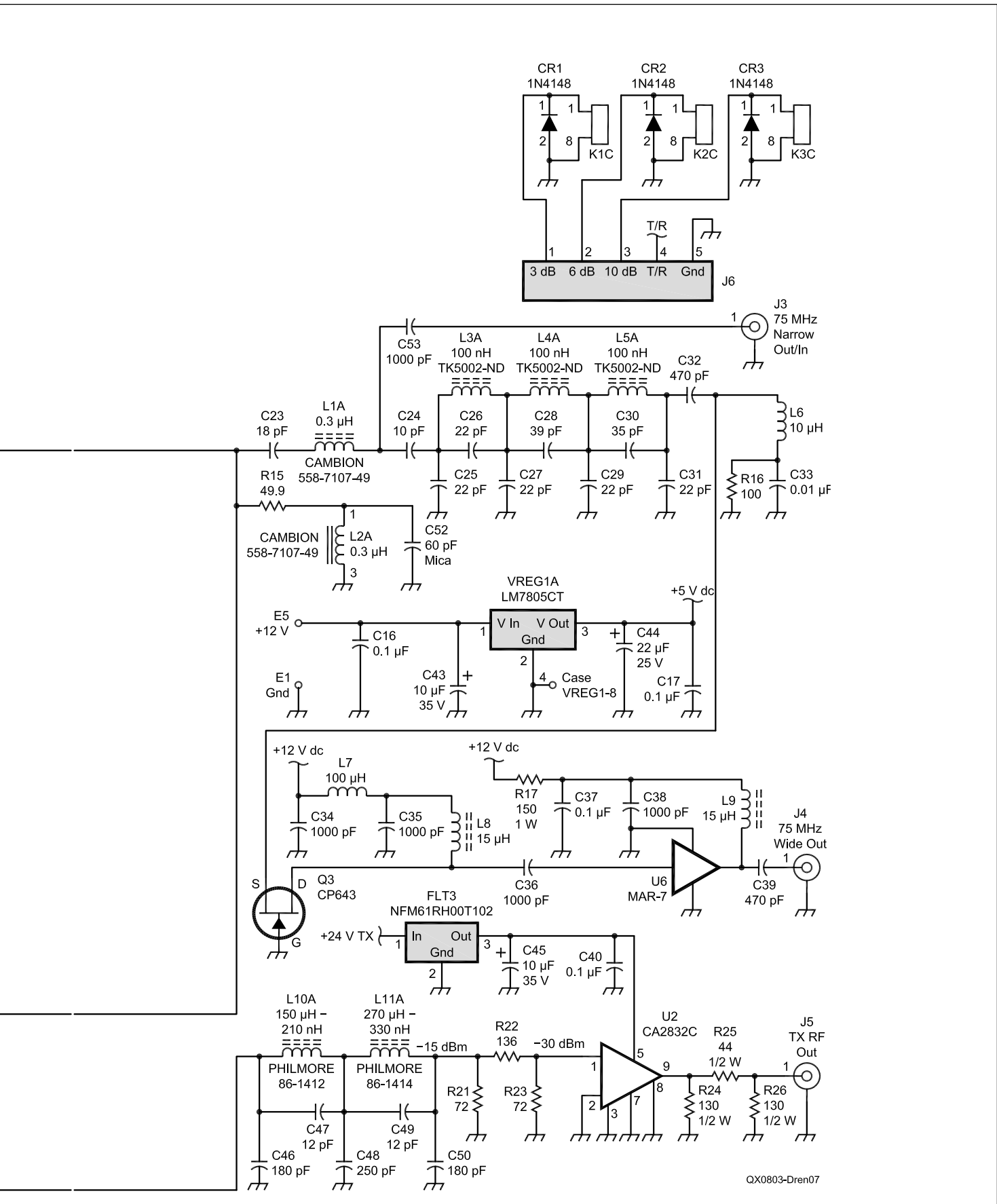


Figure 7 — Schematic diagram of the front end bilateral converter assembly, IF75BC.



automatically switched front end and IF filtering. The radio uses a DDS-Driven PLL synthesizer. Thus, the *Star-10* design resulted in a 75 MHz first IF and a 9 MHz second IF architecture, using a novel bilateral concept, a complex array of old and new technologies, circuits and packaging techniques. After ample system analysis, intense circuit design, multiple brass boarding and testing, PC board layouts were developed and four sets of boards were manufactured, populated and tested again and again before the final implementation. Two transceivers were developed using these boards, a work-in-progress prototype by KG6NK, and the featured *Star-10* model presented here.

The unpopulated double-sided, plated-through PC boards developed specifically for the *Star-10* transceiver are shown in Figure 6A. Some of the completed and tested assemblies are shown in Figure 6B. [To provide easy reference between the parts of this series, we have numbered the Figures consecutively throughout. — Ed.]

I will next discuss the major assemblies

and major design details of the *Star-10* transceiver. For clarity, you should first read Part 1 of this series in order to better understand the functionality of each of the assemblies. Part 1 is available on the ARRL *QEX* Web site at www.arrl.org/qex. You will be constantly directed to the transceiver's block diagram in Figure 2 from Part 1 to better understand where a specific assembly fits. To make the best use of printed space, only major blocks will be discussed in detail. As previously indicated, no circuit layouts, construction plans or software listings are offered in this article series.

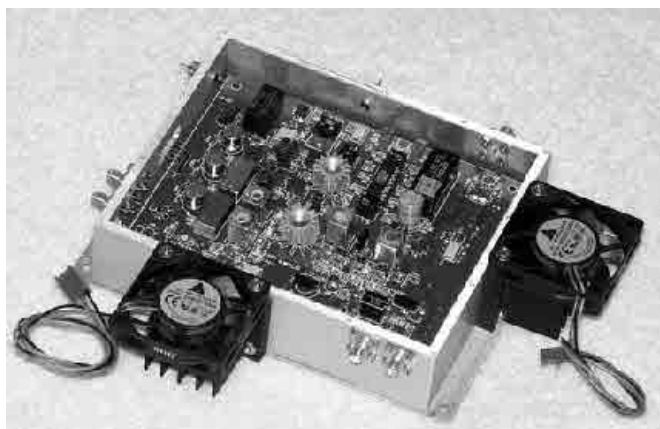
Front End (IF75BC)

As the name implies, this is the first IF (75 MHz) or the bilateral 75 MHz converter. This assembly is a key ingredient of the *Star-10* receiver design because it sets the entire system noise figure and intercept point. IF75BC operates in receive as well as transmit modes.

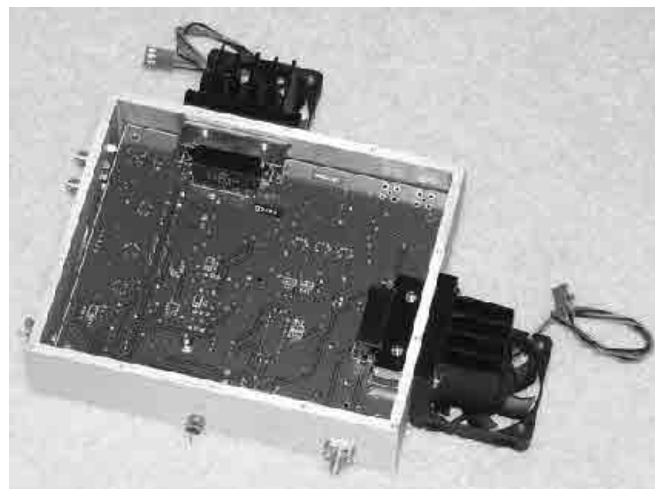
Referring to Figure 2 from Part 1, the

IF75BC assembly provides receiver up conversion for the entire HF range from 1.8 MHz to 30 MHz, to the 75 MHz IF, or down conversion from this IF to the same HF range of 1.8 MHz to 30 MHz in transmit. The IF75BC is preceded by a half-octave band-pass filter bank (composed of eight automatically selectable filters) in receive, the power linear amplifier and a similar half-octave low-pass, high power filter bank (composed of eight automatically selectable equivalent filters) in transmit. To keep intermodulation distortion under control, no PIN switching diodes are used to select filters. All filters in the *Star-10* are switched with either miniature Teledyne RF relays, or high power RF relays. These assemblies will be discussed in more detail later. A schematic diagram of IF 75BC is shown in Figure 7. The actual IF75BC board and assembly implementation are shown in Figure 8.

The 75 MHz first IF choice puts the receiver image away by 150 MHz at any frequency between 1.8 MHz and 30 MHz. This works in direct conjunction with the proper



(A)



(B)

Figure 8 — The IF75BC bilateral front-end converter assembly implementation is shown in Part A. This assembly provides crunch-proof receiver functions and doubles as the transmitter predriver. It uses class A push-pull amplifiers, a push-pull Norton amplifier equipped with very high dynamic range CP-650 FETs, and an H-mode class III mixer using the SD-5000. Two quiet, brushless fans extract the heat out of the CA2832 class A drive amplifiers located under the circuit board. IF75BC assembly dissipates approximately 30 W of dc power (at 24 V dc and 12 V dc) to insure superior dynamic range for the receiver. The unit doubles as a bilateral IF in transmit, providing RF drive signals for the follow-up power linear amplifier. Monolithic CA2832 class A amplifiers are used sparingly throughout the *Star-10* transceiver. Two CA2832 amplifiers are used in the IF75BC as shown in Part B. They are installed on the back of the circuit board. Heat is extracted through the assembly walls using two heat sinks and special brushless quiet (acoustic and electric) fans mounted on the sides of the aluminum assembly, and is further exhausted through the top of the transceiver cover. IF75BC dissipates approximately 30 W dc at 24 V dc and 12 V dc. In the *Star-10* transceiver package, the IF75BC assembly is located on the shelf shown in Part C, along with the IF9TX seen under the shelf. This shelf installs on the main shelf, which also supports the entire half octave filter bank, as can be seen in the photo at the beginning of this article.



(C)

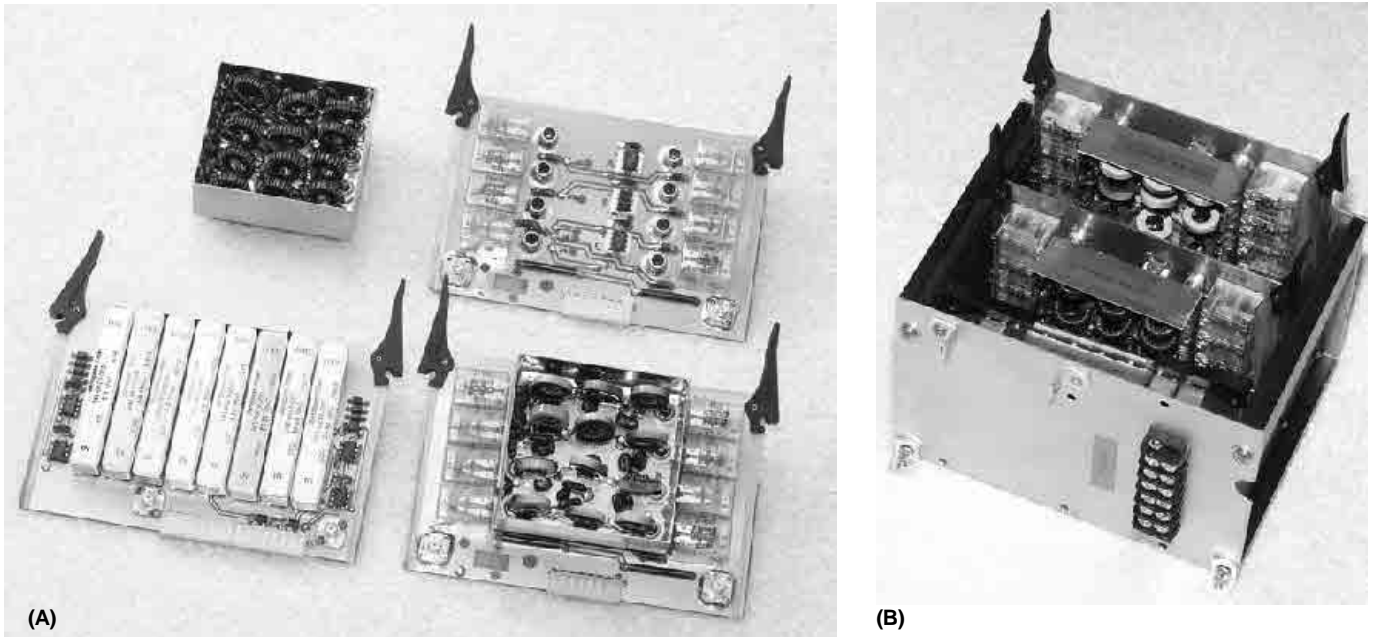


Figure 9 — Part A shows receiver and transmitter half-octave filters banks. Automatically switched half-octave filter banks are shown in Part B, where the motherboard/cage assembly holds the receiver front-end filter boards (eight filters) as well as the transmitter high-power, low-pass filter boards (eight filters). This assembly is located on a shelf shown on the right side of the transceiver, as shown in the lead photo. The DFCB command and control assembly automatically selects the filters.

half-octave filter being selected in the front-end banks. The amount of rejection provided is consequently uniform throughout the coverage due to the proper selection of the half-octave ranges. (See References 1, 2, 3, listed at the end of this article.) A high-pass receiver front end filter, which is sometimes used in general coverage designs, was found unnecessary due to the extremely good shape factor offered by the half-octave band-pass filters. Conversely, the proper half-octave low-pass filter selected in the transmit chain ensures equally good spurious and harmonic rejection throughout the entire frequency range.

Looking at the schematic diagram in Figure 7, the filtered received RF signals from the half-octave band-pass filter bank enter the receiver circuits of the IF75BC board assembly at J2 through the advanced intercept point attenuator (AIPA) and the +10 dB push-pull preamplifier located on this board. This combination allows for the programmable AIPA attenuators (part of the gain control system) to be inserted in the receiver front end if so desired. Because of the dynamic range capability of the *Star-10*, these functions have not been used extensively since good results were obtained with the preamplifier on and no attenuators.

Three front panel programmable attenuation steps are provided by AIPA: 3 dB, 6 dB and 10 dB. Commands for these selections enter the IF75BC through the J6 connector. The 3 dB and 6 dB positions are imple-

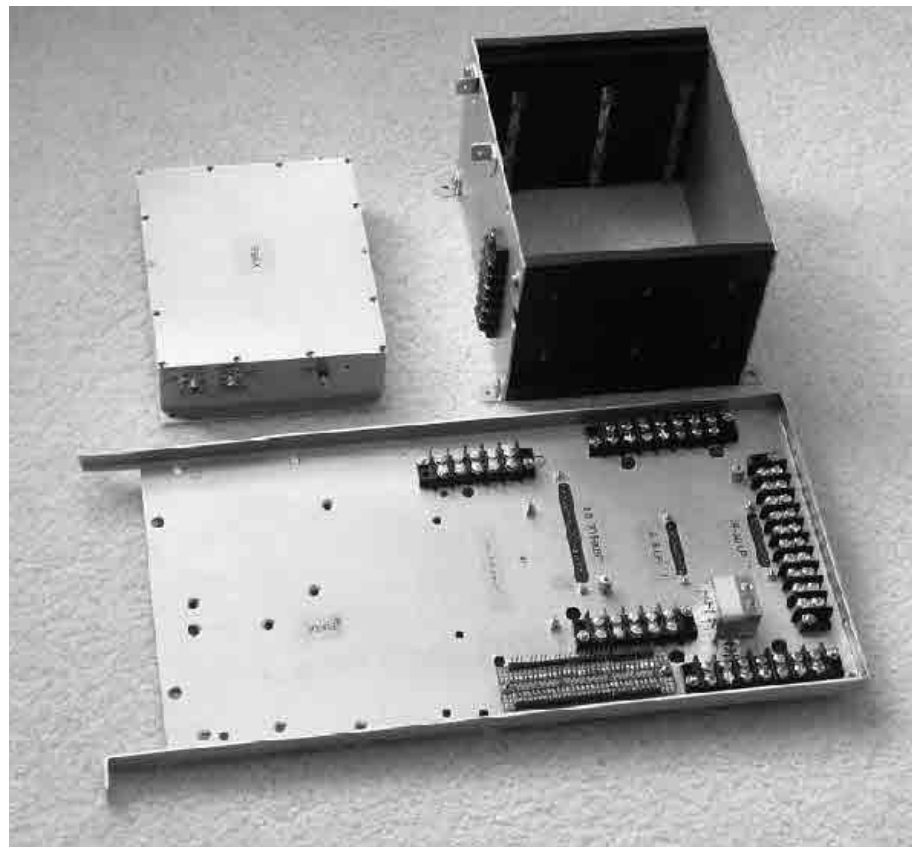


Figure 10 — View of the bottom shelf (motherboard), which holds the automatically switched half-octave filter banks and the motherboard cage (at the top right corner of the photo). Command and control lines have been wired to the connectors visible in the slots in the shelf.

mented by inserting a 3 dB or a 6 dB pad via corresponding relays (AT1, K1 and AT2, K2) in the circuit, while the 10 dB function is implemented through totally bypassing the push-pull amplifier, using K3 as shown. The preamp can always be on because of the dynamic range capability of the *Star-10*. The AIPA functions are remote controlled from the front panel via miniature RF relays located on the IF75BC board. The front panel switch (marked AIPA) that controls these attenuators also controls three LED indicators showing what is selected on the composite front panel display (dial) as shown in the lead photo.

To ensure the high dynamic range for the receiver, IF75BC uses an adaptation of a push-pull Norton amplifier, using very high dynamic range CP-650 FETs. This preamplifier, as well as other IF75BC functions, use 24 V dc in addition to 12 V dc and other voltages. The power consumption of the IF75BC front end board and assembly is around 30 W dc, requiring heat sinks as shown in Figure 8 A, B and C.

The Norton amplifier circuit was initially developed and patented by David Norton and Allen Podell in 1975 (reference 4, 5, 6). This circuit constitutes a novel development in the application of negative feedback techniques to active double-balanced mixers, in which the concept of single-transformer “loss less feedback” is employed to improve both, the intercept point and the noise figure. The Norton design uses transformer coupling to achieve “noiseless negative feedback” – a truly outstanding approach.

Loss less feedback amplifiers have been recognized as an outstanding means of providing high dynamic range, in terms of both linearity and noise figure. In the following years since its invention, various forms of the Norton amplifier have found wide usage in good communications receivers and radio astronomy applications.

A variation on the Norton amplifier was further described by Joe Reisert in *ham radio* magazine (reference 7). The circuit has been further improved by Jacob Makhinson and

was described in detail in references 8, 9, 10, 11, 12.

Looking at Figure 7, the conditioned RF signals from AIPA enter the first mixer U3 which is used in an H-mode (references 6, 7, 8, 9) biasing system. The variable high resolution LO signal from the synthesizer (FRU - FSYNTH) is presented to the mixer via J1 and U1, via a CA2832 class A monolithic amplifier (note: *Star-10* makes ample use of the Motorola CA2832 monolithic amplifiers) operating at 24 V. Thus, the LO level is built up from approximately -9 dBm to about +27 dBm. Mixer biasing is further provided through R13, R14 and U4. The H-mode mixer used is typical of the design described in the above references. However, most of these designs have been used in low IF configurations (e.g. 9 MHz) and with limited RF/LO bandwidths. They are usually fed by out of phase digital drivers which maintain tight LO jitter and phase coherence over relatively narrow frequency ranges. However, using such designs over very broad

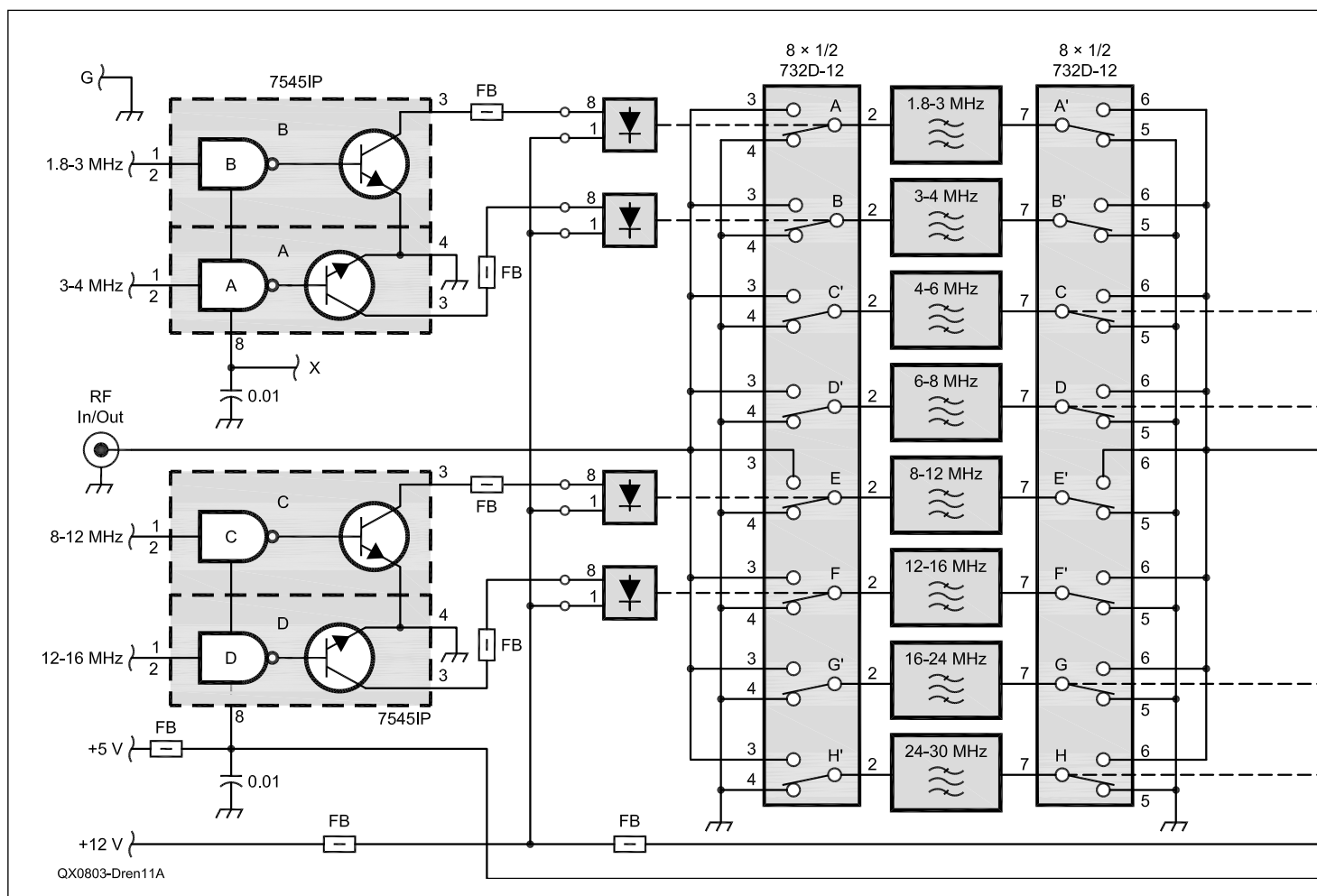


Figure 11A — The schematic diagram for the receiver band-pass filter bank.

frequency ranges such as the four octaves used in the *Star-10* would require sub - pico second rise time phase matching between the digital drivers. Because of the *Star-10* broadband nature, it was found impractical to provide LO drive via digital means. After long analysis and experimentation, it was found that using a transformer combination can provide the required phase balance over the entire frequency coverage with minor phase mismatching consequences. Following intense testing, this solution was found to be a practical compromise.

Making the preamplifier and the H-mode mixer work in the actual IF75BC board required ample circuit layout planning, where connecting paths in the double sided plated through PC board was implemented with short and balanced paths, which were trimmed equally to promote amplifier stability. Additional ferrite beads were used together with short leads to prevent oscillation. The negative biasing supply for the SD-5000 mixer was achieved using a dc-to-

dc converter at U4 as shown. Considerable care was taken in the entire board design to ensure proper ground distribution and avoid resonant features.

The transmit chain on IF75BC, when activated via the T/R relay K4, outputs RF signals to the power linear amplifier through the 30 MHz low-pass filter made of L10, L11, C46 through C50, and another class A - CA2832 monolithic amplifier, U2. Driver circuits for the RF relays on IF75BC as well as throughout the entire transceiver use high current open collector digital line drivers 75451 ICs (U5 on this board). The RF output at J5 goes further to the high power linear amplifier, and to the automatically switched half-octave low-pass filter banks, through the RF power transmitter gain control (TGC) circuits and further through the main T/R switch, to the antenna. The T/R relay on IF75BC which is facilitated through the on board K4, also provides proper switched 24 V dc to the bilateral amplifier (BILAT AMP) assembly located further down in the

75 MHz IF chain as shown in Figure 2, Part 1 of this article series.

There are two 75 MHz IF receiver outputs on the IF75BC; the first is diplexed via L2, C52, C53 and is further output at J3 to be input to the quartz crystal roofing filter assembly, FL75. This signal serves in receive as well as in transmit as the narrow 75 MHz IF output/input. The other output at J4 serves as the 75 MHz wide IF (500 kHz) intended for spectrum analysis and noise blanker functions to be achieved further in IF9NB. This wide band signal follows the path from C24 through the 500 kHz band pass filter made of L3 through L5 and C25 through C32 and further through Q3 and U6. This completes the IF75BC assembly description.

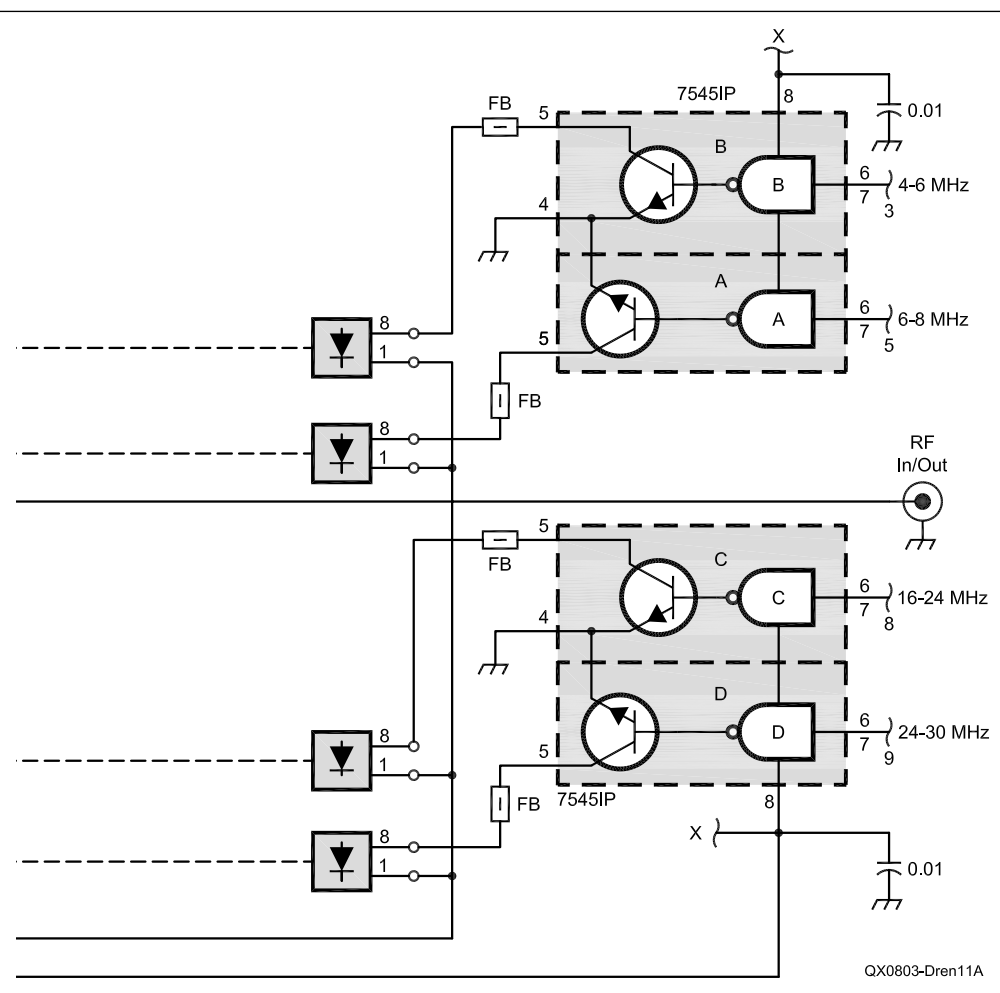
Receiver and Transmitter Half-Octave Filter Banks

Looking at the *Star-10* transceiver block diagram from Figure 2 of Part 1, the IF75BC assembly is preceded by the half-octave band-pass and low-pass filters banks as shown in Figure 9. The actual location of this assembly in the *Star-10* transceiver package can be seen on the right side of the leading photo at the beginning of this Part.

The design of these filters and their functionality in a general coverage HF transceiver or receiver has been previously described in great detail in references 1, 2 and 3. The *Star-10* transceiver uses this design in a new mechanical implementation specific to this transceiver package.

There are eight automatically selectable band-pass receiver filters (bottom left board of Figure 9 A) and eight high-power low-pass similar filters (the remaining assemblies shown in Figure 9 A). The filter banks are plug in shielded assemblies as shown. They insert into the PC boards that contain the control circuits utilizing 75451 line drivers to switch corresponding RF relays, which in turn use commands from the DFCB assembly microprocessor to select the proper receive and transmit combination. The boards equipped with the plug in filter banks (as shown) are in turn, plug-in assemblies themselves. They insert into a machined motherboard cage assembly as shown in Figure 9 B. Command signals coming from DFCB board and RF connectors are provided at the bottom of the assembly which is supported by the bottom shelf of the *Star-10* system as shown in Figure 10.

The schematic diagram for the receiver's band-pass filters - bank is shown in Figure 11 A. The schematic diagram for the high power low-pass filters banks (two assemblies) is shown in Figure 11 B. There are eight band-pass filters in the receiver assembly and four low-pass filters in each of the two low-pass assemblies, for a total of eight equivalent



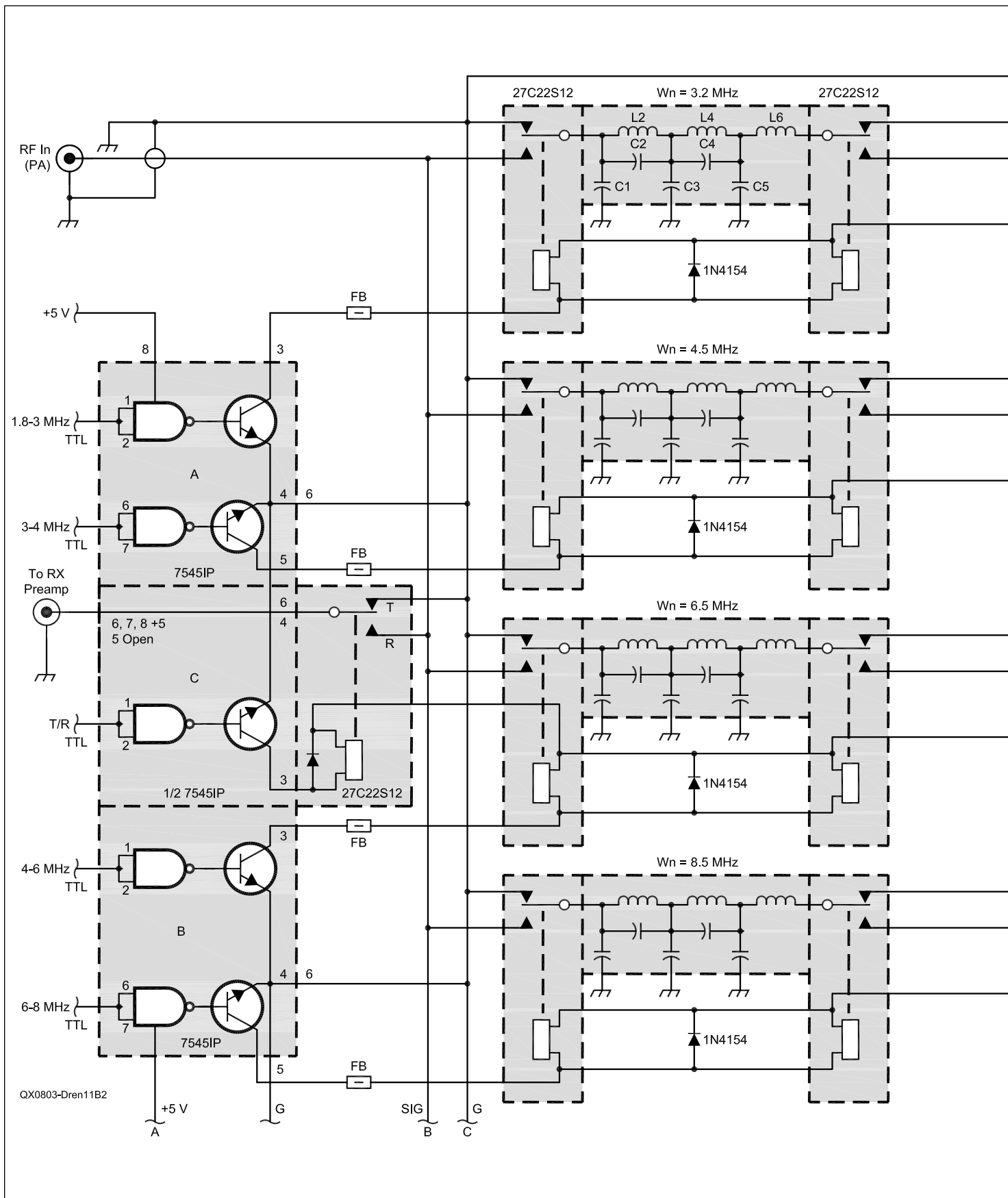
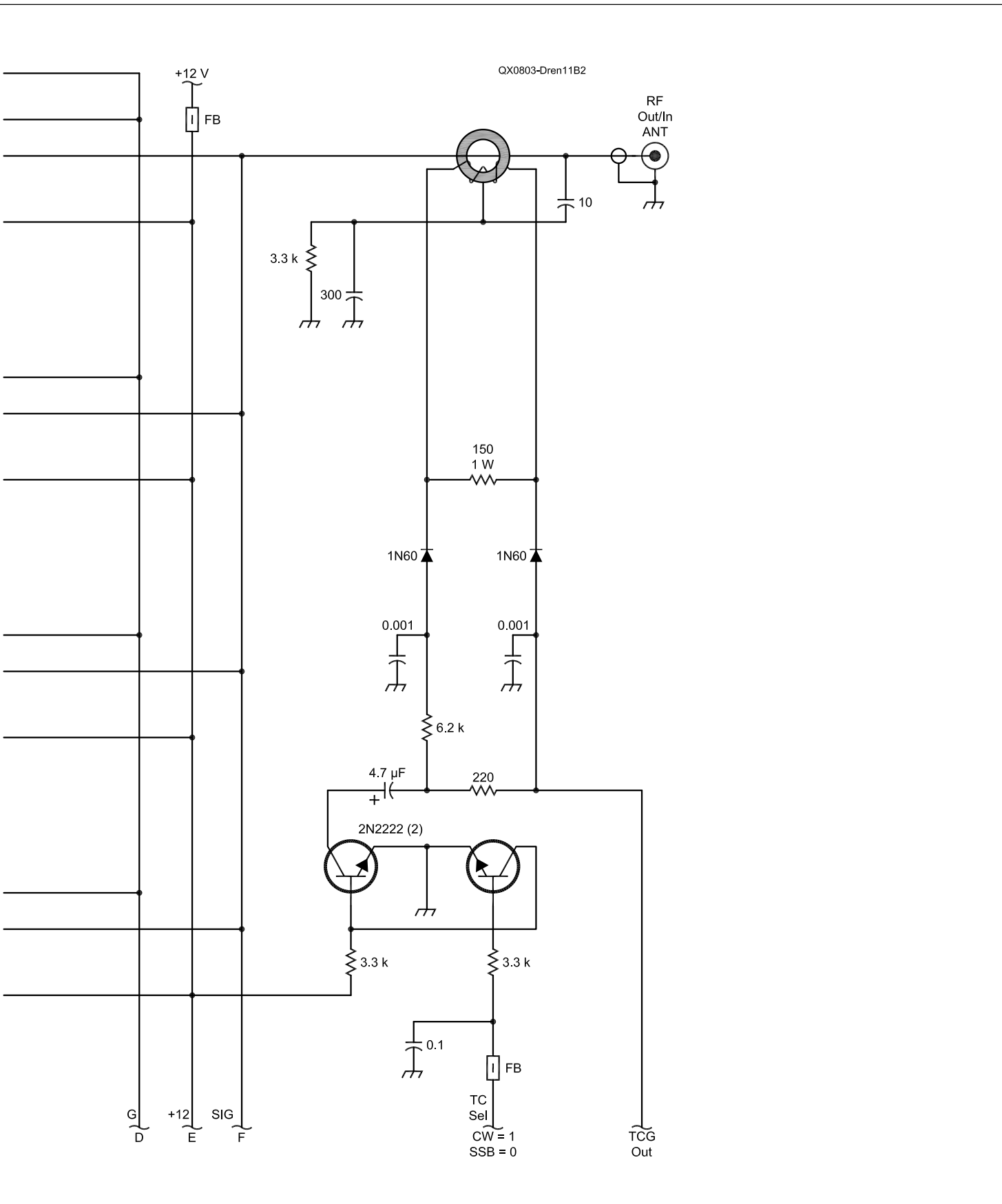


Figure 11B — The schematic diagram for the high-power, low-pass filter banks.



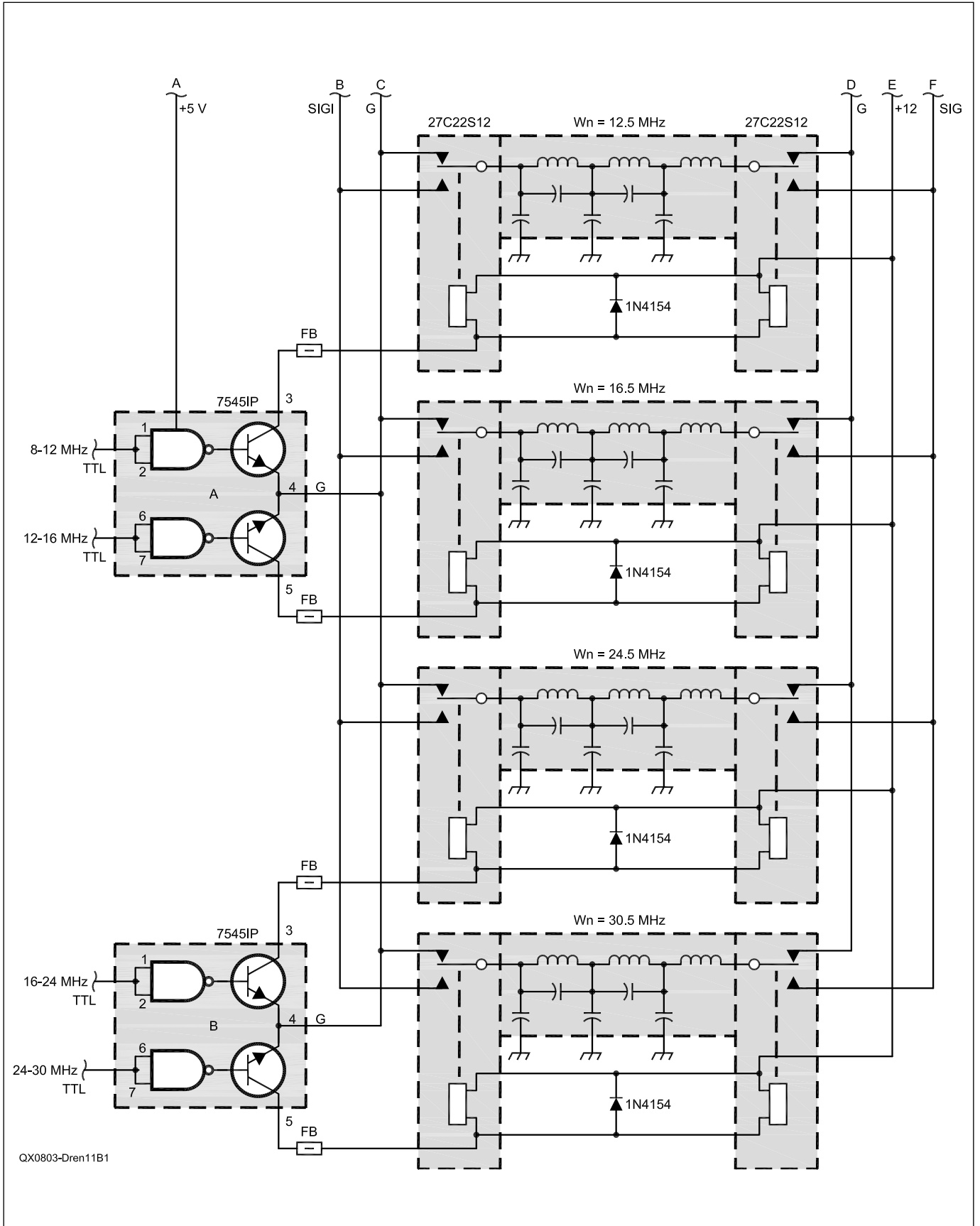
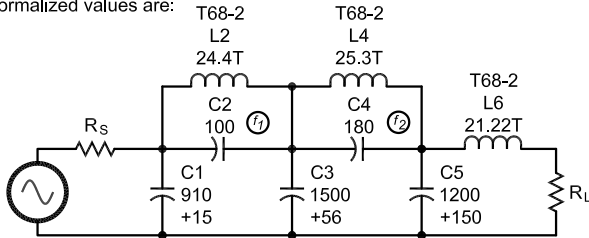


Figure 11B continued

#1

$f_c = 3.2$ MHz Band = 1.8 – 3 MHz
 Reject 6 MHz by 60 dB
 f_c : Reject = 1.875:1

Use A C0615C $\theta = 35^\circ$ Filter
 Minimum Attenuation At 6 MHz = 67.8 dB
 Normalized values are:



$R_S = 1$	$R_L = 1$
$C_1 = 0.9316$	$C_2 = 0.1082$
$L_2 = 1.368$	$C_3 = 1.564$
$C_4 = 0.1880$	$L_4 = 0.1466$
$C_5 = 1.371$	$L_6 = 1.033$

$f_1 = 2.5989$	$f_2 = 1.9051$
----------------	----------------

the denormalized values are:

$R_S = 50$	$R_L = 50$
$C_1 = 926.7^* \text{ pF } (910 + 15)^{**}$	$C_2 = 107.6 \text{ pF } (100)$
$L_2 = 3.40 \text{ }\mu\text{H}$	$C_3 = 1556 \text{ pF } (1500 + 56)$
$C_4 = 187 \text{ pF } (180)$	$L_4 = 3.65 \text{ }\mu\text{H}$
$C_5 = 13.64 \text{ pF } (1200 + 150)$	$L_6 = 2.568 \text{ }\mu\text{H}$

$f_1 = 8.316$ MHz	$f_2 = 6.0963$ MHz
-------------------	--------------------

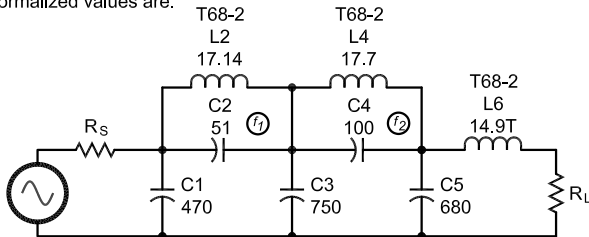
tune L_2, C_2 for an attenuation peak at f_1
 tune L_4, C_4 for an attenuation peak at f_2

* Design value
 ** Actual value used

#3

$f_c = 6.5$ MHz Band = 4 – 6 MHz
 Reject 12 MHz
 f_c : Reject = 1.846:1

Use A C0615C $\theta = 35^\circ$ Filter
 Minimum Attenuation At 12 MHz = 67.8 dB
 Normalized values are:



$R_S = 1$	$R_L = 1$
$C_1 = 0.9316$	$C_2 = 0.1082$
$L_2 = 1.368$	$C_3 = 1.564$
$C_4 = 0.1880$	$L_4 = .1.466$
$C_5 = 1.371$	$L_6 = 1.033$

$f_1 = 2.59897$	$f_2 = 1.9051$
-----------------	----------------

the denormalized values are:

$R_S = 50$	$R_L = 50$
$C_1 = 456.2 \text{ pF } (470)$	$C_2 = 53 \text{ pF } (51)$
$L_2 = 1.675 \text{ }\mu\text{H}$	$C_3 = 766 \text{ pF } (750)$
$C_4 = 92 \text{ pF } (100)$	$L_4 = 1.79 \text{ }\mu\text{H}$
$C_5 = 671.4 \text{ pF } (680)$	$L_6 = 1.265 \text{ }\mu\text{H}$

$f_1 = 16.893$ MHz	$f_2 = 12.383$ MHz
--------------------	--------------------

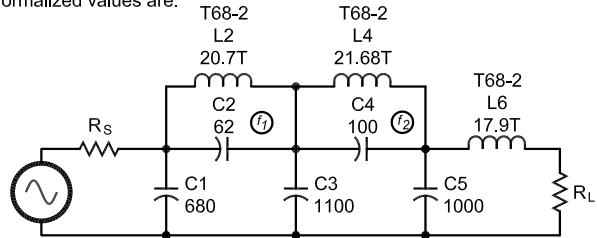
tune L_2, C_2 for an attenuation peak at f_1
 tune L_4, C_4 for an attenuation peak at f_2

#2

QX0803-Dren11C

$f_c = 4.5$ MHz Band = 3 – 4 MHz
 Reject 9 MHz
 f_c : Reject ratio = 2:1

Use A C0615C $\theta = 32^\circ$ Filter
 Minimum Attenuation At 9 MHz = 72.8 dB
 Normalized values are:



$R_S = 1$	$R_L = 1$
$C_1 = 0.9492$	$C_2 = 0.08912$
$L_2 = 1.393$	$C_3 = 1.601$
$C_4 = 0.1540$	$L_4 = 1.518$
$C_5 = 1.395$	$L_6 = 1.034$

$f_1 = 2.8385$	$f_2 = 2.06813$
----------------	-----------------

the denormalized values are:

$R_S = 50$	$R_L = 50$
$C_1 = 671.4 \text{ pF } (680)$	$C_2 = 63 \text{ pF } (62)$
$L_2 = 2.46 \text{ }\mu\text{H}$	$C_3 = 1132.4 \text{ pF } (1100)$
$C_4 = 108.9 \text{ pF } (100)$	$L_4 = 2.68 \text{ }\mu\text{H}$
$C_5 = 986.7 \text{ pF } (1000)$	$L_6 = 1.83 \text{ }\mu\text{H}$

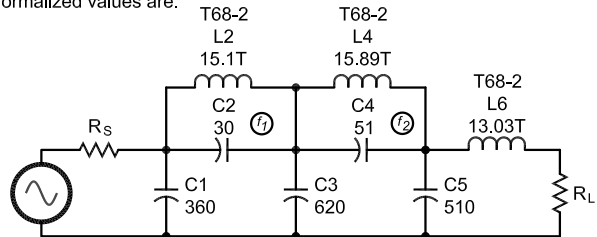
$f_1 = 12.773$ MHz	$f_2 = 9.3066$ MHz
--------------------	--------------------

tune L_2, C_2 for an attenuation peak at f_1
 tune L_4, C_4 for an attenuation peak at f_2

#4

$f_c = 8.5$ MHz Band = 6 – 8 MHz
 Reject 18 MHz
 f_c : Reject = 2.11:1

Use A C0615C $\theta = 31^\circ$ Filter
 Minimum Attenuation At 18 MHz = 74.5 dB
 Normalized values are:



$R_S = 1$	$R_L = 1$
$C_1 = 0.9547$	$C_2 = 0.08325$
$L_2 = 1.400$	$C_3 = 1.612$
$C_4 = 0.1436$	$L_4 = 1.535$
$C_5 = 1.402$	$L_6 = 1.034$

$f_1 = 2.9287$	$f_2 = 2.1298$
----------------	----------------

the denormalized values are:

$R_S = 50$	$R_L = 50$
$C_1 = 357.5 \text{ pF } (360)$	$C_2 = 31.2 \text{ pF } (30)$
$L_2 = 1.31 \text{ }\mu\text{H}$	$C_3 = 603.7 \text{ pF } (620)$
$C_4 = 53.8 \text{ pF } (50)$	$L_4 = 1.44 \text{ }\mu\text{H}$
$C_5 = 525 \text{ pF } (510)$	$L_6 = 0.968 \text{ }\mu\text{H}$

$f_1 = 24.894$ MHz	$f_2 = 18.1033$ MHz
--------------------	---------------------

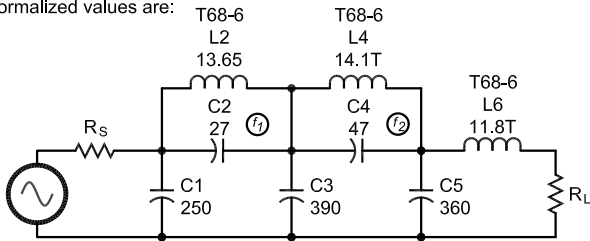
tune L_2, C_2 for an attenuation peak at f_1
 tune L_4, C_4 for an attenuation peak at f_2

Figure 11C — Design values for the low-pass filter banks. The band-pass design is directly derived from the low-pass design.

#5

$f_c = 12.5$ MHz Band = 8 – 12 MHz
Reject 24 MHz
 f_c : Reject = 1.92:1

Use A C0615C $\theta = 34^\circ$ Filter
Minimum Attenuation At 24 MHz = 69.4 dB
Normalized values are:



$R_S = 1$	$R_L = 1$
$C_1 = 0.9377$	$C_2 = 0.101$
$L_2 = 1.376$	$C_3 = 1.577$
$C_4 = 0.1761$	$L_4 = 1.484$
$C_5 = 1.379$	$L_6 = 1.034$
$f_1 = 2.6741$	$f_2 = 1.9561$

the denormalized values are:

$R_S = 50$	$R_L = 50$
$C_1 = 238.8$ pF (250)	$C_2 = 25.9$ pF (27)
$L_2 = 0.876$ μ H	$C_3 = 401.6$ pF (390)
$C_4 = 44.8$ pF (47)	$L_4 = 0.945$ μ H
$C_5 = 351.1$ pF (360)	$L_6 = 0.658$ μ H
$f_1 = 33.426$ MHz	$f_2 = 24.451$ MHz

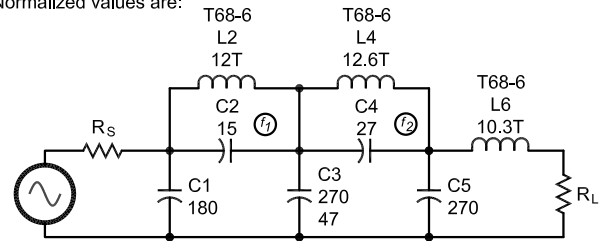
tune L_2, C_2 for an attenuation peak at f_1
tune L_4, C_4 for an attenuation peak at f_2

#6

QX0803-Dren11C

$f_c = 16.5$ MHz Band = 12 – 16 MHz
Reject 36 MHz
 f_c : Reject ratio = 2.18:1

Use A C0615C $\theta = 30^\circ$ Filter
Minimum Attenuation At 36 MHz = 76.3 dB
Normalized values are:



$R_S = 1$	$R_L = 1$
$C_1 = 0.96$	$C_2 = 0.0776$
$L_2 = 1.408$	$C_3 = 1.623$
$C_4 = 0.1337$	$L_4 = 1.551$
$C_5 = 1.410$	$L_6 = 1.034$
$f_1 = 3.02499$	$f_2 = 2.19586$

the denormalized values are:

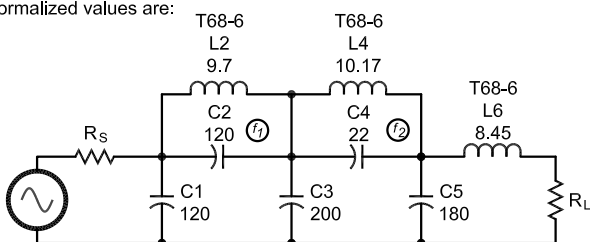
$R_S = 50$	$R_L = 50$
$C_1 = 185.19$ pF (180)	$C_2 = 14.9$ pF (15)
$L_2 = 0.679$ μ H	$C_3 = 313.1$ pF (270 + 47)
$C_4 = 25.8$ pF (27)	$L_4 = 0.748$ μ H
$C_5 = 272$ pF (270)	$L_6 = 0.4987$ μ H
$f_1 = 49.9123$ MHz	$f_2 = 36.2317$ MHz

tune L_2, C_2 for an attenuation peak at f_1
tune L_4, C_4 for an attenuation peak at f_2

#7

$f_c = 24.5$ MHz Band = 16 – 24 MHz
Reject 48 MHz
 f_c : Reject = 1.96:1

Use A C0615C $\theta = 33^\circ$ Filter
Minimum Attenuation At 48 MHz = 71.1 dB
Normalized values are:



$R_S = 1$	$R_L = 1$
$C_1 = 0.9436$	$C_2 = 0.09523$
$L_2 = 1.385$	$C_3 = 1.589$
$C_4 = 0.1648$	$L_4 = 1.501$
$C_5 = 1.387$	$L_6 = 1.034$
$f_1 = 2.75377$	$f_2 = 2.0103$

the denormalized values are:

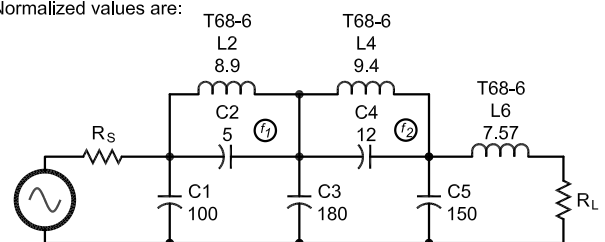
$R_S = 50$	$R_L = 50$
$C_1 = 122.6$ pF (120)	$C_2 = 12.37$ pF (12)
$L_2 = 0.449$ μ H	$C_3 = 206.4$ pF (200)
$C_4 = 21.4$ pF (22)	$L_4 = 0.487$ μ H
$C_5 = 180.2$ pF (180)	$L_6 = 0.336$ μ H
$f_1 = 67.467$ MHz	$f_2 = 49.292$ MHz

tune L_2, C_2 for an attenuation peak at f_1
tune L_4, C_4 for an attenuation peak at f_2

#8

$f_c = 30.5$ MHz Band = 24 – 30 MHz
Reject 72 MHz
 f_c : Reject = 2.36:1

Use A C0615C $\theta = 27^\circ$ Filter
Minimum Attenuation At 72 MHz = 82 dB
Normalized values are:



$R_S = 1$	$R_L = 1$
$C_1 = 0.9747$	$C_2 = 0.06212$
$L_2 = 1.429$	$C_3 = 1.654$
$C_4 = 0.1066$	$L_4 = 1.595$
$C_5 = 1.430$	$L_6 = 1.035$
$f_1 = 3.3568$	$f_2 = 2.4244$

the denormalized values are:

$R_S = 50$	$R_L = 50$
$C_1 = 101.7$ pF (100)	$C_2 = 6.5$ pF (5)
$L_2 = 0.373$ μ H	$C_3 = 172.6$ pF (180)
$C_4 = 11.1$ pF (12)	$L_4 = 0.416$ μ H
$C_5 = 149.2$ pF (150)	$L_6 = 0.270$ μ H
$f_1 = 102.38$ MHz	$f_2 = 73.944$ MHz

tune L_2, C_2 for an attenuation peak at f_1
tune L_4, C_4 for an attenuation peak at f_2

half-octave filters (1.8 to 3, 3 to 4, 4 to 6, 6 to 8, 8 to 12, 12 to 16, 16 to 24, and 24 to 30 MHz). The chosen electrical design for all filters is the Cauer (elliptical) approach. This type of filter has an in-band characteristic similar to that of a Chebyshev filter; it also has a more abrupt transition band characteristic than the monotonically increasing attenuation of the Chebyshev approach. This design was chosen because of the superior rejection and the relatively easier execution and tuning procedures required. Shown in Figure 11 C are the electrical schematics and design values for all the low-pass filter banks. The band-pass design was directly derived from the low-pass implementation. For a much more in depth discussion on the actual design of these filters, you are directed to my article series on references 1 and 2, which is available on my Web site listed at the end of this article.

75 MHz Bilateral IF

The roofing filter assemblies (FL75), the 75 MHz Bilateral Amplifier (BILAT AMP), and the 75 MHz to 9 MHz Bilateral Converter (IF9BC) will be described together because they constitute the 75 MHz bilateral IF. Looking at the *Star-10* transceiver block diagram from Figure 2 of Part 1, these three assemblies follow the IF75BC providing further signal processing through the 75 MHz bilateral IF (BILAT AMP), and selective signal conditioning through the FL75 roofing filter assembly.

A second conversion to the 9 MHz IF stage (used in receive and transmit) is facilitated through the IF9BC assembly. Physically, the above assemblies are partly located on the left side of the transceiver under the shelf shown in Figure 8 C. The BILAT AMP assembly is located in the center area of the bottom side of the main shelf (for a view of the shelf, see Figure 10) as shown in Figure 12 (the smaller assembly in the center equipped with a fan).

The BILAT AMP and the FL75 roofing filter assemblies are shown in Figure 13. The schematic diagram for the BILAT AMP assembly is shown in Figure 14. The performance characteristics of the bilateral amplifier are shown in Table 1.

Looking at Figure 14, the 75 MHz BILAT AMP uses two back-to-back CA2832 monolithic amplifiers which were discussed earlier. As can be seen, only one of the amplifiers is on at the time, the default being the receiver chain at the top of Figure 14. Power is applied selectively to the respective circuit via the T/R function through the switched 24 V dc lines from IF75BC. In transmit, the power is switched on to the bottom circuit and the top circuit remains dormant for the duration of transmit. Natural isolation between the active

circuit and the dormant circuit is provided via the inherent isolation (>20 dB) allowed by the passive splitter/combiner arrangement shown.

One of the 75 MHz IF outputs from IF75BC enters the first section (A) of the roofing filter FL75 (see Figure 2 in Part 1) as shown. Again, all RF interconnects between assemblies in the *Star-10* are 50 ohms, making it easy to use miniature coaxial cables

equipped with SMA connectors. The output of the first FL75 filter section is then input to the BILAT AMP at J1, where it enters the first splitter/combiner PSC2-1 (A1) at pin 1 as shown. The receiver path continues at pin 5 of the PSC2-1 and is output to the BIPA circuit located on the IF9BC assembly. The BIPA circuit is a 30 dB –programmable – from the front panel – PIN diode attenuator circuit that will be discussed in more detail later. The return path from the BIPA circuit is input back into the receiver's 75 MHz IF and is further amplified in the BILAT AMP assembly by the CA2832 amplifier at U1, to be recombined with the isolated transmitter path through another PSC2-1 (A2). The output of the BILAT AMP assembly is then output at J2 and is further input to the second section (B) of the FL75 roofing filter assembly. This functionality is true in receive as well as transmit providing true bilateral functionality for the entire 75 MHz IF. It should be noted that the 75 MHz filter assembly has been split in two sections and is intentionally isolated by the amplifier in order to cope with the relatively high IF levels seen at these points in the circuits (see system analysis

Table 1

Bilateral Amplifier (BILAT AMP) Specifications

Mode of operation: Bidirectional OR function (one way active at any given time)
 Operating frequency: 75 MHz
 Gain (max): +36 dB
 NF: 5 dB
 1 dB compression point (CP1): +35 dBm
 IP3: +50 dBm
 RF in (max): +5 dBm
 RF out (max) +32 dBm
 Vcc: +24 V dc
 Ic: 450 mA (one-way active)
 Amplification Class: AA

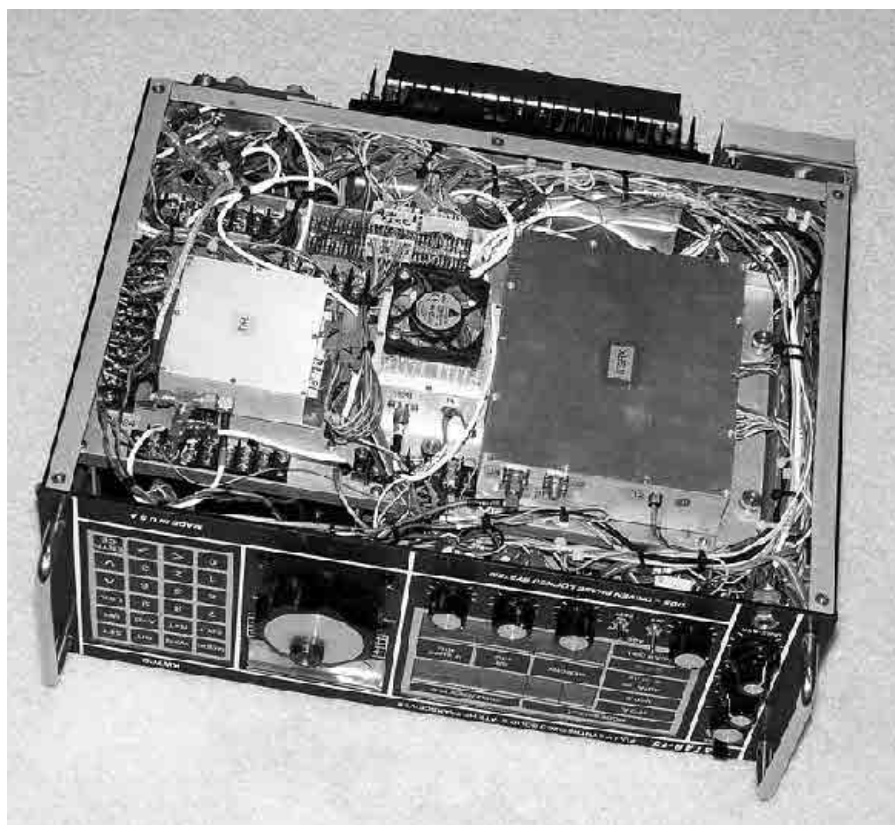


Figure 12 — Bottom view of the *Star-10* transceiver, with the back of the main shelf exposed. Shown in the center is the 75 MHz bilateral amplifier (BILAT AMP) using two back-to-back monolithic CA2832 class A amplifiers (one used in receive and the other in transmit), isolated from each other via splitters/combiners. These high dynamic range amplifiers are capable of 35 dB gain, a 5 dB noise figure and a +50 dBm IP3. Cooling is achieved via another brushless fan extracting the heat through the bottom panel.

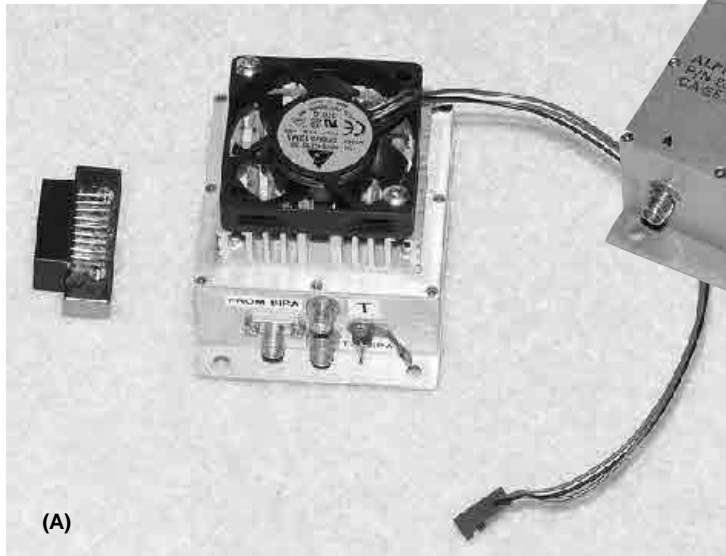


Figure 13 — The physical implementation of the BILAT AMP assembly is shown in Part A. Two back-to-back class A CA2832 amplifiers (one shown at left for size) are packaged together in this assembly. They are passively isolated from each other via a splitter/combiner assembly which provides 20 dB of natural isolation between receive and transmit functions. Switched 24 V dc is selectively provided to the amplifiers depending on the receive or transmit function selected by the T/R assembly via the IF75BC T/R relay. BiPA attenuation is inserted as shown in Figure 2 of Part 1 of the article. The schematic diagram of the BILAT AMP assembly is shown in Figure 14. Part B shows the roofing filter FL75 assembly. It contains two four-pole filters (eight poles) with a 3 dB bandwidth of approximately 10 kHz. These high intercept filters have been especially designed and manufactured for the *Star-10* by Temex Inc. Initially, a fifth overtone filter set was designed and tested. The initial concern was about the maximum amount of RF drive level these filters will see at this point in the system (approximately +5 dBm), at what duty cycle, and how their aging (calculated at 32 years) will suffer under these conditions, their insertion loss and their group delay properties. A second set was designed and manufactured by Alpha Components Inc., using a fundamental Gaussian design, which can provide better resistance to high drive levels.

from part 1 of the article). Thus, the first roofing filter is different in design than the second roofing filter.

The roofing filters assembly contains two four-pole filters (eight poles composite) with a 3 dB bandwidth of approximately 10 kHz. These high intercept filters have been especially designed and manufactured for the *Star-10* by Temex Inc. Initially, a fifth over tone filter set was designed and tested. The initial concern was about the maximum amount of RF drive level these filters will see at this point in the system (approximately +5 dBm maximum), at what duty cycle, and how their aging (calculated at 32 years) will suffer under these conditions, their insertion loss and their group delay properties. A second set was designed and manufactured by Alpha Components Inc., using a fundamental Gaussian design which can provide better resistance to high drive levels. Although a narrower bandwidth was desirable, at 75 MHz, a 10 kHz bandwidth was the best that could be done considering all other design criteria.

It should be noted that despite popular belief, narrowing bandwidth in roofing filters for up-convert transceivers, although very desirable, it is not by far as important as creating crunch proof front ends such as done in IF75BC. Roofing filters of 3 to 4 kHz bandwidth at 75 MHz that withstand high RF levels are hard to realize and manufacture consistently. High dynamic range 75 MHz roofing filters with a 3 dB bandwidth of 10 kHz and high intercept points are, however, possible. Reducing the first IF frequency to a lower frequency, can ease the design of these filters at the cost of more demanding front end filtering to cope with image and spurious rejection. Going to low first IFs of, say, 9 MHz

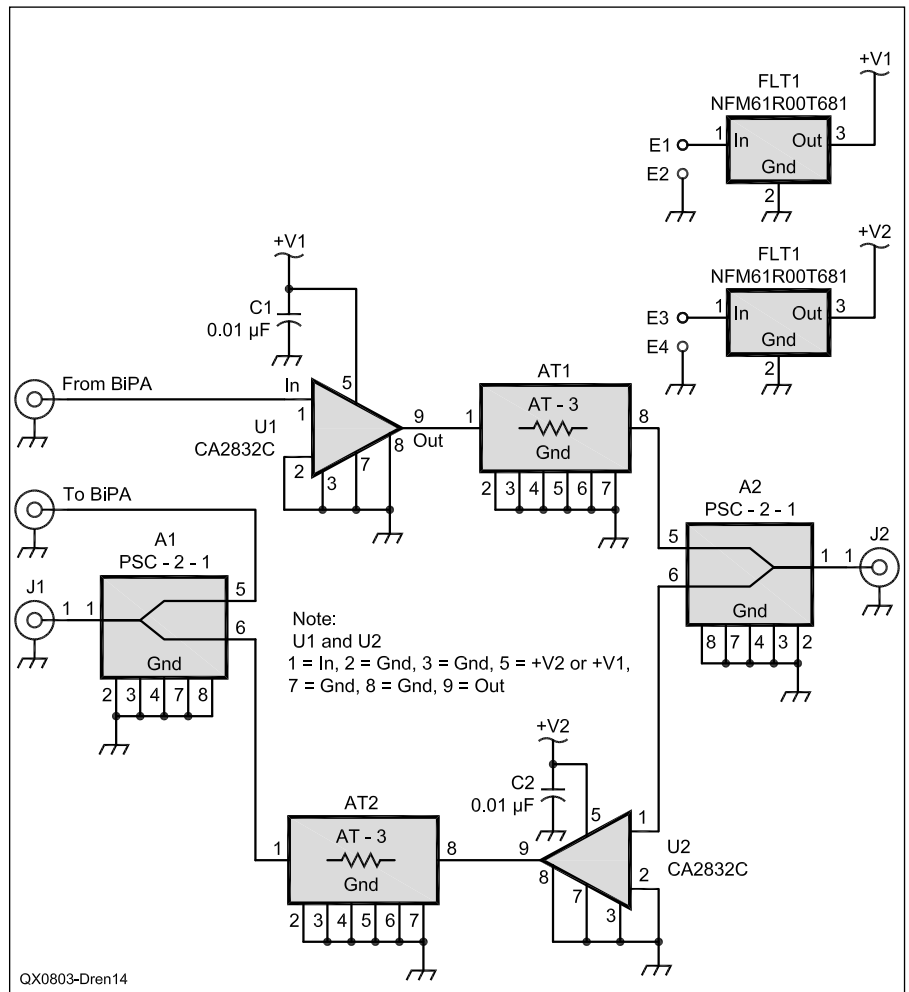


Figure 14 — This is the schematic diagram for the BILAT AMP assembly. This circuit provides high dynamic range selective amplification - bilateral functionality with automatic passive isolation (without using relays) between the active section and the off section, depending on whether the receive or transmit function is selected. The customary 3 dB impedance matching pads at the output of the amplifiers were later eliminated in the interest of gain and noise figure.

can allow for narrow roofing filters of 2 to 3 kHz (compatible with the ultimate bandwidth required of SSB signals); however, the entire idea of a high performance general continuous coverage transceiver can be thrown out the window, resulting in a compromise — channelized band-only, coverage.

Returning to the BILAT AMP assembly, the AT1 and AT2 pads seen in the BILAT AMP have been provided for amplifier matching. However, after long experimentation, they have been removed from the circuit in the interest of gain and noise figure improvements.

The output of the second section of FL75 is input to the IF9BC assembly along with the wide (500 kHz) 75 MHz IF signal intended for spectrum analysis (see Figure 2 in Part 1). The IF9BC assembly is the second bilateral converter which provides 9 MHz receiver IF signals to IF9RX and accepts 9 MHz transmitter IF signals from IF9TX. The wide band 9 MHz IF is further input to IF9NB, which in turn, provides oscilloscope, spectrum analyzer and noise blanker functions for the transceiver. Again, this is shown in the block diagram in Figure 2 of Part 1.

Looking at Figure 15, the two 75 MHz paths are input at J1 (wide) and J3 (narrow) to be converted to 9 MHz IFs separately via two independent high level mixers paths (Mix 1 and 2) in IF9BC using class II, TAK-3H mixers as shown.

Figure 15 shows the 84 MHz fixed frequency LO coming from the MRU (master reference unit) / PLXO, which is filtered and amplified by a class A amplifier and enters the IF9BC at J2. The signal is split by the A1 splitter (another PSC2-1) and is presented equally to the two TAK-3H mixers with a level of +17 dBm. The top mixer IF output is filtered through a wide bandwidth band-pass filter, and is finally amplified by AR1 (a MAR-8 device) to be output to the IF9NB assembly at J4. The narrow-band 9 MHz IF (with a bandwidth equal to the composite bandwidth of the two 75 MHz roofing filters at FL75) coming from MIX2 (the other TAK-3H mixer) is conditioned via the diplexer circuit of L10, C16, R5, L9 and C15, and is split by A2. The first half is output via a 1.5 dB pad through J5 to go to the narrow band receiver IF, IF9RX. The other half goes through another 1.5 dB pad and J6 to be connected with the narrow band transmitter IF when activated. I will explain more about this in Part 3.

I will now discuss the previously mentioned BIPA function using a Pi configuration PIN attenuator provided on IF9BC. This attenuator provides adjustable front panel and first IF/RF gain and noise blanking gating, coming from the IF9NB. It could also be used as a second AGC loop (not implemented yet).

In Figure 15, the 75 MHz input coming from the BILAT AMP is at J7. The attenuated output resulting from the BIPA circuit is available at J8. Control is provided via E2A and B. The BIPA attenuator function is packaged on a 24 pin PC board layout which follows a 24 pin IC module physical design approach. A picture of the BIPA assembly is shown in Figure 16. The schematic diagram of the assembly is shown in Figure 17.

Looking at Figure 17, BIPA uses four voltage controlled 5082-3080 PIN diodes in a Pi configuration. The design was inspired by Raymond Waugh's article in *Microwave Journal* (reference 13). This design approach provides very good impedance matching and flat attenuation over a wide frequency band and can be used in many applications. In fact, I used this circuit in the 9 MHz transmit IF as a CW drive controller as we will discuss later in Part 3.

This attenuator design is very good. After extensive testing at 75 MHz, it was found that with a 3.5 V bias at pin 24 and a control voltage of 0.3 V dc to 10.2 V dc at pins 10, 11, and 12, a range of 43 dB (-45 dB to -2 dB minimum insertion loss) of attenuation can be obtained. Less than 2 dB insertion losses can be obtained with higher control voltages according to reference 13. With the circuit operated at 0 dBm (a rather high level) the third order IMD was -65 dB; at +10 dBm, third order IMD was -50 dB. Additional tests were conducted using 20 kHz tones spacing at 9 MHz (for the IF9TX function) with better results (-70 dB). The BIPA control on *Star-10*, with improved attenuation characteristics can be used not only for manual gain control, but also for muting the IF chain as commanded by the noise blanker. It can also serve as the second AGC control loop in the middle of the receiver chain, for an improved AGC system.

It was found that the minimum insertion loss of the BIPA circuit as applied in the *Star-10* system is about 2 to 3 dB (depending on cables and connectors used). When plugging this into the dynamic range analysis from Part 1, it can be seen that the MDS can be improved if this minimum insertion loss number could be reduced further. If implementing this circuit, a special effort should be made to further reduce its minimum insertion loss through increasing the bias voltage to the rail. This proved helpful in improving the MDS performance. An MDS of -136 dBm (versus the initial -132 dBm) was obtained by improving the minimum insertion loss and/or shorting out the BIPA circuit. This circuit can use a shorting feature utilizing a miniature RF relay similar to the one implemented in the preamp from the IF75BC assembly. The BIPA circuit is a remarkable circuit with outstanding attenuation range and IMD performance.

Master Reference Unit (MRU) / PLL Oscillator (PLXO84)

Next, I will direct our discussion from the receiver and transmitter signal path to the coherent local oscillators (LO) system used in the transceiver. As I previously explained in Part 1, *Star-10* is a “fully coherent” or “fully synthesized” system. This means that all local oscillator frequency sources in the double conversion superheterodyne implementation are locked to a single high stability - high spectral purity source whose performance is reflected in the total long term stability and phase noise performance of the system and is directly translated into the receiver's and transmitter's performance. A high performance master oscillator is required to provide reference frequencies for the synthesizer and all LOs. This master frequency source is the MRU (master reference unit) which generates the 84 MHz reference frequency local oscillator to be used further by the synthesizer (FRU) - FSYNTH and also as a direct fixed LO for converting the 75 MHz bilateral IF to the 9 MHz bilateral IF in IF9BC. Thus, the 84 MHz - MRU LO serves as both, a high quality reference for the two DDSs in the FRU - FSYNTH, as well as a high quality fixed LO for the second conversion. A fully coherent system with equally good phase noise performance at all mixer ports results.

Before going into the circuit description of the MRU, it should be noted that in calculating the phase noise contributions of all LOs in a complex coherent RF system such as *Star-10*, a careful synthesizer analysis should be performed to insure that they are all fully compatible with each other and with the MDS - phase noise and spurious performance of the radio itself. This means that synthesizer performance at all receiver/transmitter LO ports should be equally good throughout as phase noise translates directly dB per dB (minus the mixer loss) into the MDS of the radio within the IF band-pass of interest. Many receiver and transceiver designers do not take this fact into consideration as witnessed by receiver MDS being sometimes obscured (phase noise limited) by the converted poor phase noise. This rule also applies to frequency doublers of lower reference frequencies (for example 32 MHz \times 2 for 64 MHz) being commonly used to obtain master reference frequencies, implementation that loses phase noise performance by 6 dB ($20 \log 2$) through the doubling process by the time it gets to the synthesizer and reflects badly in the LO outputs.

Synthesizer design should start with the highest technologically feasible reference frequency and dividing it down from there if necessary (not multiplying up as some companies do) and partitioning the synthesis for

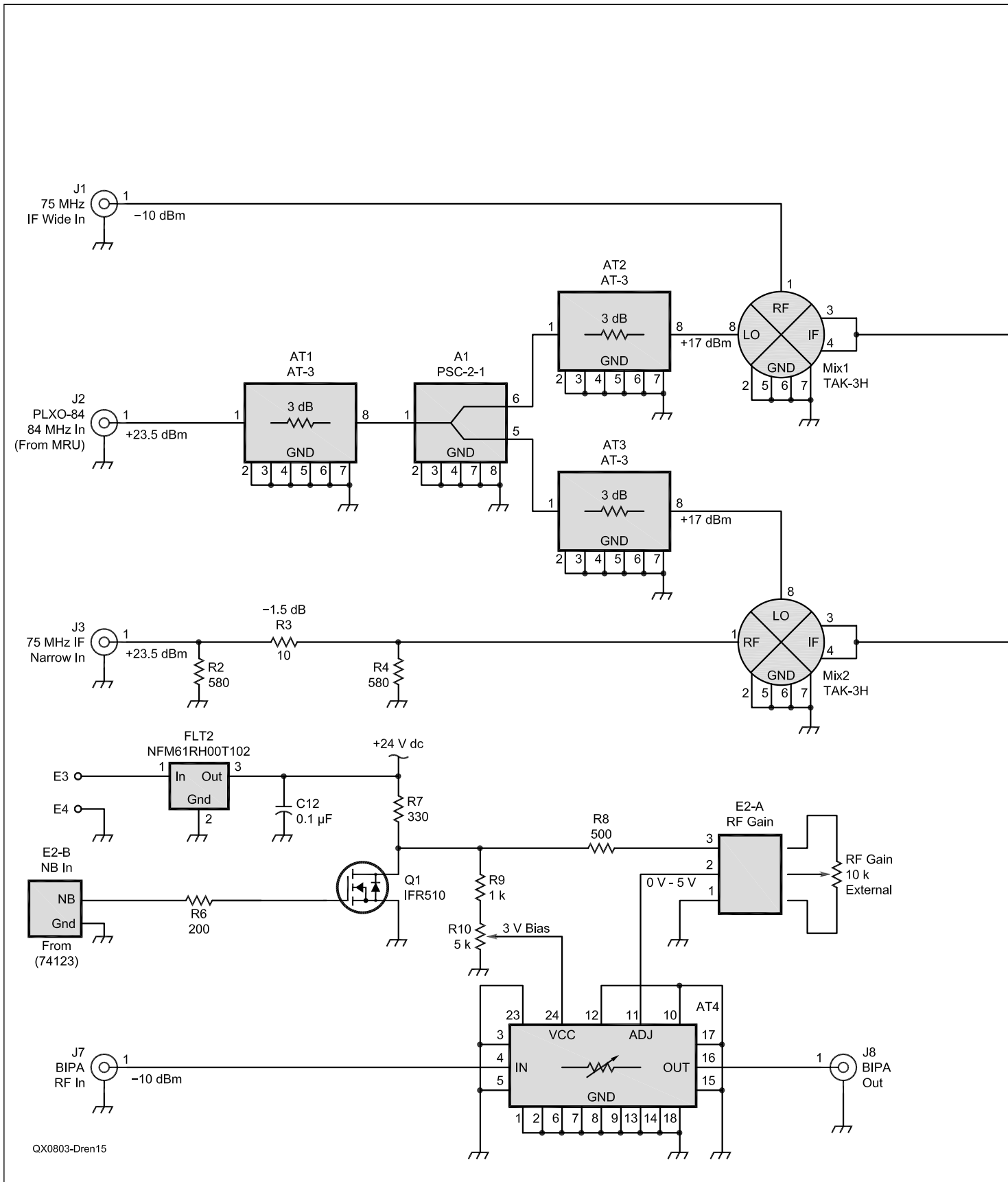
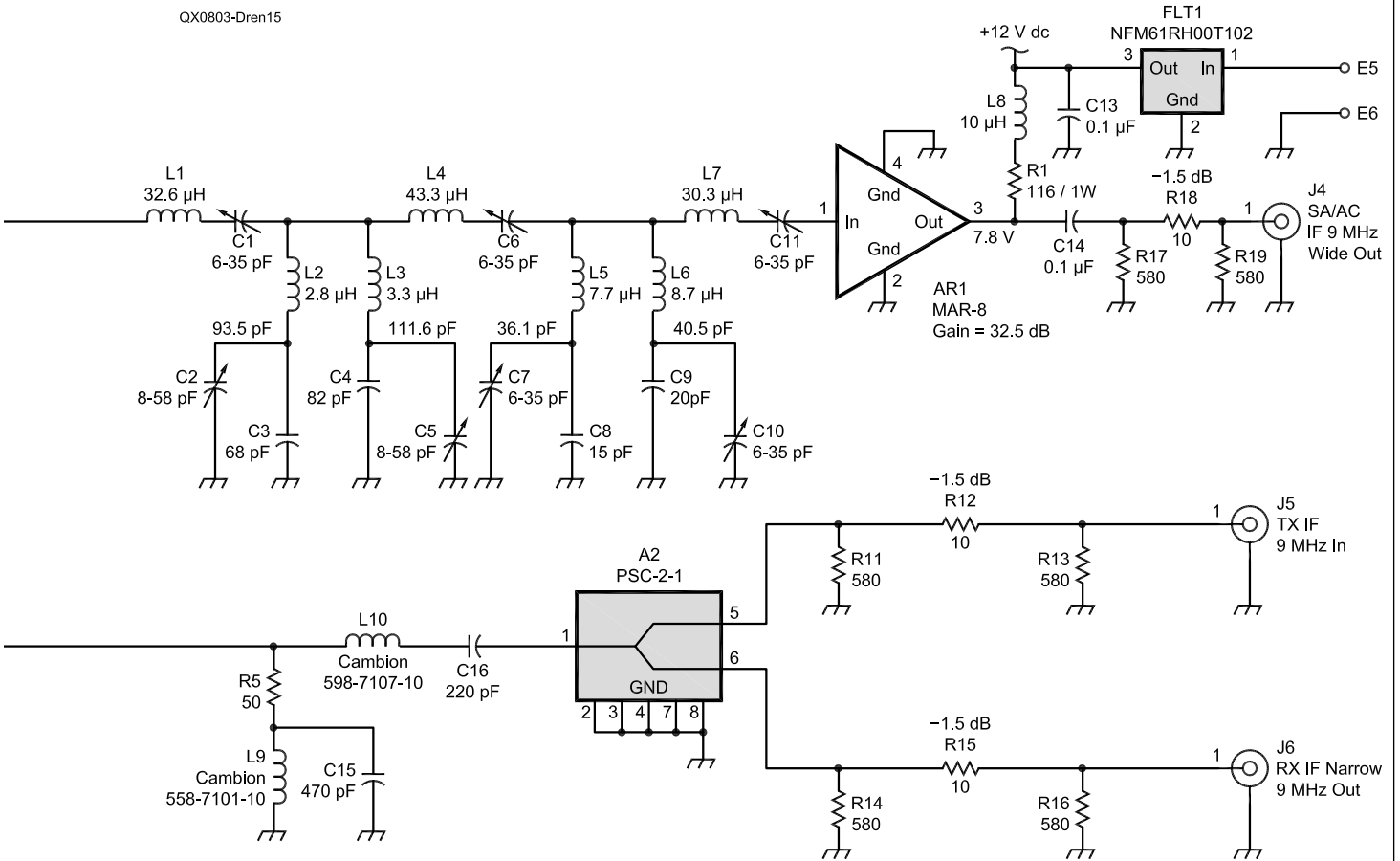


Figure 15 — This schematic diagram shows the circuit for IF9BC, the 9 MHz IF/bilateral converter.

QX0803-Dren15



the various conversions such as to be fully comparable and balanced between all conversion stages. It does not do a system any good to have a good synthesizer as the first LO, while the second and third LOs in the multiple-conversion RF system are inferior in phase noise performance. The composite results will always reflect the worst LO performance.

The *Star-10* MRU schematic diagram is shown in Figure 18. The actual MRU assembly implementation is shown in Figure 19. Looking at Figure 2 of Part 1, it can be seen that the MRU consists of a 10 MHz OCXO providing the system's long-term stability of 1×10^{-8} after a 30 seconds warm-up, and an 84 MHz PLXO, locked to the stable 10 MHz OCXO for high Q – good phase noise performance of the 84 MHz master reference.

Looking at Figure 18, the *Star-10* MRU utilizes an 84 MHz - precision cut (0.001%) fifth overtone Quartz crystal (X1) with one side of the crystal grounded in a phase-locked series resonant Colpitts oscillator arrangement comprised of Q1 (2N5179), L2, L3, C3, C4, R2, R3 and R4. The Colpitts approach was chosen because of its well-known circuit stability while the 0.001% Quartz crystal cut was chosen to guarantee initial start-up almost on frequency before locking occurs. C3 and C4 are high Q, silver mica capacitors customary of the Colpitts implementation.

Looking at Figure 18, the 84 MHz Colpitts oscillator is initially tuned within its narrow resonance range via L2 and L3, which were calculated to resonate the Colpitts circuit on the fifth overtone of the crystal. Additional tweaking was required to bring the circuit into resonance due to board stray elements with L3 being the key-tuning element. This coil is wound using seven turns of #20 wire on a 1/4 inch molded plastic form and using a high-Q aluminium core as an initial frequency control element. L2 is wound in a similar fashion. More detail about this kind of circuit and its PLXO implementation can be found in reference 14, which is available on my Web site listed at the end of this article.

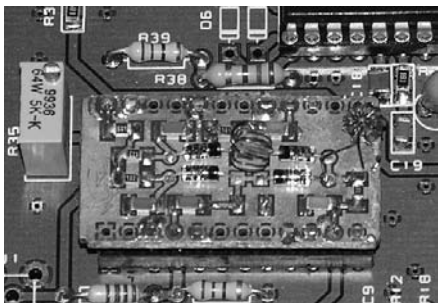


Figure 16 — Actual implementation of the BIPA Pi attenuator used in the IF9BC and the IF9TX assemblies.

The initial free running 84 MHz oscillator is digitally divided down by 84 for a 1 MHz square wave reference signal to be phase compared against a 1 MHz precision frequency signal obtained from the 10 MHz OCXO, as compared against the 10 MHz WWV signal. Upon power on of the *Star-10*, the default-received frequency is the 10 MHz WWV. An exclusive OR phase detector is used to obtain a dc correction signal which is fed back to the 84 MHz Colpitts oscillator via a simple loop filter and a varactor.

Here is how it works. Upon applying power to the MRU assembly, the high performance, low phase noise Colpitts Quartz oscillator starts up almost on frequency due to its 0.001% precision cut. The clean sine wave generated is further amplified by Q2, a 2N5109 transistor. The signal is then filtered using a similar 84 MHz Quartz crystal at X2 and is presented to the divide by two digital divider U1, a UPB1509. This high quality chip has analog to digital conditioning circuits, which allow for a clean 42 MHz signal to be produced. The 42 MHz analog signal is further conditioned/filtered in the IC for extremely low jitter, only to be filtered again via a 42 MHz tubular Quartz crystal filter at X3. The signal is finally presented to U2, a MAX999 low jitter comparator. The threshold of this chip is adjusted via a ten-turn potentiometer, R10. The MAX999 comparator is billed to guarantee a 4.5 ns propagation delay time at 100 MHz. This implies low jitter performance with rise times in the range of 2 ns or less, but experiments comparing

the 84 MHz directly through this device showed a relatively noisy signal. Thus, the divide by two conditioning resulted. Using a 42 MHz (less than half its frequency spec) signal into the comparator showed superior and stable (low jitter) results.

The clean 42 MHz square wave signal at U2 pin 1 is further presented to a digital divider string comprised of U3 and U4, two 74161 chips for a divide by 42 (7 and 6) function. A clean 1 MHz square wave results from the 84 MHz Colpitts oscillator, which is further presented to U9A, an exclusive OR phase detector. Further signal conditioning is achieved using U6, a high-speed 54S00 used as sequential gates. The other side of the phase detector is presented with a highly accurate 1 MHz comparison signal derived from the 10 MHz OCXO through another MAX999 comparator and a 50% duty cycle – divide by 10, IC at U8, a 74LS290 part.

It should be noted that the exclusive OR phase detector was chosen on purpose because of its narrow Pi/4 capture range which is exactly what is needed to lock a 0.001% deviation Quartz crystal over the operating temperature range of interest. Using a wider phase detector would result in more searching and additional jitter translating into inferior phase noise performance (something some engineers never learn). Exclusive OR phase detectors need 50% duty cycle digital signals, and locked condition is achieved when the two reference signals are out of phase by 90 degrees. These conditions are fully achieved in the *Star-10* MRU design

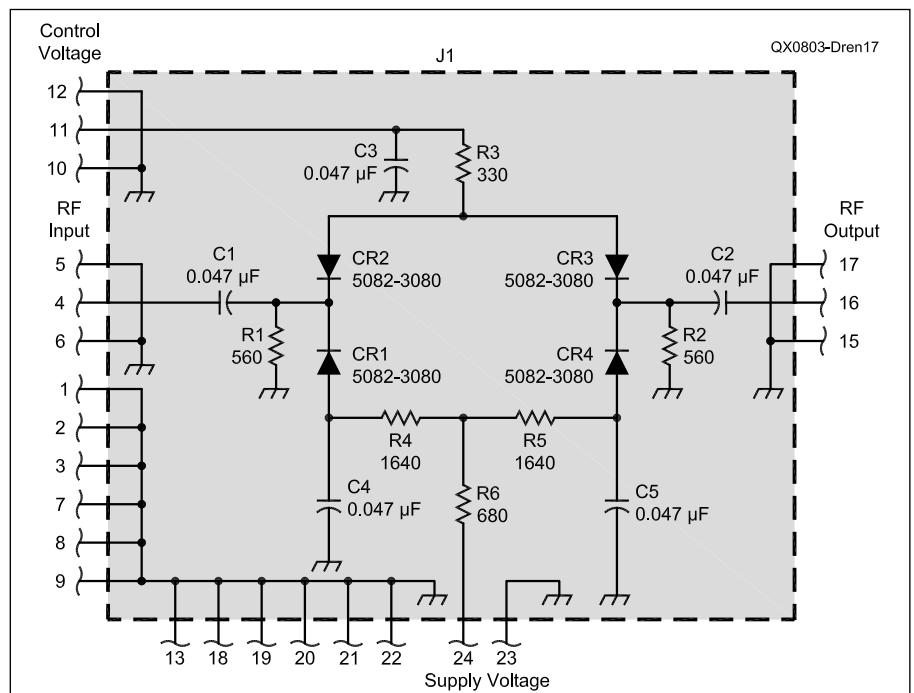


Figure 17 — This is the BIPA circuit diagram.

(note: A quieter mixer type phase detector was briefly considered, but found unnecessary since superior phase noise performance was already achieved with the simple exclusive OR design – see Specification table in Part 1).

The loop correction voltage is obtained at U9A pin 3. The signal is applied through the loop filter comprised of R11, R12 and C19 to the varactor CR1, a BB109. The loop correction signal (2.5 V dc when locked) is fed back to the 84 MHz Colpitts oscillator at the point between C3 and C5 which also serves as the output point of the locked 84 MHz oscillator to be amplified by Q3, Q4, Q6, and filtered by X4, X5, over two channels to provide +10 dBm to +13 dBm fixed reference signals to FSYNTH and serve as a second LO drive in IF9BC. Two additional fifth order tubular narrow band pass filters visible in Figure 19 help reducing further any harmonic spurious content.

It was initially feared that the 1 MHz reference square waves would generate multiple markers at every MHz throughout the HF range. Because of the comprehensive filtering, used, this has not been the case.

For more in depth information on the works of a PLXO MRU and its exclusive OR phase detector, please refer to references 14, 15 and 17.

Operation of the MRU is simple and automatic. Upon turning the power ON to the *Star-10* transceiver, the loop searches within the first 30 seconds for the 10 MHz OCXO signal, which is forced into a quick, warm up mode (the oven heats up). The 84-MHz signal searches back and forth quickly at a decreasing frequency of approximately 10 Hz and down until the oven in the 10 MHz OCXO reaches its internal temperature (over 100 degrees F) and an exact 1 MHz reference signal is obtained and heard by the receiver beating against the 10 MHz WWV signal. A front panel yellow LED reports to the operator this lock-up process. At this point (MRU locked), the receiver can be redirected to the frequency of interest via the keypad, or via the optoencoder using the proper digit underscore marker on the main dial. All LOs in the *Star-10* are now coherent with the MRU and WWV within 1×10^{-8} and operation can begin. The radio is now guaranteed to be exactly on frequency in receive or transmit regardless of where it is tuned within the 1.8 MHz to 30 MHz range. No drift.

Frequency Reference Unit (FRU) Frequency Synthesizer - (FSYNTH)

The frequency synthesizer in the *Star-10* transceiver is a microwave DDS-Driven PLL running from 770 MHz to 1050 MHz. The idea of DD-Driven PLL is not new. I introduced this idea at RF Expo – 1988,

in Anaheim, California (see reference 15). Since then, the majority of transceivers on the market use this concept to generate high-resolution local oscillators frequencies. The synthesizer in *Star-10* goes a step further by generating the LO frequencies at ten times the required frequency range, or 770 MHz to 1050 MHz for improved phase noise performance after a division by 10, which facilitates a 6 dB improvement at the divided down 77 MHz to 105 MHz. This design takes advantage of the reduction in percentage bandwidth offered by the microwave design by using a single VCO (instead of four). The FSYNTH design has been discussed in detail in references 16 and 17. Additional information can be found in reference 18. The schematic for the FSYNTH assembly is shown in Figure 20 and its physical implementation is shown in Figure 21.

Looking at Figure 20, the FSYNTH assembly uses two DDSs, both AD 9850 to generate the variable PLL reference for the DDS-Driven PLL LO as well as the BFO LO. The 50-ohm 84 MHz reference signal coming from the MRU PLXO is input to the FSYNTH assembly at J1. From this point on, it is equally distributed between the two AD 9850 DDSs at pins 9 of U1 and U2. The word-clock commands information for both DDSs coming from the DFCB command and control assembly are input at J1. The command and control assembly will be discussed later. The resolution of the top DDS (U1) is 1 Hz and results in 10 Hz after it gets multiplied by 10 in the PLL loop of the DDS-Driven PLL part of FSYNTH. The highly filtered (to prevent spurious) BFO DDS has a resolution of 10 Hz. The ultimate resolution of FSYNTH as reflected in the transceiver's ultimate resolution from 1.8 MHz to 30 MHz is 10 Hz. For a much more in depth explanation of how the FSYNTH assembly works, please refer to reference 17, page 5. This reference is available on my Web site, which is listed at the end of this article.

Although new and improved DDS devices have evolved since the introduction of the AD9850, the fact remains that spurious performance is still the main challenge in DDS systems used as simplistic direct synthesizers, despite new and clever noise cancelling techniques that have been recently introduced. (See Analog Devices AD9959 Application Note: www.analog.com/UploadedFiles/Data_Sheets/AD9959.pdf, p 11.)

As such, the AD9850, if used properly, remains the workhorse of the Analog Devices family of DDS ICs even after all these years. An AD9850 DDS device used in a well-controlled, tight-loop, DDS-driven PLL can indeed exceed the spurious performance of simplistic DDS-only synthesizers

using even the most modern DDS devices.

The secret of this superior performance lays in a combination of design parameters, primarily in choosing a correct Nyquist reference frequency (References 15, 16, 17), and the proper interface of the DDS with the PLL phase detector, combined with a well designed loop filter in the PLL.

The FSYNTH performance has been improved since its original design through constant tweaking of the loop filter and a better selection of parts in the microwave divider section and the squaring circuits. This design is capable of -133 dBc/Hz performance from 2 kHz through 20 kHz offset at the divided down output. This performance has been tested and documented as shown in Figure 22. Further phase noise improvements will be discussed in Part 3.

Additional improvements in phase noise performance can be obtained by altering the loop bandwidth and other circuits at the cost of other parameters such as end-to-end synthesizer lock-up split operation and others.

Command and Control Assembly (DFCB)

The command and control assembly - DFCB is the heart of the *Star-10* transceiver. It provides the smarts and the friendly user interface for the system. The system control is achieved through the microprocessor board (part of DFCB) which houses the PIC-17C44 chip discussed in Part 1, its associated hardware, software, and the back-light LCD display assembly viewable through the front panel. This is packaged together on the DFCB, and is used together with the keypad data entry board and the optoencoder and all other user interfaces and controls located behind the front panel of the transceiver as shown in Figure 23.

The command and control system addresses all frequency and mode commands in the FRU — FSYNTH, as well as the various associated frequency selection commands to the half-octave front end filter banks, the ultimate bandwidth and mode selection commands for the receiver IF9RX and IF9TX, the T/R control commands, debouncing delayed Morse code key commands which work in conjunction with the synthesizer split lock-up functions and even display light intensity and multiple sound feed-back tones audible through the receiver's audio amplifier upon depressing keys on the key pad data entry shown on the right side of Figure 23.

The microprocessor code embedded into the command and control system is represented by what the *Star-10* transceiver really does, as commanded from the front panel of the radio. The command and control - DFCB system is primarily capable of addressing

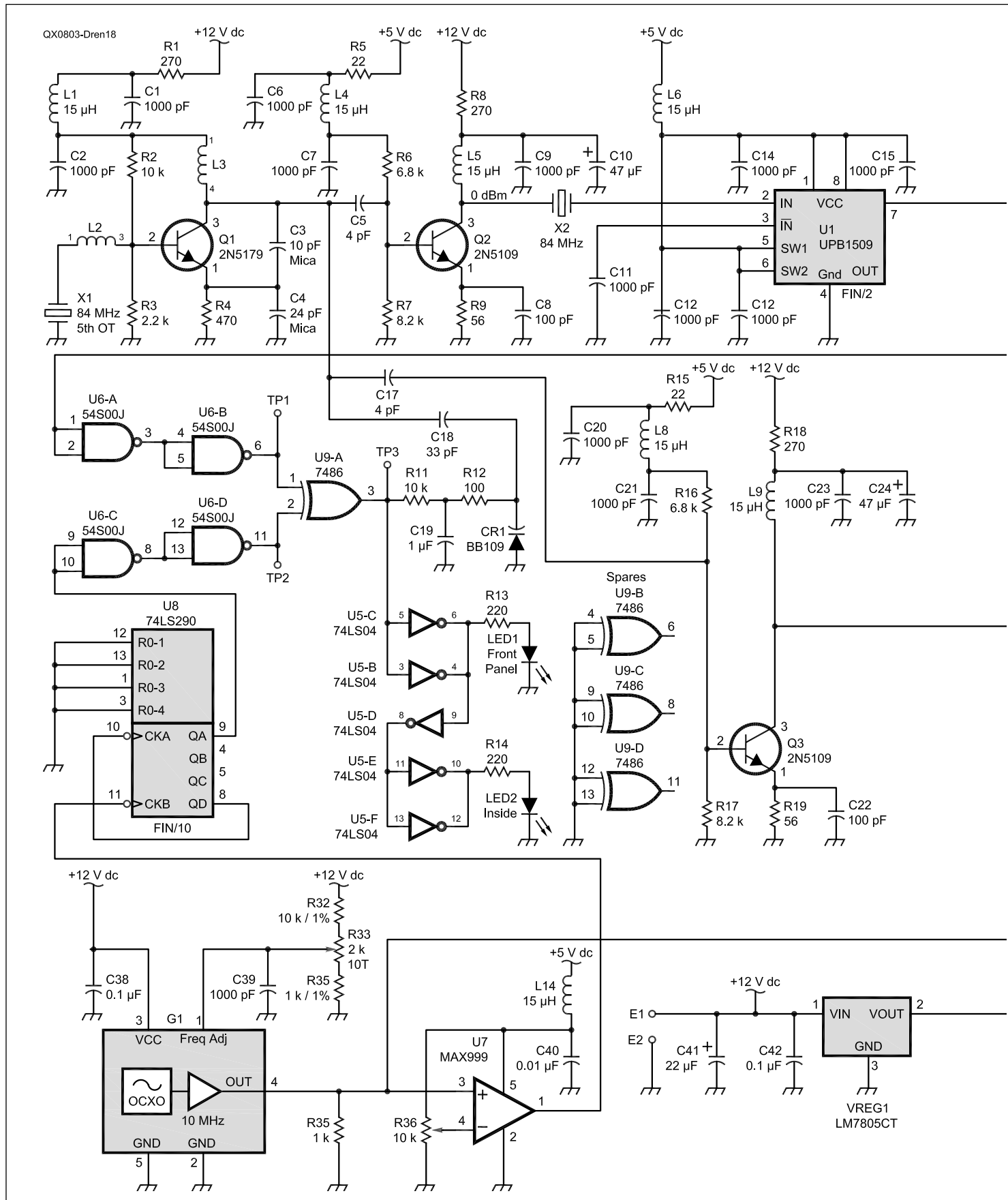
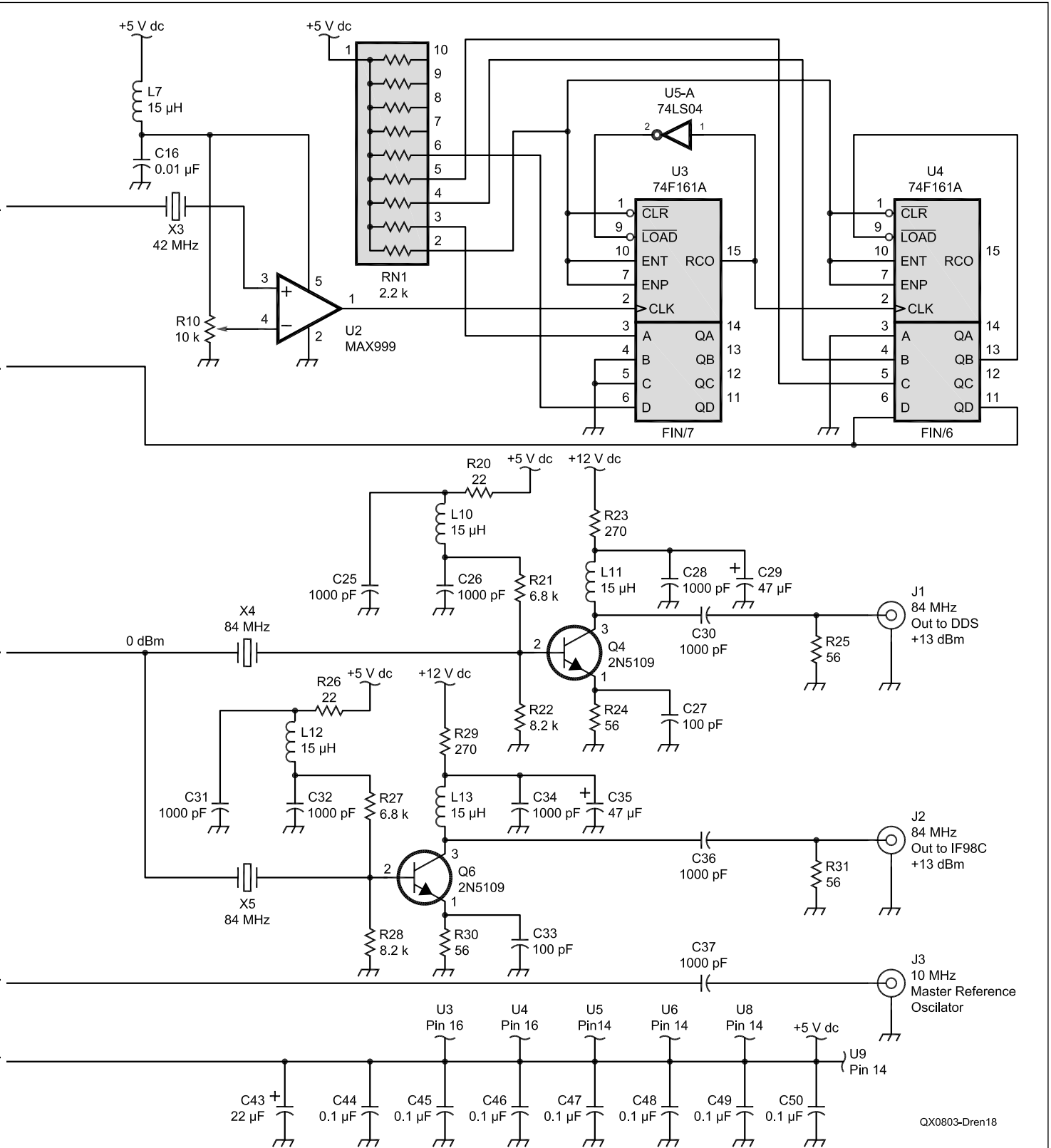


Figure 18 — Circuit diagram of the MRU.



either the main loop DDS-Driven PLL or the BFO DDS. The main synthesizer loop (the DDS-Driven phase-locked microwave loop) is controlled through direct keypad entry as taken over by the optoencoder. When in the mode select mode, the keypad controls the microprocessor such that the BFO/DDS-2 follows a fixed programmed function/frequency offsets from the nominal 9 MHz and as changed by the USB, LSB, CW, CWN, AFSK commands requirements. This programmability along with the entire transceiver's frequency sources programmability was previously shown in Table 1 of Part 1. Up/Down arrow commands are used on the keypad to enter RIT and RX and TX - PBT offsets. The PBT function allows selected TX or RX offsets to vary ± 1.5 kHz moving the IF BW and other sources in either side of the zero in either transmit or receive by using the main tuning knob. Once set, the IF PBT remains memorized, to be reset back only by the power off function. The RIT function accessible through the main knob when in RIT mode, allows for ± 9.9 kHz received frequency offset from nominal and gets reset to nominal zero by turning the transceiver power off. The schematic diagram of the DFCB assembly is shown in Figure 24.

Looking at Figure 24, the heart of the command and control system, DFCB is the PIC-17C44 microprocessor at U4. As can be seen, all I/O ports have been thoroughly used by the *Star-10* design. The microprocessor runs at 32 MHz as shown using the Quartz crystal oscillator X1 at pins 19 and 20. The reason for this frequency choice was described in Part 1 of this article series. Harmonics and products of this oscillator are outside of the receiver bandwidth. The switching RF noise produced by the display (which can be heard on a pocket AM Broadcast radio held in front of the display) does not impact the receiver because of the considerable shielding of the assemblies. There is absolutely no impact on the receiver MDS.

The keypad interface is shown on the left side of the drawing. The keys are arranged in a matrix of switches that address the microprocessor through closing user commanded keys via J4 A and B and through the 74HCT138 decoder demultiplexer at U2. Two OPTREX DMC-16230 N - EB displays (DISP 1 and DISP 2) using multiple green LEDs behind a dot matrix LCD for backlighting, are wired and addressed in parallel from the I/O ports as shown. Contrast adjustments are provided through R2 and R3. A switched "bright" function is facilitated by pulling more current through the display LEDs via the IFR510 FET at Q1. The bright command as well as the sound feedback command are implemented via the microprocessor by touch-pushing the main

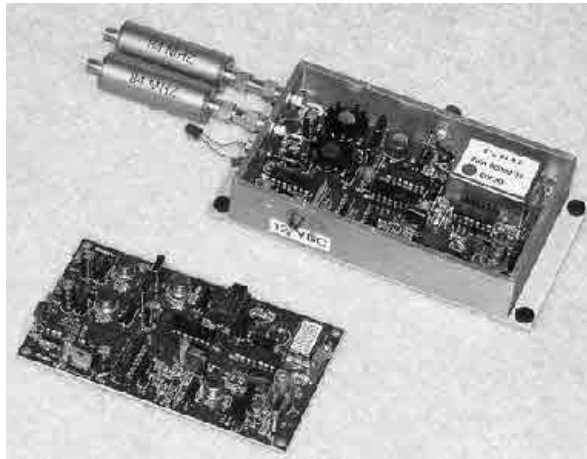


Figure 19 — The *Star-10* MRU assembly uses an 84 MHz PLXO for good phase noise as locked to a 10 MHz OCXO (WVV compared) for long term stability of 1×10^{-8} . A simplified version was also developed using a 16.8 MHz TCXO (bottom photo) but was abandoned due to the inferior stability of the TCXO as compared with the OCXO.

tuning knob through the push-push switch provided in the optoencoder. The optoencoder is an inexpensive 32 positions Clarostat unit wired through J2 directly into the I/O ports as shown. The 99 memories function is provided by the permanent memory IC, 25C060 at U1. Memorizing a frequency is easy by using the MR and ENTR functions on the keypad. The memorized frequencies are not erased with power off. They can only be erased by using the keypad and entering a new frequency in an addressed memory number from 1 to 99. The half-octave filters (receiver band-pass and transmitter low-pass) are selected automatically by the microprocessor and output through another 74HCT138 — a three to eight line decoder demultiplexer at U3 and through a tri-state inverting octal buffer, 74HC240 at U6. These logic signals are further carried via connector J5 to the half-octave filter banks via the mother board connectors located on the back of the main shelf as previously discussed. The logic arrangement at U5 A, B, C and D is intended for debouncing functions through the I/O interface connectors. Additional command and control signals are provided from this assembly to the FSYNTH, IF9RX, IF9TX and the T/R assembly via the J1 and J3 connectors. As with all other assemblies in the *Star-10*, proper voltages and regulation are provided via on-board variable and fixed regulators, in this case, a 7805 at VREG1. For reason of simplicity, the three LEDs that work in conjunction with the AIPA selector have not been shown in Figure 24. This completes the DFCB assembly description.

9 MHz Narrow Band Receiver IF (IF9RX)

I will next discuss the receiver narrow-band IF — IF9RX. Its design was briefly presented in Part 1 of this series. The ultimate receiver bandwidth requirements are established through the IF9RX assembly and its custom made Quartz crystal fil-

ters. Commands are received through the command and control assembly, DFCB. Conversely, the transmitted bandwidth for the SSB/AFSK transmit functions is established through a similar filter bank in the IF9TX assembly. This will be discussed later in Part 3 of this series.

As can be seen from Figure 2 of Part 1, the IF9BC main receiver output is further input to the IF9RX assembly. This IF path achieves the ultimate receiver bandwidth selection and amplification as commanded by the command and control assembly, DFCB.

The IF9RX board provides approximately 100 dB of AGCed gain (80 dB AGC control plus filter insertion loss compensation) using three high dynamic range (+15 dBm IP3) AD-603 logarithmic/linear IF blocks from Analog Devices. This choice was made after an intense search for the right amplifier device. Initially, the old and popular MC-1590 device was considered based on prior art (reference 19). After intense IP3 tests in the KG6NK laboratory using two-tone signals (1.5 kHz apart) at 9 MHz, with and without AGC applied, the IP3 performance of the MC-1590 was found to be inferior. The idea was quickly abandoned.

Several other choices were considered. Among them were the Analog Devices AD600, AD602, AD603, AD604, AD605 and Cougar AGC230. The Cougar device, while offering a third order intercept point of +21 dBm, was too expensive for this application. After ample conversations with Dana Whitlow of Analog Devices, I zeroed in on the AD603, an inexpensive high performance device. This is a low noise device with a bandwidth of 90 MHz, which can be powered from a single 10 V supply. It is a voltage-controlled amplifier, which provides gains of +9 dB to +51 dB (42 dB) and a "linear in dB" accurate and stable range suitable for a linear — in dB — S-meter indicator. It offers a -67 dBm AGC threshold. Its IP3 is +15 dBm. Its noise figure is billed at 8.8 dB. Quick system calculations revealed that if using two AGCed

AD603 devices cascaded with switched in Quartz crystal filters and followed by a third AD603 programmed to compensate for filters insertion loss can provide slightly over 100 dB gain with about 80 dB of AGC. Gain system implications revealed that AGC action and consequently S-meter action would start at approximately -103dBm signal at the receiver antenna input or an S-3 signal level. This was deemed as a good enough compromise considering the circuit complexity and a linear range of 70 dB shown on the S-meter from an S3 to an S9 plus 40 dB signal level.

Several breadboards were constructed and tested together with Dana Whitlow and Constantin Popescu, (KG6NK) using these ideas, and based on Analog Devices recommendations (see reference 20). An actual to-size first cut board was laid out courtesy of Bruno Santalucia (I6YPK). Because of the 100 dB gain provided by this important board, and the limited board size of 5.5 × 4.5 inches, the IF9RX board had to be laid out again to prevent possible oscillation. A special effort was made by KD7KEQ to provide extra ground stitching for the final layout.

The IF9RX concept was briefly discussed in Part 1 of this series. A block diagram and discussion appears in Figure 5 of Part 1. The IF bandwidth selection is provided by four 8-pole crystal filters for a total of 32 possible poles of selectivity. Instead of selecting individual filters as in conventional IF designs, the *Star-10* IF9RX filter assemblies are combined in a cascaded AND function (rather than an OR function) for a total of 32 poles (plus the 8 poles composite roofing filter) of superb selectivity. This cascaded architecture makes the IF9RX a unique design that works in tandem with the system's command and control software.

As shown in Figure 5 of Part 1, two 8 pole crystal filters with a bandwidth of 2.4 kHz are always used at the beginning and the end of the 9 MHz IF chain for good noise management. This idea was inspired by standard RF design procedures and by reference 18. Additional 8 pole crystal filters of narrower bandwidths are inserted or removed between the gain stages (for a maximum of 32 poles in CW Narrow mode) depending on the mode selection and as commanded by the DFCB. The selection is achieved with miniature RF Teledyne relays, just as in the front end of the radio (no diode switching for RF paths in this radio). Automatic insertion loss compensation control is achieved depending on the diverse filters configurations chosen so there is no difference in signal amplitude and S-meter reports when changing filters and bandwidths.

The schematic diagram for the IF9RX is shown in Figure 25 and the actual implementation of the assembly is shown in Figure 26.

Here is how it works. Looking at Figure 25, the 9 MHz receiver IF signal coming from one side of the bottom splitter in IF9BC is input to the IF9RX assembly at J3. It is then passed through the first 8-pole, 2.4-kHz-wide quartz filter, XF1. This filter and XF4 (an exact similar filter intended to limit the noise content of amplifiers) are always in the circuit. Two cascaded AD603 amplifiers U1 and U2 follow the first filter. They are AGCed at point A via the circuit containing Q8, Q9, Q10 and U7A. The AGC signal is derived at U3 as shown. AGC ON/OFF and time constant (FAST/SLOW) functionality from the front panel are provided through J1 along with IF gain and MUTE functions (through Q7). The attack time is fast in all modes (<2 ms) while the fast decay time is 0.5 seconds and the slow decay time is 4 seconds. The output of the AGCed amplifiers at U2 is further cascaded via additional Quartz filters XF2 and XF3. The operator controls the filter selection and insertion loss compensation from DFCB via the keypad depending on the mode and bandwidth selected. The filters are merrily inserted in the circuit or shorted out using miniature Teledyne RF relays as shown. Control signals are applied to U4, U8 and the relays (K1, K2, K3, K4, K5) via J1 and J2 as shown. The output of XF3 is further presented the third AD603 at U3 which inserts fixed gain compensation as set by R33 and R40 depending on the narrow filters selected (XF2 or XF3).

It should be noted that "narrow" means different things in different modes. In SSB for instance, "narrow" means that XF2 (1.8 kHz) was selected, while in CW or AFSK, "narrow" selects XF2 (1.8 kHz) and XF3 (500 Hz) for a total of 32 poles of cascaded selectivity. Conversely, "wide" means different things in different modes: In SSB for instance, "wide" uses XF1 and XF4 (both 2.4 kHz, 16 pole filters) while in CW, "wide" selects XF2 (1.8 kHz) together with XF1 and XF4 for 24 poles of filtering. The intelligence for these selections is actually built into the DFCB assembly and is part of the software design. The computer in DFCB actually understands which mode was selected from the keypad and makes the right decisions accordingly.

Metering functionality by switching from the S-meter function in receive to the RF power meter function in transmit is provided through J2 via K5. IF gain control is wired to the front panel control potentiometer via the J1 connector.

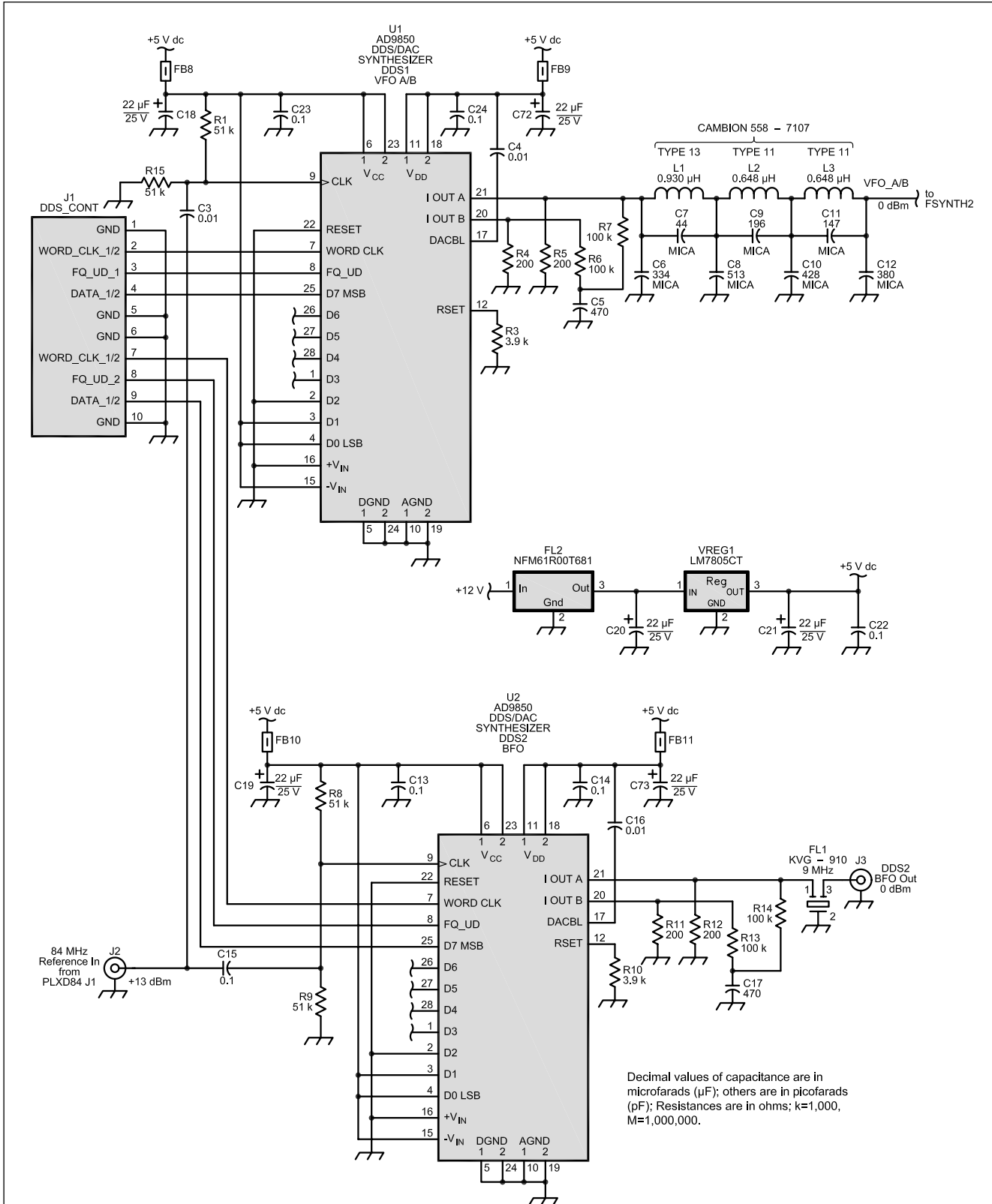
Some of the circuits in IF9RX are powered directly from 12 V dc. The AD603 amplifiers are powered from the +12 V dc input E1 through U5, a programmable LM317 regulator set at 10 V dc. Additional 5 V dc power is supplied to the 75451 line drivers (U4 and U5) via a 5 V dc regulator, U6.

Despite its relatively simple apparent design, the IF9RX assembly has been a challenging IF to implement, because of the very high gain requirements and the relatively small space available on the board. Its novel cascaded functionality has proven to be well worth the extra effort of diverting from the classic "one filter at the time" mode selection of the past.

This concludes Part 2 of this article series. In Part 3, I will discuss the receiver product detector Assembly (PDAF), the transmit / receive (T/R) controller, the 9 MHz transmitter IF (IF9TX), additional assemblies, power linear amplifier, the EMI-quiet switching power supply, putting it all together, the final performance tests and conclusions as well as the lessons learned.

References

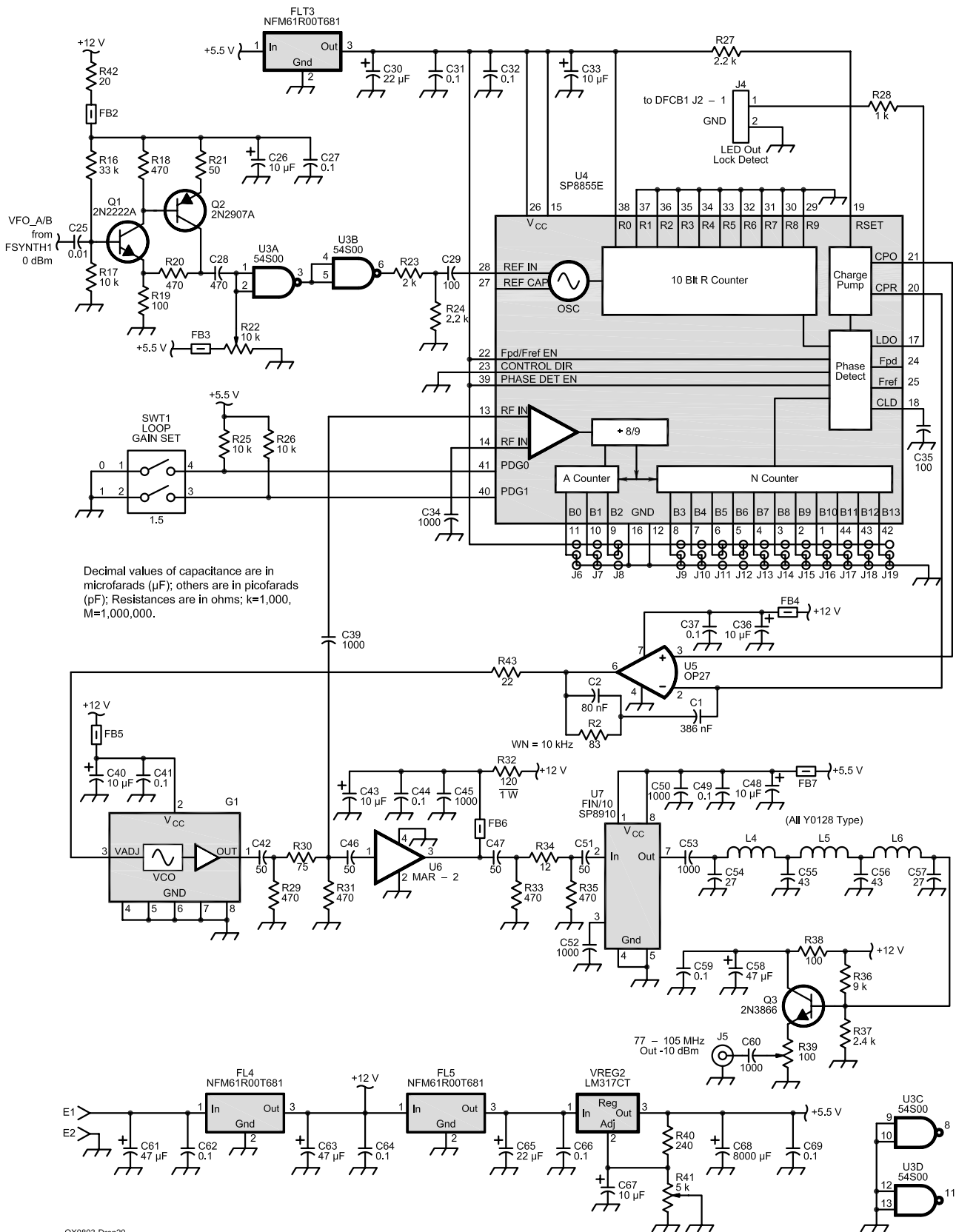
- 1) Cornell Drentea, "Automatically Switched Half-octave Filters, Part 1," *ham radio*, Feb 1988, pp 10-13, 15, 17, 18, 21, 22, 24-26, 28, 29, 31, 32. This article is available on the author's Web site: members.aol.com/cdrentea/myhomepage/index.html.
- 2) Cornell Drentea, "Automatically Switched Half-octave Filters, Part 2," *ham radio*, Mar 1988, pp 29, 30, 33, 34, 36, 37, 39, 41, 44. This article is available on the author's Web site: members.aol.com/cdrentea/myhomepage/index.html.
- 3) Cornell Drentea, *Radio Communications Receivers*, McGraw Hill 1982, 1983, 1984, p 1393.
- 4) David Norton and Allen Podell, Transistor Amplifier with Impedance Matching Transformer, U.S. Patent 3,891,934, June 1975.
- 5) David Norton, "High Dynamic Range Transistor Amplifiers Using Lossless Feedback," *Proceedings of the 1975 IEEE International Symposium on Circuits and Systems*, 1975, pp. 438-440.
- 6) David Norton, "High Dynamic Range Transistor Amplifier using Lossless Feedback," *Microwave Journal*, May 1976, p 53.
- 7) Joe Reisert, "VHF/UHF World, High Dynamic Range Receivers," *ham radio*, Nov 1984, pp 97-105.
- 8) Jacob Makhinson, "A High Dynamic Range MF/HF Receiver Front End," *QST*, Feb 1993, pp 23-28.
- 9) Colin Horrabin, "Technical Topics, High Performance Mixer," *RadCom*, Oct 1993, pp 55, 56.
- 10) Mark Wilson, K1RO, Ed., *The ARRL Handbook*, 2008 Ed, Chapter 11, Mixers, Modulators and Demodulators, ARRL, 2007, pp 11.26, 11.27.
- 11) Sergio Cartoceti, "A Doubly Balanced 'H-Mode' Mixer for HF," *QEX*, Jul/Aug 2004, pp 23-32.
- 12) Chris Trask, *Distortion Improvement of Lossless Feedback Amplifiers Using Augmentation*, ATG Design, P.O. Box 25240 Tempe, AZ 85285.
- 13) Raymond Waugh, "A Low Cost Surface Mount PIN Diode Pi Attenuator," *Microwave Journal*, Vol 35, No. 5, May 1992.
- 14) Cornell Drentea, "High Stability Local Oscillators for Microwave and Other Applications," *ham radio*, Nov 1985, pp 29-35, 37, 38.
- 15) Cornell Drentea, "Designing Frequency Synthesizers," RF Technology Expo, 1988, Disneyland Hotel, Anaheim, CA, Feb 10-12, 1988, Session B-1, Frequency Synthesis.



Decimal values of capacitance are in microfarads (μF); others are in picofarads (pF); Resistances are in ohms; k=1,000, M=1,000,000.

QX0803-Dren20

Figure 20 — Schematic diagram for the Star-10 frequency reference unit (FRU), FSYNTH.



Decimal values of capacitance are in microfarads (μF); others are in picofarads (pF); Resistances are in ohms; k=1,000, M=1,000,000.

- 16) Cornell Drentea, "Beyond Fractional-N, Part 1," *QEX*, Mar/Apr 2001, pp 18-25. This article is available on the author's Web site: members.aol.com/cdrentea/myhomepage/index.html.
- 17) Cornell Drentea, "Beyond Fractional-N, Part 2," *QEX*, May/June 2001, pp 3-9. This article is available on the author's Web site: members.aol.com/cdrentea/myhomepage/index.html.
- 18) Vadim Manassewitsch, *Frequency Synthesizers, Theory and Design*, Wiley 1976.
- 19) Wes Hayward, W7ZOI, "A Competition Grade CW Receiver," *QST*, Mar 1974, pp 16-20, 37.
- 20) Analog Devices, Low Noise Variable Gain Amplifier AD-603, Application Note.

Additional Reading

- Mark Wilson, K1RO, Ed, *The ARRL Handbook*, 2008 Ed., Chapter 10, Oscillators and Synthesizers, and Chapter 11, Mixers, Modulators and Demodulators, ARRL, 2007.
- Ulrich Rohde, "Communication Receivers for the Year 2000," *ham radio*, Part I, Nov 1981, Part II, *ham radio*, Dec 1981.
- Cornell Drentea, *The Art of RF System Design*, a three day comprehensive course (members.aol.com/cdrentea/myhomepage/)
- James Tsui, *Digital Techniques for Wideband Receivers*, SciTech Publishing, ISBN 1-891121-26-x.
- Oran E. Brigham, *The Fast Fourier Transform*, Prentice Hall, ISBN 0-13-307496-x.
- Cornell Drentea, United States Patent 7,139,545, Ultra-wideband fully synthesized high-resolution receiver and method.
- Ulrich Rohde, "Digital HF Radio: A Sampling of Techniques," paper presented at the Third International Conference on HF Communication Systems and Techniques, London, England, February 26-28, 1985.
- Ulrich Rohde and Jerry Whitaker, *Communications Receivers, DSP, Software Radios, and Design*, Third Edition, McGraw Hill, ISBN 0-07-136121-9.
- Peter Vizmler, *RF Design Guide, Systems, Circuits and Equations*, Artech House, ISBN 0-89006-754-6.
- Ulrich Rohde, "Recent Advances in Shortwave Receiver Design," *QST*, Nov, 1992, pp 45-55.
- Ulrich Rohde, "Key Components of Modern Receiver Design," *QST*, May, Jun, Jul, Dec 1994.
- Lawrence E. Larson, *RF and Microwave Circuit Design for Wireless Communications*, Artech House, ISBN 0-89006-818-6.
- Ulrich Rohde and A. K. Poddar, "Theory of Intermodulation and Reciprocal Mixing: Practice, Definitions and Measurements in Devices and Systems," Part 1, *QEX*, Nov/Dec 2002, Part 2, *QEX*, Jan/Feb 2003.
- Ulrich Rohde, "High Intercept Point. Broadband, Cost Effective and Power Efficient Passive Reflection FET DBM," EuMIC Symposium, 10-15 Sep 2006, UK.
- Ulrich Rohde and A. K. Poddar, "Low Cost, Power-Efficient Reconfigurable Passive FET Mixers," 20th IEEE CCECE 2007, 22-26 Apr 2007, British Columbia, Canada.
- Ulrich Rohde and A. K. Poddar, "Switching FET Broadband DBM for Wireless Applications," IEEE Sarnoff Symposium, 30 April - 02 May 2007, Princeton, NJ.
- Donald D. Weiner and John E. Spina, *Sinusoidal Analysis and Modeling of Weakly Nonlinear Circuits*, with application to nonlinear interference effects, Van Nostrand Reinhold, ISBN 0-442-26093-8.
- Nonlinear System Modeling and Analysis with Applications to Communications Receivers, Signatron, prepared for Rome Air Development Center, AD-766 278, NTIS, US Department of Commerce.

Figure 21 — Actual FSYNTH assembly implementation.

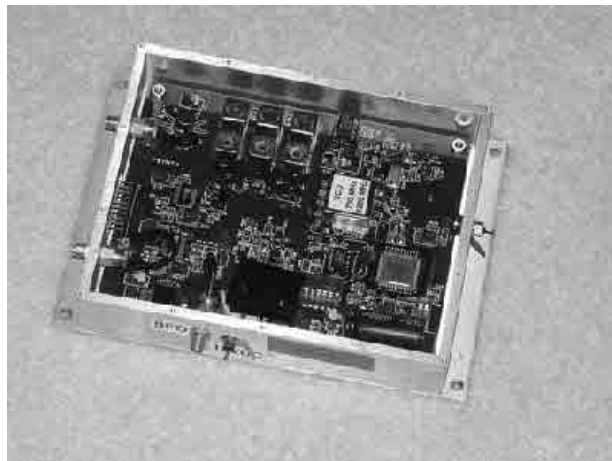


Figure 22 — Phase noise performance of the Star-10 FSYNTH assembly shows a close in performance of -133 dBc/Hz at 4 kHz. The photo shows total performance from 500 Hz to 20 kHz from the carrier. This test was performed directly at the output of the synthesizer at 89.2 MHz (14.2 MHz). A rather tight loop bandwidth was chosen (see reference 17) and shows the normal "hump" created by the super imposing of the VCO phase noise with the loop bandwidth. The FSYNTH loop bandwidth is optimized here for close in performance (from 500 Hz through 4 kHz) since this noise content is reflected dB per dB through the transceiver's mixers especially in the receiver performance.

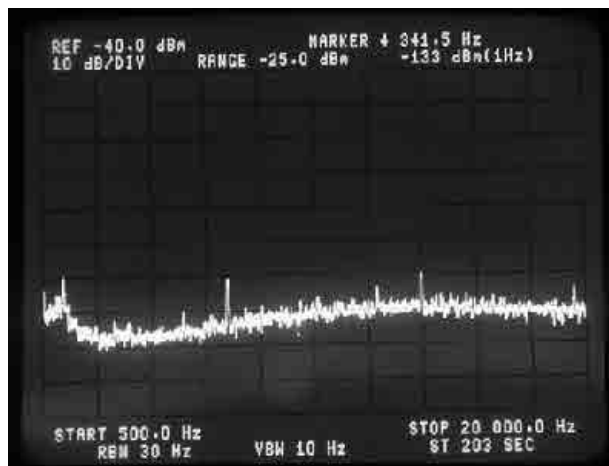
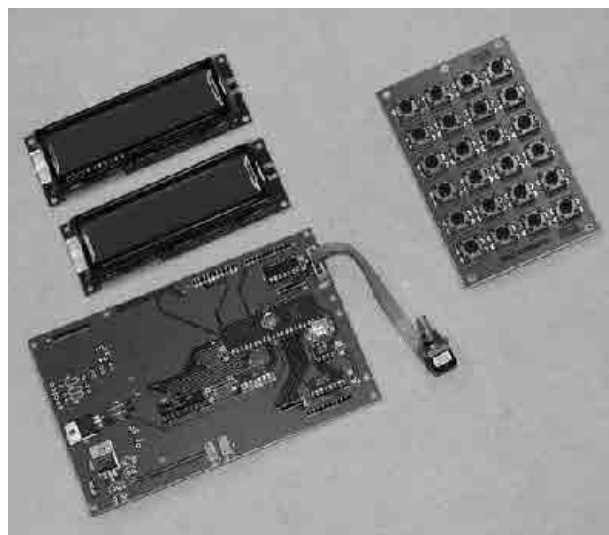


Figure 23 — The command and control assemblies behind the front panel contain the main DFCB board (with microprocessor shown), the optoencoder, the 64 characters displays that plug into DFCB board and the key pad board, all interconnected with ribbon cables. See text.



Cornell Drentea, United States Patent 4,584,716, Automatic Dual Diversity Receiver through Image Recovery.

Cornell Drentea, United States Patent 6,882,310, Direct Sampling Receiver.

William F. Egan, *Frequency Synthesis by Phase Lock*, John Wiley & Sons, ISBN 0-471-08202-3.

Alain Blanchard, *Phase-Locked Loops*, John Wiley & Sons, ISBN 0-471-07941-3.

Floyd M. Gardner, *Phaselock Techniques*, John Wiley & Sons, ISBN 471-29156 0.

Ulrich Rohde, *Digital PLL Frequency Synthesizers, Theory and Design*, Prentice Hall, ISBN 0-13-214239-2.

P. V. Brennan, *Phase-Locked Loops: Principles and Practice*, MacMillan Press, ISBN 0-333-65571-0.

Dan H. Wolaver, *Phase-Locked Loop Circuit Design*, Prentice Hall, ISBN 0-13-662743-9.

John B. Anderson, *Digital Transmission Engineering*, IEEE Press, ISBN 0-7803-3457-4.

James Hardy, *High Frequency Circuit Design*, Reston, ISBN 0-8359-2824-1.

Bernard Sklar, *Digital Communications: Fundamentals and Applications* (with System View), Prentice Hall, ISBN 0-13-084788-7.

Cornell Drentea, United States Patent 7,324,797, Bragg-Cell Application to High Probability of Intercept Receiver.

Ferrel G. Stremmer, *Introduction to Communication Systems*, Addison Wesley, ISBN 0-201-07251-3.

Roland E. Best, *Phase-Locked Loops: Design, Simulation, and Applications*, McGraw Hill, ISBN 0-07-134904-9.

Doug Smith, *Digital Signal Processing Technology*, ARRL, ISBN 0-87259-819-5.

Albert D. Helfrick, *Electrical Spectrum and Network Analyzers*, Academic Press, ISBN 0-12-338250-5.

George W. Stimson, *Airborne Radar*, SciTech and IEEE Press, ISBN 1-891121-01-4.

James R. Rowland, *Linear Control Systems: Modeling, Analysis and Design*, John Wiley & Sons, ISBN 0-471-03276-x.

Ralph S. Carson, *Radio Concepts*, John Wiley & Sons, ISBN 0-471-62169-2.

Herbert L. Krauss, Charles W. Bostian, Frederick H. Raab, *Solid State Radio Engineering*, John Wiley & Sons, ISBN 0-471-03018-x.

Ralph S. Carson, *High-Frequency Amplifiers*, John Wiley & Sons, ISBN 0-471-86832-9.

Philip E. Pace, *Low Probability of Intercept Radar Receivers*, Artech House, ISBN 1-58053-322-1.

William E. Sabin, Edgar O. Schoenike, *Single-Sideband Systems and Circuits*, McGraw Hill, ISBN 0-07-054407-7.

Anatol L. Zverev, *Handbook of Filter Synthesis*, John Wiley & Sons, ISBN F 471 98680-1.

Ronald E. Crochiere and Lawrence R. Rabiner, *Multirate Digital Signal Processing*, Prentice Hall, ISBN 0-13-605162-6.

Lee R. Watkins, *Comprehensive Filter Design*, Motorola Inc., 1997.

Scott R. Bullock, *Transceiver and System Design for Digital Communications*, Noble, ISBN 1-884932-14-2.

James A. Cherry and Martin Snelgrove, *Continuous-Time Delta-Sigma Modulators for High-Speed A/D Conversion: Theory, Practice and Fundamental Performance Limits*, Kluwer Academic, ISBN 0-7923-8625-6.

Paul A. Lynn, *An Introduction to the Analysis and Processing of Signals*, Howard W Sams, ISBN 0-672-22253-1.

Andrew F. Inglis, *Electronic Communications Handbook*, McGraw Hill, ISBN 0-07-031711-9.

Paul J. Nanhin, *The Science of Radio*, American Institute of Physics, ISBN 1-56396-347-7.

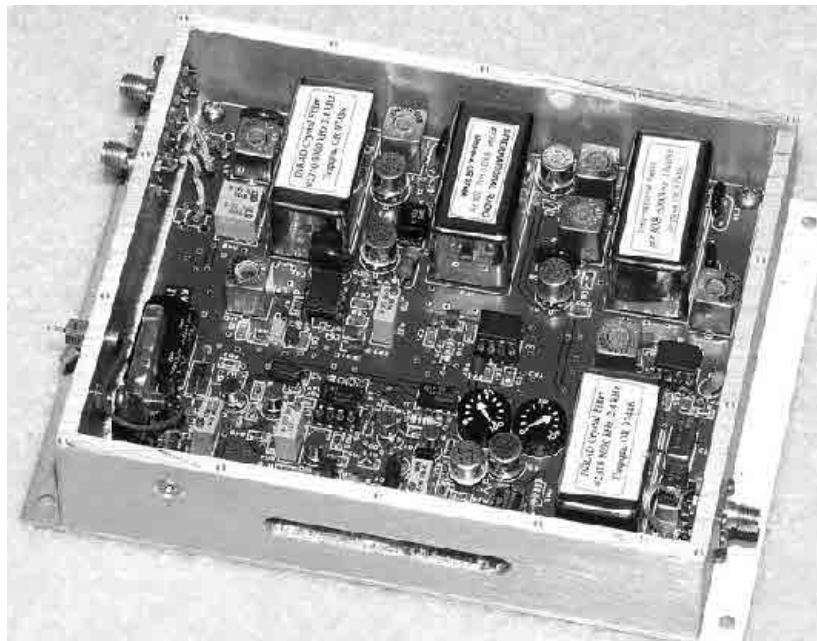


Figure 26 — Actual implementation of the IF9RX assembly. A specific double side ground plane stitched - plated through layout is used to maximize isolation between input circuits and output circuits in order to prevent oscillation in this very high gain (100 dB) assembly. All Quartz filters on the assembly have been expressly manufactured for the Star-10 by International Filter Company.

Heinrich Meyr and Gerd Ascheid, *Synchronization in Digital Communications: Phase - Frequency - Locked Loops and Amplitude Control*, John Wiley & Sons, ISBN 0-471-50193-x.


Lucien Boithias, *Radio Wave Propagation*, McGraw Hill, ISBN 0-07-006433-4.




Merrill Skolnik, *Radar Handbook*, Second Edition, McGraw Hill, 1990, Section 3.9.

T. T. Brown, "Mixer Harmonic Chart," *Electronics Magazine*, Apr 1951, pp 24, 132, 134.

Cornell Drentea, KW7CD, has been a ham since 1957. He has built many radios and transceivers and made his passion for designing "radios" his lifelong profession. As an amateur radio operator, he is known for his extensive RF technology articles in magazines such as ham radio, Communications Quarterly, RF Design, and QEX. Professionally, Cornell is an accomplished RF technologist, an engineer and a scientist with over 40 years of hands-on experience in the aerospace, telecommunications and electronics industry. He received his formal education abroad with continuing studies and experience achieved in the United States. Cornell has presented extensively on RF design topics at technical forums such as IEEE, RF-Expo, Sensors-Expo and has given comprehensive professional postgraduate courses in RF receiver design, synthesizer design, sensors and communications. He has published over 80 professional technical papers and articles. He is the author of the book, Radio Communications Receivers, McGraw Hill, ISBN 0-8306-2393-0 and ISBN 0-8306-1393-5, 1982. You can find out more about Cornell, on his web site: members.aol.com/cdrentea/myhomepage/

NATIONAL RF, INC.



 <p>VECTOR-FINDER Handheld VHF direction finder. Uses any FM xcvr. Audible & LED display. VF-142Q, 130-300 MHz \$239.95 VF-142QM, 130-500 MHz \$289.95</p>	 <p>ATTENUATOR Switchable, T-Pad Attenuator, 100 dB max - 10 dB min BNC connectors AT-100, \$89.95</p>
 <p>DIP METER Find the resonant frequency of tuned circuits or resonant networks—ie antennas. NRM-2, with 1 coil set, \$219.95 NRM-2D, with 3 coil sets (1.5-40 MHz), and Pelican case, \$299.95 Additional coils (ranges between 400 kHz and 70 MHz avail.), \$39.95 each</p>	 <p>DIAL SCALES The perfect finishing touch for your homebrew projects. 1/4-inch shaft couplings. NPD-1, 3/4 x 2 1/4 inches 7:1 drive, \$34.95 NPD-2, 5/8 x 3 1/8 inches 8:1 drive, \$44.95 NPD-3, 5/8 x 3 1/8 inches 6:1 drive, \$49.95</p> <p style="font-size: small;">S/H Extra, CA add tax</p>

NATIONAL RF, INC
7969 ENGINEER ROAD, #102
SAN DIEGO, CA 92111

858.565.1319 FAX 858.571.5909
www.NationalRF.com

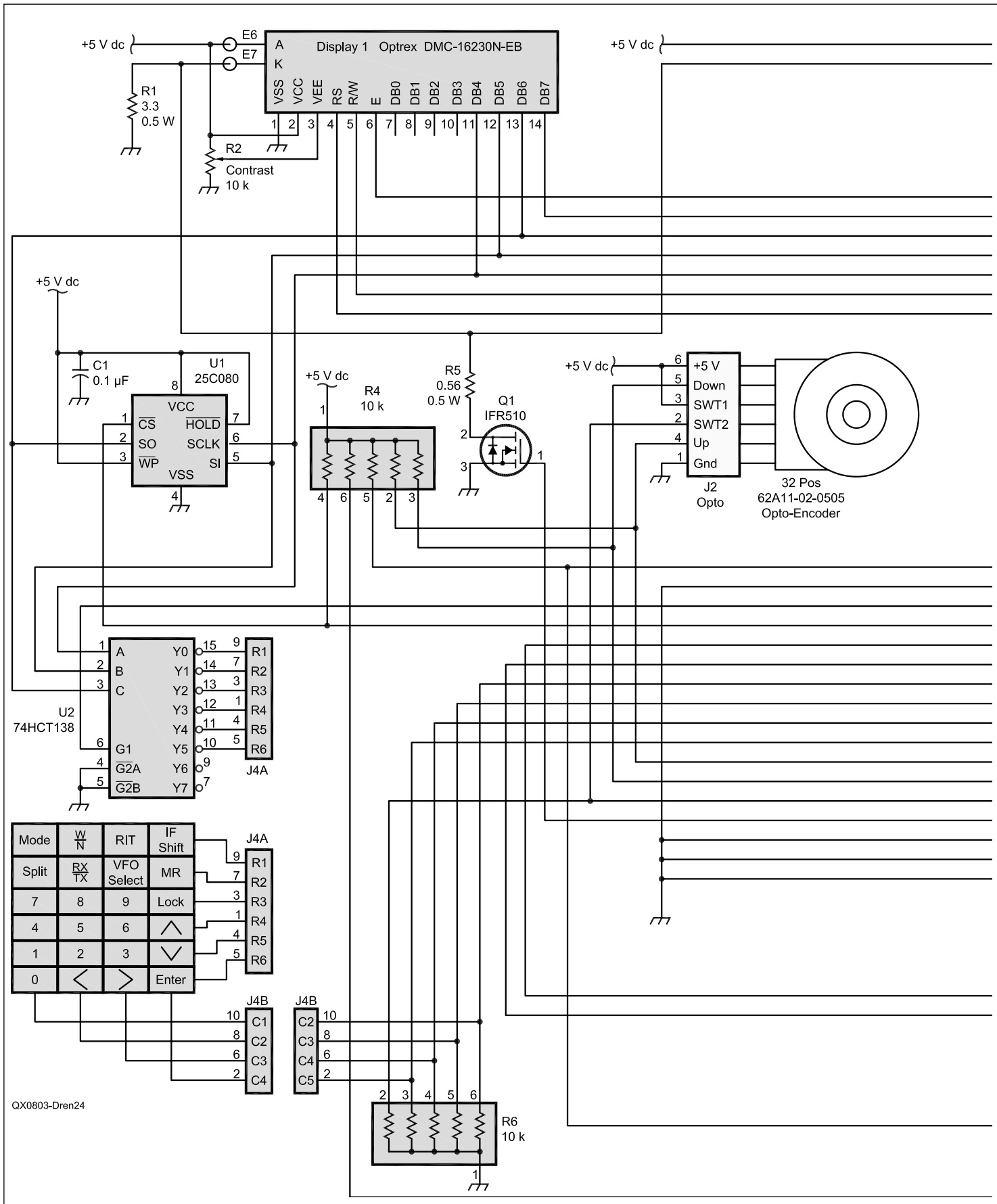
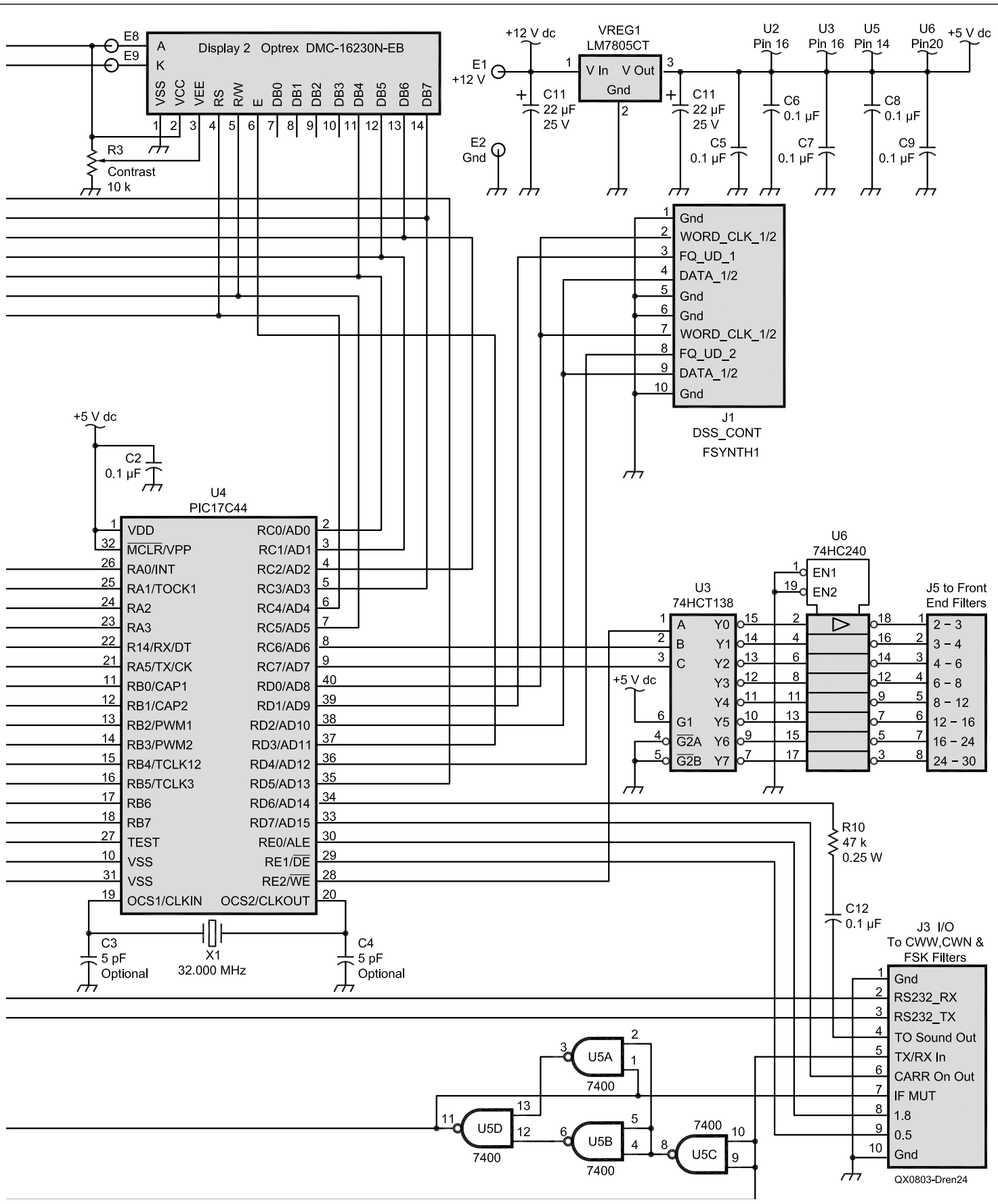


Figure 24 — Schematic diagram of the DFCB command and control system.



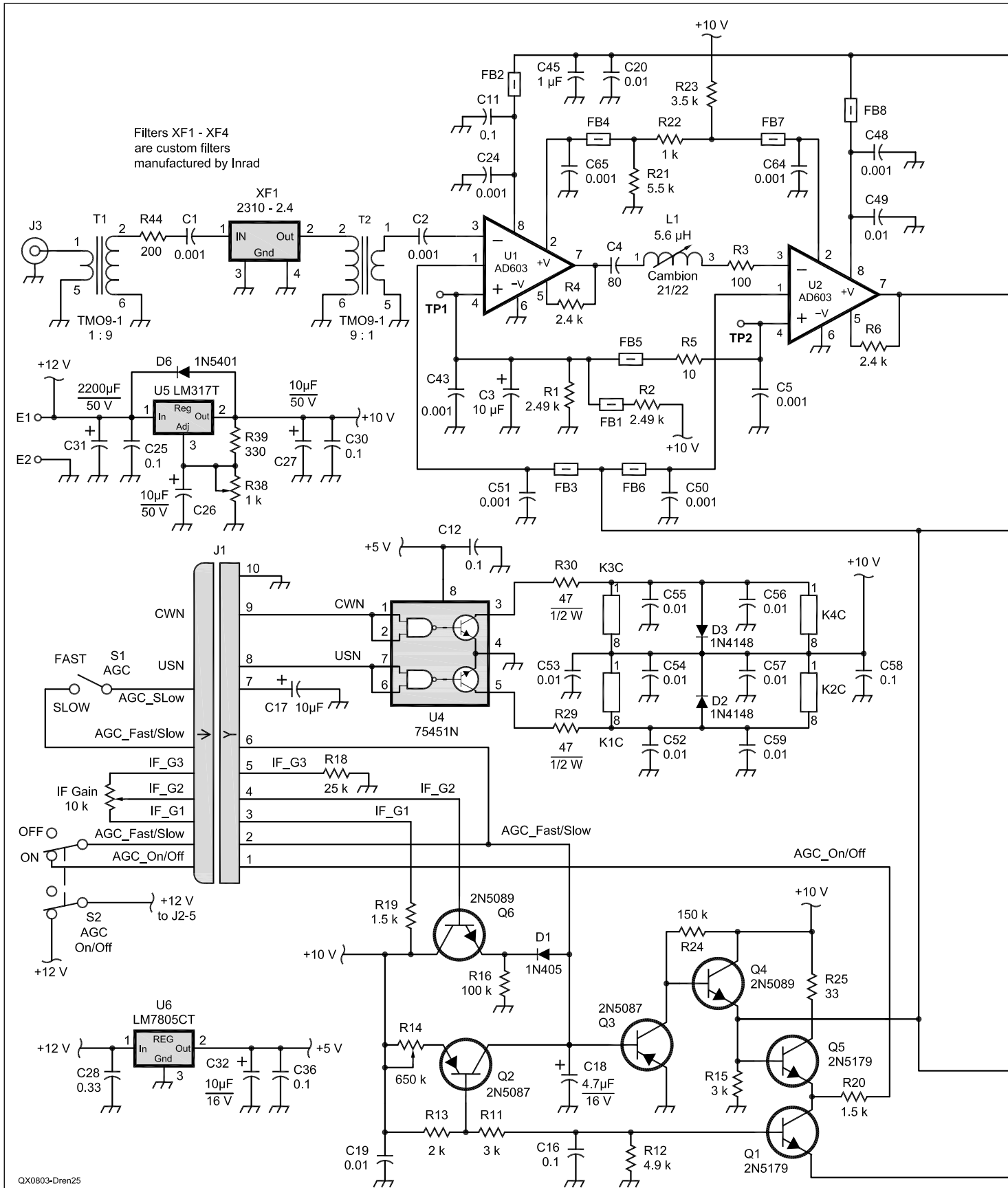
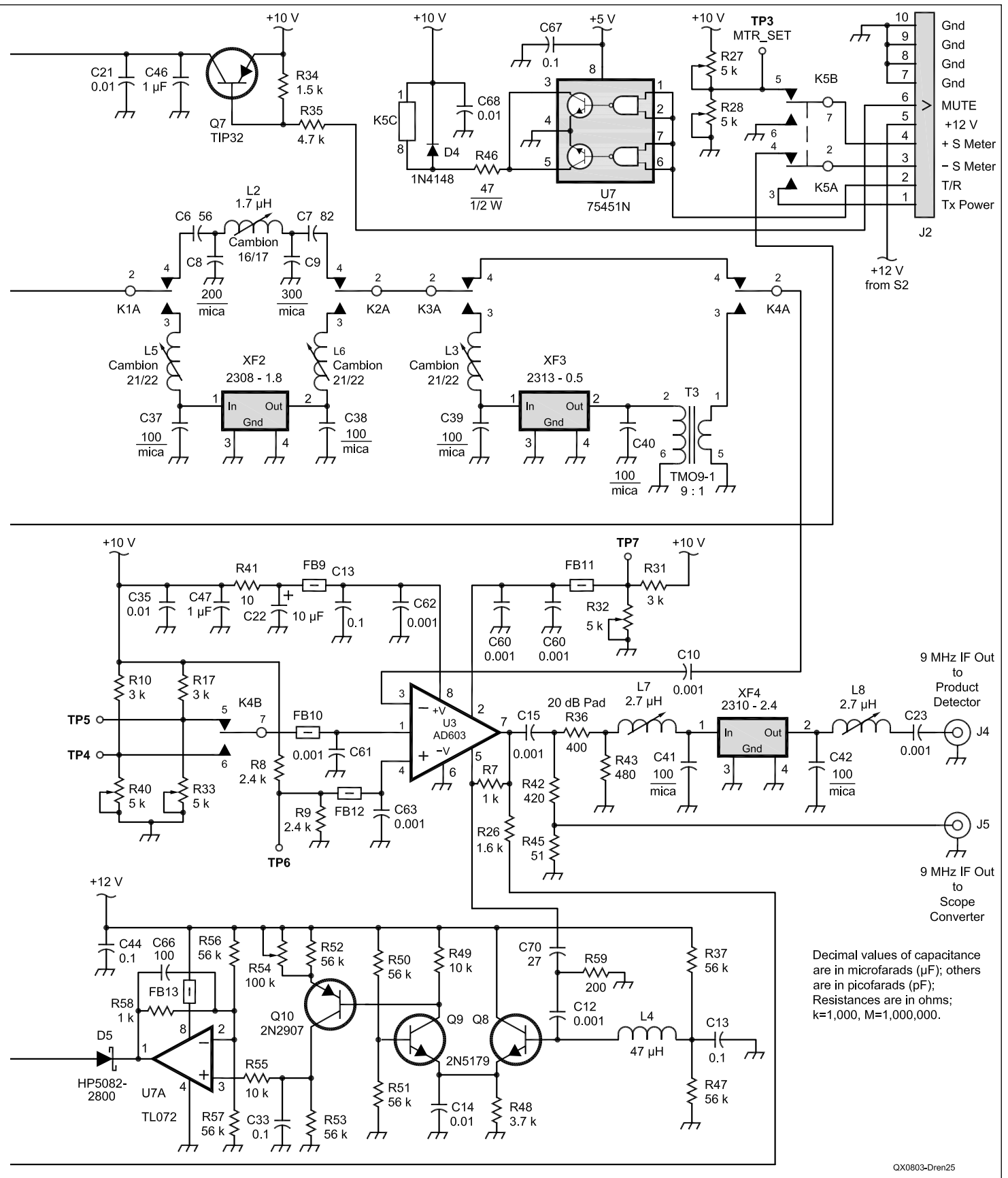


Figure 25 — Schematic diagram of the IF9RX assembly. Two 2.4 kHz - wide filters (one at the IF input and one at the IF output) are always in the circuit. Additional filters for SSB narrow (1.8 kHz) and CW/AFSK narrow (500 Hz) are inserted or shorted out from the command and control DFCB assembly using the keypad and the intelligence built into DFCB microprocessor. Two AD603s are used for AGCed gain and



Decimal values of capacitance are in microfarads (μF); others are in picofarads (pF); Resistances are in ohms; k=1,000, M=1,000,000.

a third AD603 is used after the 1.8 kHz filter and the 500 Hz filter to compensate for the insertion loss of the selected filters. All filters are cascaded in an AND function rather than selected individually in an OR function, to optimize shape factor and depending on the mode and bandwidth selection. 32 poles of maximum filtering are possible.



Carbon Composition, Carbon Film and Metal Oxide Film Resistors

Resistance, inductance and capacitance data was measured for various resistor construction types

While it's no secret in the Amateur Radio community that carbon composition (CC) resistors drift with age, I had filed that bit of knowledge in the back of my mind, as it's been some time since I built a project with a CC resistor.¹ Like all good builders, I'm a pack rat, and recently ran across a stash of a few hundred ½ W CC resistors when looking in a remote corner of the garage for a hose nozzle. These resistors were purchased new in the early 1960s, to the best of my knowledge, and were still in International Resistance Corporation original factory "Grip Reel" packaging. Curiosity led me to measure these resistors to see if they were still "in spec" after 45 years or more in uncontrolled storage. Those measurements suggested further exploration to see how these "new old stock" parts stacked up with modern carbon film and metal film general purpose resistors, in terms of tolerance, high frequency response, inductance and stray capacitance.

Carbon Composition Construction

With CC resistors now largely relegated to special purposes, they may not be familiar to newer amateurs.² Ohmite, one of the few remaining manufacturers of CC parts, describes their construction this way:

Carbon composition resistors are manufactured by extruding a blend of carbon and organic binders inside a phenolic outer body. The extrusion is cut to length, leads inserted, cured, and marked to form a finished resistor. The carbon and binder mixture is adjusted to produce different resistance values. The resistors are sorted for 5%, 10%, and 20% tolerance values.³

Figure 1 is a notional diagram of a typical CC resistor, and Figure 2 is a 4700 Ω, 2 W CC resistor cut in half longitudinally. The carbon particles are microscopic and cannot be separated from the binder

material with the naked eye.

Figure 1 has several points of note:

1) Contact between conducting carbon particles is mechanical and depends upon the pressure exerted by the binding material. This pressure, and hence the resistor value, can vary with time, vibration and temperature cycling.

2) The body is not hermetically sealed; hence moisture may ingress and increase inter-particle resistance, thereby increasing the resistor value.

3) Since the material is not homogenous,

capacitance between particles provides an alternative path, as illustrated in Figure 3. At radio frequencies, therefore, the resistor value will be below its dc resistance.⁴

4) The relatively large end plugs also have capacitance between them.

5) The CC resistor structure lends itself to minimum inductance as it is a straight, linear conductor.

6) Since the construction relies upon mechanical contact between adjacent particles, CC resistors are prone to generating excess noise.

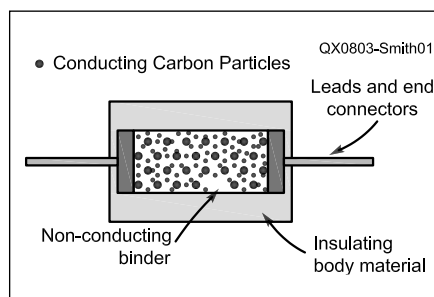


Figure 1 — This diagram illustrates the typical construction of a carbon composition resistor.

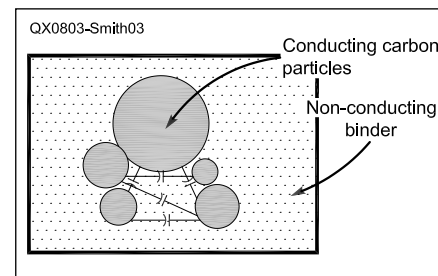


Figure 3 — The mixture of carbon particles and nonconducting binder material is not homogenous. In addition to the conductive path through carbon particle contact, there is some capacitance between nearby particles, creating a capacitive alternate path through the resistor for ac signals.

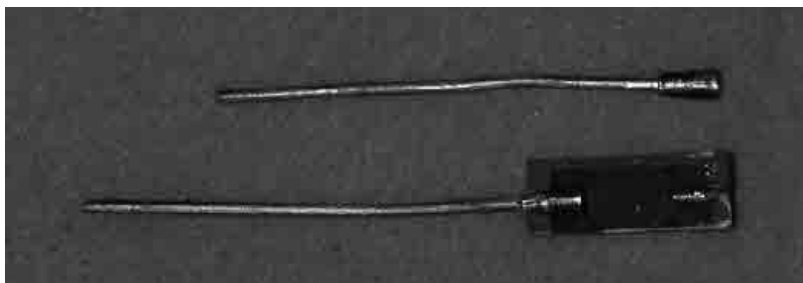


Figure 2 — This photo shows a 4700 Ω, 2 W carbon composition resistor that has been cut in half along its length.

¹Notes appear on page 53.

7) Heat generated during a short-term overload is distributed relatively uniformly through the entire resistor.

Carbon and Metal Film Construction

As their name suggests, carbon film (“CF”) and metal film resistors use a thin film of carbon or metal or metal oxide as the resistive element. Carbon film is commonly used for 5%, ¼ W parts, with metal or metal oxide film found in precision and high power resistors. The film is deposited over a ceramic tube, trimmed to final resistance value, and given a protective coating and color coding stripes or other identification.

The conceptual rub in this statement, however, is “trimmed to final resistance.” The film is deposited with a thickness and composition so that the resistance is significantly below the desired value. The deposited film is mechanically cut away until the target resistance is achieved, using either a laser or a diamond-tipped tool. Each CF resistor is individually measured and trimmed, a highly automated process. Figure 4 shows three ¼ W CF resistors with the protective coating removed. All three resistors exhibit a spiral pattern. These resistors, at least, are combination inductors and resistors. I’ve also checked 1 W and 2 W metal oxide film resistors and found them to also have the same spiral cut pattern. It would be possible to trim the film with a less inductive pattern, but all the resistors I’ve looked at are spiral cut. Later in this article, we’ll explore whether this inductance is actually a problem, and whether CF resistors look inductive or capacitive at HF and VHF.

To summarize the CF construction-related issues:

1) It avoids most of the particle-associated flaws of the CC resistor, as the resistance is a single structure.

2) Spiral trimming forms an inductor, albeit of low value.

3) Since each individual part is measured and trimmed, adherence to tolerance will be better than for a CC part.

4) Both the ceramic substrate and film retain usefulness at elevated temperatures, with 100°C or greater ratings common.

5) The film composition can be selected for temperature stability, with metal film being better than carbon film.

6) During a short-term overload, it is possible for a “hot spot” to form and damage the conductive film causing an open circuit.

Surface Mount Construction

Surface mount resistors are commonly available in “thick film” and “thin film” types. Both are constructed on a ceramic (usually alumina) substrate, generally with a fired-glass protective coating. Thick film

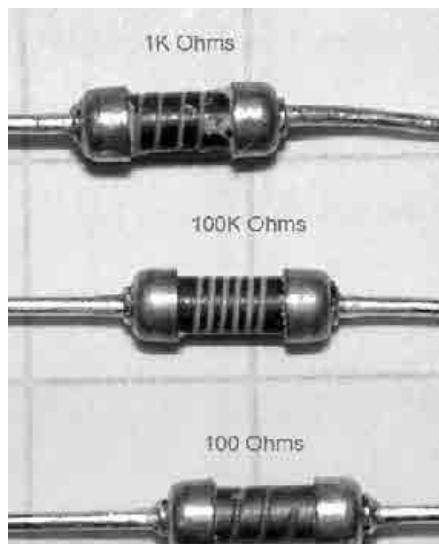


Figure 4 — Here are three carbon film resistors, shown with their protective coating removed. The spiral cuts into the conductive film are easy to see.

parts are manufactured with a process similar to printing — a paste containing a conductive material, such as ruthenium dioxide, is silk screened onto a large substrate and then baked at a high temperature until it fuses into a solid. By varying the conductive/non-conductive mix of the paste, different resistances are produced.

Thin film parts sputter or vacuum deposit the film onto the substrate, which can be alumina or more exotic materials, such as

quartz or Beryllium oxide. Thin film material includes tantalum nitride, ruthenium dioxide and nickel chromium, among others. If more complex structures are required, the deposited material can be further processed by photo etching, similar to the way integrated circuits are manufactured.

Abrasive or laser trimming is used to bring both thick and thin film parts into tolerance. Likewise, cutting the larger substrate into individual parts, coating them with a glass surface, applying end caps and printing component values is required for both thin and thick film resistors.

To summarize surface mount construction-related performance issues:

1) Parts have no leads and physically small size, reducing their stray inductance and capacitance. Their structure is a linear conductor, which further minimizes inductance.

2) Individually trimmed parts will be close to nominal value.

3) Thin film parts are generally manufactured in tighter tolerances than thick film parts and are more expensive.

Sample Parts Tolerance

I started my research into resistors out of curiosity over the old ½ W CC resistors found in my garage, and my first measurements looked at the resistance of these old parts. The values varied from 3.3 kΩ to 1 MΩ, with a mix of 5% and 10% tolerance, and generally between five and ten parts of each value. Figure 5 compares the mean

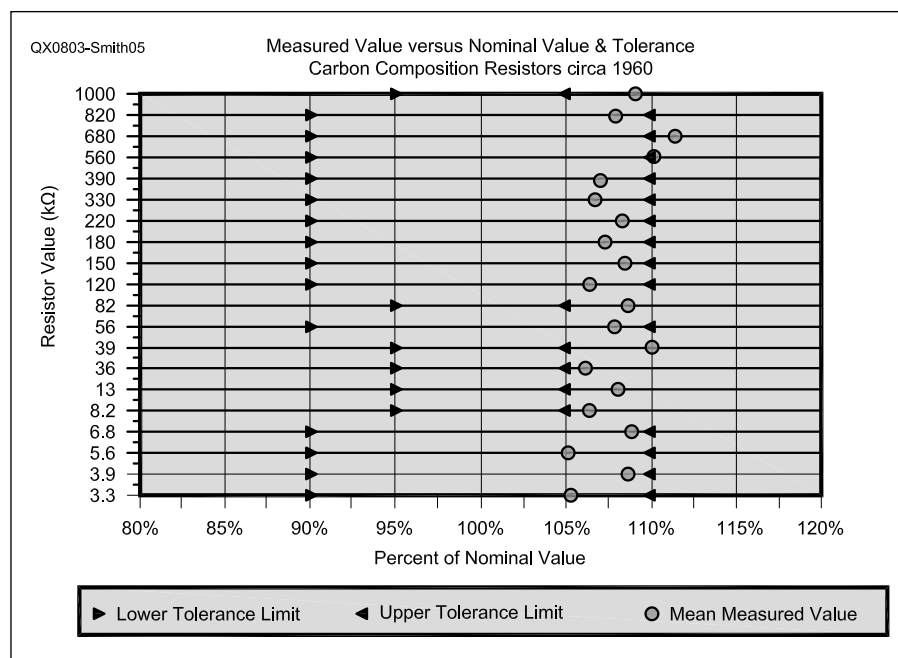


Figure 5 — This graph shows the average measured values of some old carbon composition resistors compared with their nominal values (100%). The limits show the 5% tolerance and 10% tolerance range.

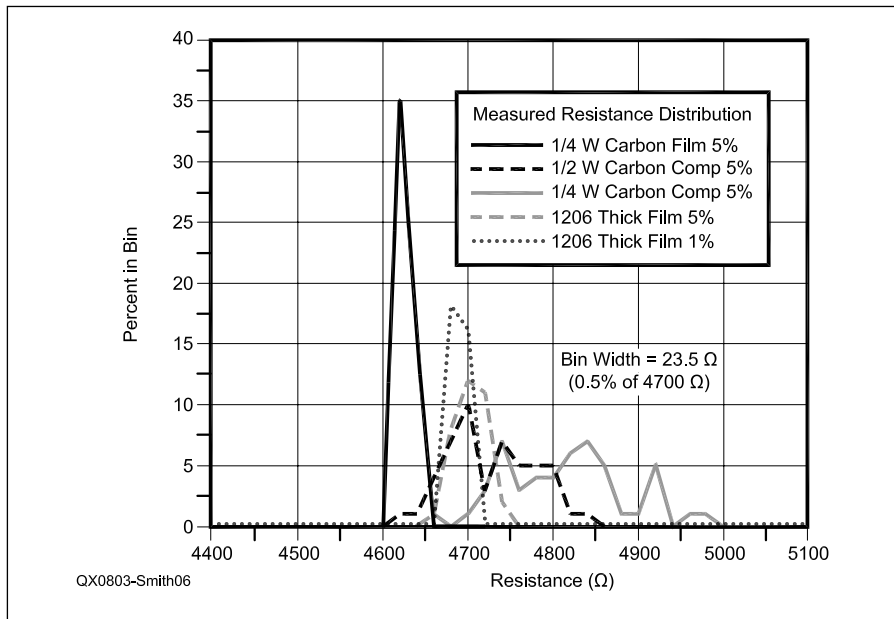


Figure 6 — This graph compares measured values of several resistor construction types.

value of these resistors to their tolerance limits. By “mean value” I mean the average of all of the resistors of each value. In measuring the CC resistors, I found one or two that were clearly defective, and excluded them from the data.

I used a General Radio 1658 Digibridge to measure these values, after first verifying its accuracy by comparing it against new 0.1% tolerance resistors as well as an HP 3456A and an HP3568A digital meter. The verification showed agreement well within the Digibridge’s rated $\pm 0.1\%$ accuracy. The Digibridge makes resistance measurements at 1 kHz, while the two HP digital meters operate at dc. For resistor values and construction considered in this article, there is no difference at the 0.1% level between 1 kHz and dc data. All three instruments use Kelvin “four-wire” techniques, effectively canceling test lead resistance. I used a Quadtech 1689-9601 BNC adapter box with Quadtech 7000-05 “Chip Component Tweezers” to measure surface mount parts with the 1658. This combination extends the $\pm 0.1\%$ four-wire measurement ability of the 1658 to the tweezers tip.

As Figure 5 shows, the mean values have all shifted upward, by at least 5%, and there’s

no obvious correlation between the nominal value and degree of shift. Further, the 5% and 10% tolerance parts seem to have shifted similar percentages. In fact, none of the 5% parts had a mean value within tolerance. Some individual resistors were within 5% tolerance, but those were uncommon.

The normal explanation for upward drift in CC resistors is storage under humid conditions which causes changes in particle-to-particle contact. Age alone, even under dry storage conditions, also causes a similar upward drift in component value for the same reason, although humidity apparently accelerates the drift. The resistors in my garage were exposed to 20 years of hot, humid northern Virginia summers and cold winters, as well as being at least 40 years old. To test the degree of drift, I purchased 100 new CC resistors, manufactured by Xicon, with a 4.7 k Ω nominal value in $\frac{1}{4}$ and $\frac{1}{2}$ W ratings. I measured 50 of each power rating as well as 50 4.7 k Ω , $\frac{1}{4}$ W carbon film resistors. I also measured 34 5% 4.7 k Ω 1206 thick film surface mount resistors and 34 1% 4.7 k Ω 1206 thick film surface mount resistors. Figure 6 and Table 1 present the results of those measurements. Interestingly, three of the 50 new $\frac{1}{4}$ W CC resistors were outside

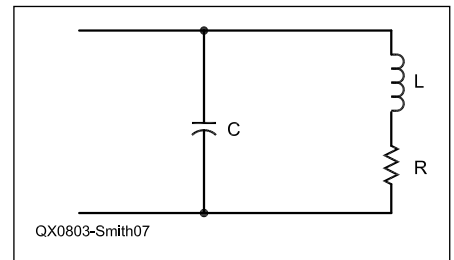


Figure 7 — This simple model is often used to characterize the performance of a resistor at HF.

the 5% tolerance band. More important, of course, is that even *new* CC resistors are far more likely to be above their nominal 4700 Ω value than below nominal value. Of course, this data is drawn from a limited number of parts, and may not necessarily apply to other manufacturers’ parts or even to other samples of Xicon CC resistors. It does suggest, however, that caution should be exercised even with new CC parts, and checking their value before use is advisable.

Of equal interest is the performance of the CF and thick film parts. All are quite close to nominal value, and have a tightly grouped spread of values. As we might expect, carbon film resistors are below nominal value — the blanks are low and trimming increases resistance. As a matter of manufacturing economy, therefore, we would expect the expensive trimming process to terminate when the part is within an acceptable tolerance, rather than continuing trimming to center on the nominal value. The mean resistance of the 50 CF resistors is -1.56% from nominal, which suggests this particular lot was manufactured with a trimming cutoff around -1.5% . The standard deviation at 6.4 Ω (0.14% of nominal value) is extremely good for a 5% part. Indeed, these CF parts demonstrate a standard deviation nearly as good as the 1% thick film surface mount resistors. Of course, the 1% resistors are closer to nominal value; with a mean value only -0.2% below 4700 Ω .

Radio Frequency Performance

As we’ve seen from looking at how resistors are constructed, there’s reason to wonder how they behave at radio frequencies. From

Table 1
Mean and Standard Deviation, New 4700 Ω Resistors

Resistor Type	Number of Samples	Mean Resistance (Ω)	Standard Deviation (Ω)
$\frac{1}{4}$ W carbon film, 5%	50	4626.6	6.4
$\frac{1}{2}$ W carbon composition 5%	50	4728.3	49.5
$\frac{1}{4}$ W carbon composition 5%	50	4813.6	70.3
$\frac{1}{4}$ W 1206 5% thick film	34	4703.1	17.7
$\frac{1}{4}$ W 1206 1% thick film	34	4690.4	5.6

our quick survey, we expect the CC resistor to show decreased resistance with increasing frequency, as the carbon granules are partially bypassed by particle-to-particle capacitance. CF resistors, in contrast, should look more like inductors as frequency increases, with some bypassing effect from turn-to-turn distributed capacitance. Surface mount parts have no spirals or particle-to-particle construction, and we expect skin depth and end-cap-to-end-cap capacitance to dominate high frequency performance. Leaded parts will additionally exhibit series inductance from the leads, as well as capacitance between end caps. And, of course, stray capacitance from the resistor body to ground or other nearby circuit elements will affect how the resistor looks at high frequencies.

Figure 7 is a simple model commonly used to characterize a resistor's HF performance. C is stray capacitance across the resistor body resulting from capacitance between end caps, particle-to-particle capacitance in CC resistors and, in the case of spiral-cut film resistors, distributed capacitance between turns. L is the resistor's self-inductance. For a spiral-cut film resistor, it will be mostly from the solenoid-type windings. In a carbon composition resistor, it will be that of a straight conductor. (In all cases, of course, lead wire inductance is present, as is the inductance of the loop formed by the resistor and its leads when connected to the test fixture.) R is the resistance. Film resistors will have a higher RF resistance than dc resistance due to skin effect, although for the resistors I measured the difference is overshadowed by other effects. Carbon composition resistors also have skin effect factors, but the internal capacitance between conducting granules more is important, which leads to a bypass effect.

To assess these effects, I measured a selection of resistors with an HP 8752B vector network analyzer and homemade test fixture, as summarized at Table 2. The associated sidebar "Parallel or Series" provides more details on my test setup. Vector network analyzers are tremendously useful tools in radio work, but become significantly less accurate where the component being tested has resistance or reactance outside the range 5Ω to $2 \text{ k}\Omega$.⁵ Hence, I've limited my resistor choice to two values, 47Ω and $4.7 \text{ k}\Omega$. Although above the recommended $2 \text{ k}\Omega$ limit, the $4.7 \text{ k}\Omega$ VNA data is consistent with my measurements using a Boonton 250A RX Meter.⁶

End Cap Capacitance

I also determined the capacitance between end caps for $\frac{1}{4}$ W carbon film and 2 W metal oxide film bodies by mechanically removing their conducting film with an abrasive and measuring the end-to-end capacitance with a General Radio 1658 Digibridge at 1 kHz.

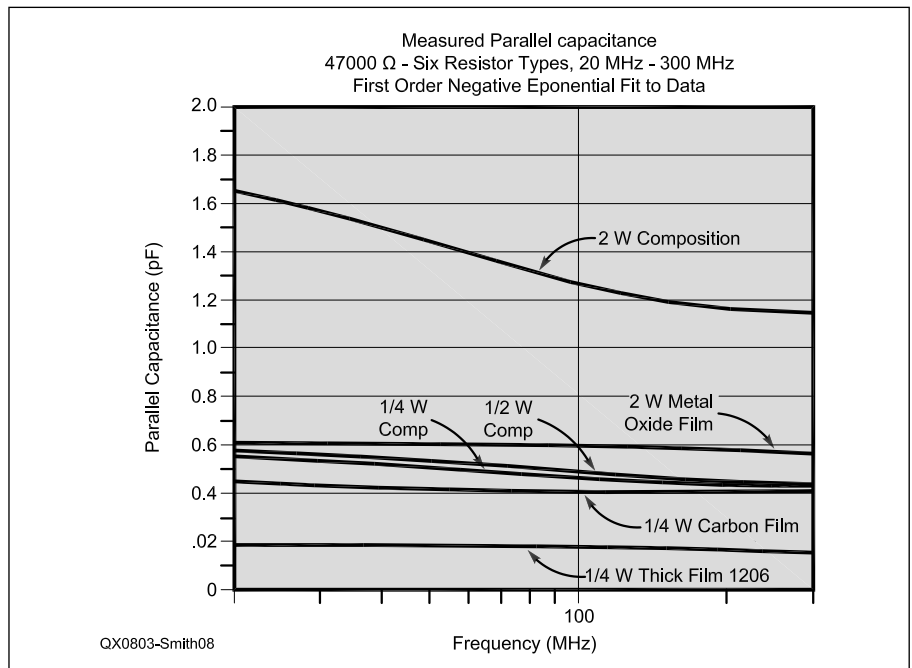


Figure 8 — This graph shows the measured parallel (shunt) capacitance of the various resistor construction types tested.

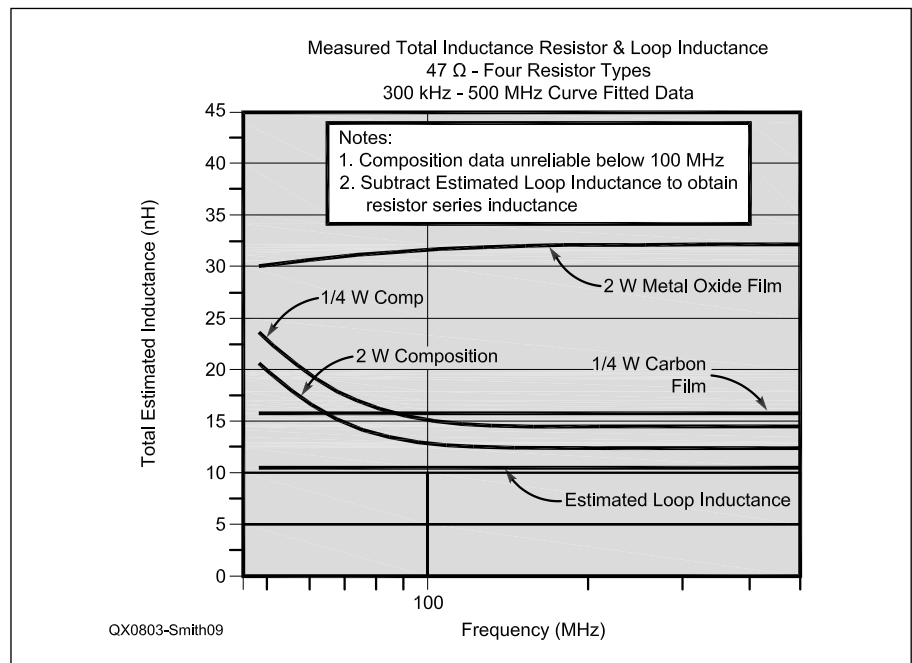


Figure 9 — This graph represents the measured inductance for the resistor construction types tested.

Table 2
Resistors Tested

Construction	Value (Ω)	Power Rating (W)	Frequency Range
Carbon Composition	4700	$\frac{1}{4}$, $\frac{1}{2}$ and 2	300 KHz - 300 MHz
	47	$\frac{1}{4}$ and 2	300 KHz - 500 MHz
Carbon Film	4700	$\frac{1}{4}$	300 KHz - 300 MHz
	47	$\frac{1}{4}$	300 KHz - 500 MHz
Metal Oxide Film	4700	2	300 KHz - 300 MHz
	47	2	300 KHz - 500 MHz
Thick Film (1206 surface mount)	4700	$\frac{1}{4}$	300 KHz - 300 MHz

The ¼ W carbon film resistors had a capacitance of 0.08 pF. (As a cross-check, the end-cap capacitance is 0.072 pF measured with an 8752B VNA at 100 MHz.)

The 2 W metal oxide film resistors had a capacitance of 0.15 pF.

In modeling a film resistor, of course, the turn-to-turn distributed capacitance should also be considered.

Measured Total Capacitance

For our RLC resistor model of Figure 7, the imaginary part of Equation 10 (from the sidebar) is the susceptance measured by the VNA:

$$IM(Y) = B = \frac{-j\omega [L(1 - \omega^2 LC) - CR^2]}{R^2 + \omega^2 L^2} \quad [\text{Eq A}]$$

C is the total shunting capacitance, which includes end-cap to end-cap and turn-to-turn capacitance plus uncompensated strays to the test fixture. Rather than using Equation A to solve for C based on measured B, R and computed L, we first see if it is possible to ignore the R and L terms. As demonstrated later in this analysis, for resistors of the type studied, we know the maximum expected L is 83.6 nH, representing a 2 W metal oxide film part with eight spiral turns. Based on the end cap measurements and other data, we expect the total shunting capacitance to be between 0.3 pF and 1.5 pF, with lower values of C causing the most error in neglecting R and L. Substituting R = 4700 and C = 0.3 pF into Equation A and comparing the results with L = 0 and L = 83.6 nH shows that up through 500 MHz we may ignore R and L and assume B represents only the shunting capacitance, with less than 1.5% error in computing the true shunting C. My calculations use this simplifying assumption.

Figure 8 presents the measured total shunting capacitance for the six resistor types measured. The excess capacitance over the end-cap to end-cap measurements in the CF and metal oxide film parts represents turn-to-turn capacitance, along with some strays to the test fixture.

All three CC resistors show the shunting capacitance diminishes with increasing frequency at a more rapid rate than the film resistors.⁷ I tried to keep the lead length of all test parts equal, except, of course, the surface

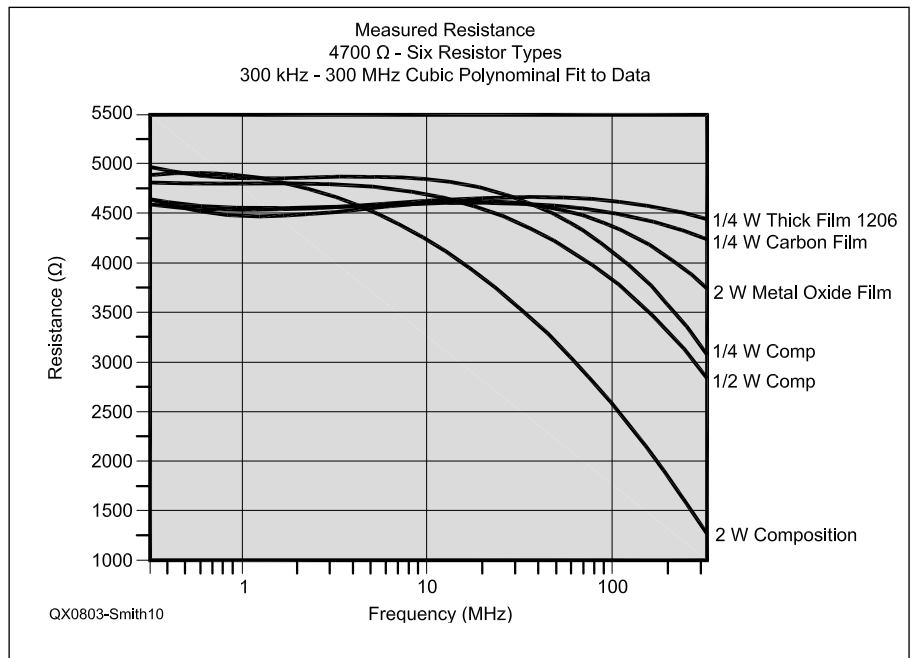


Figure 10 — The actual resistance of the resistor construction types tested is shown on this graph.

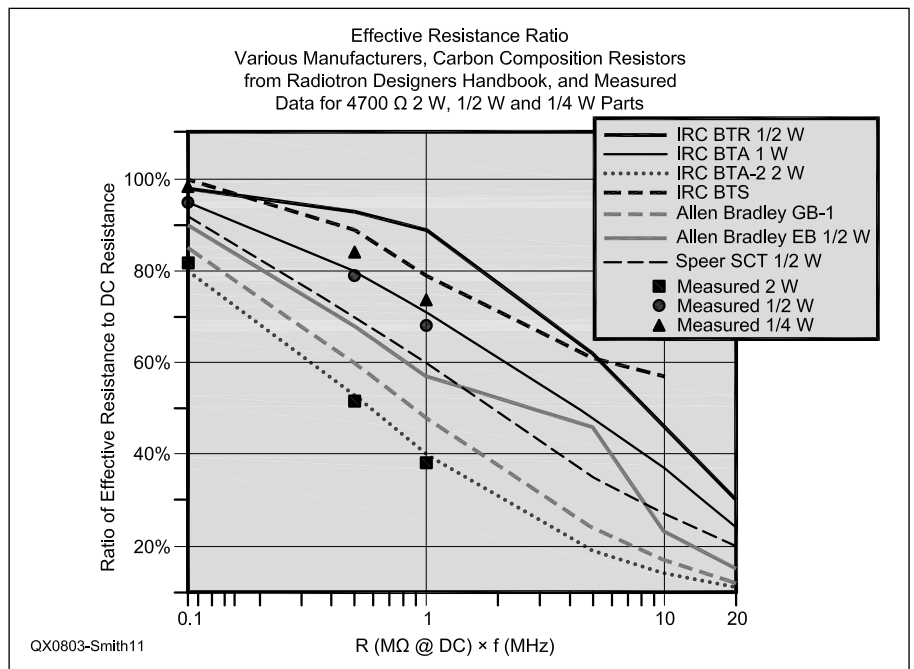


Figure 11 — The effective resistance value of carbon composition resistors will vary with frequency, generally according to the graphs shown for various manufacturers.

Table 3
Measured Resistor Inductance

47 Ω Resistor Type	Raw Measured Inductance at 200 MHz (nH)	Net Inductance (nH)	Number Turns for Film Part	Predicted Net Inductance (nH)
¼ W carbon film	15.7	5.7	2.5	4.7
2 W metal oxide film	31.8	21.8	4.25	23.6
¼ W carbon composition	15.1	5.1	—	—
2 W carbon composition	11.7	1.7	—	—

mount resistor, so the downward capacitance versus frequency tilt of the film parts likely represents the effect of internal and lead inductance effectively cancelling part of the parallel capacitance, as well as test fixture and calibration imperfections. (The resistor and leads form a loop with an estimated inductance of about 10 nH.) The cancellation effect and fixture errors are roughly the same for all leaded parts tested, so the extra downward slope of the CC parts is a real effect, not a measurement artifact.

Measured Inductance

It's also possible to measure the resistor's inductance directly via the real part of the admittance. Looking only at the real part of the admittance, we find:

$$\text{Re}(Y) = G = \frac{R}{R^2 + \omega^2 L^2} \quad \text{Equation B}$$

Equation B may be solved for L with measured G and the assumption that R does not change with frequency (which we know to be close to true for film resistors).

In this case our accuracy problem is the reverse of measuring shunting capacitance, where we needed R to be large. To measure the inductance, we want R to not be too much greater than ωL . Otherwise, the R^2 term dominates, reducing the change in measured $\text{Re}(Y)$ with frequency and increasing measurement error. Based on the expected range of inductance value, I selected 47 Ω as a suitable R.

Figure 9 shows the total inductance extracted from measuring four 47 Ω resistors, along the estimated loop inductance, comprised of the resistor and leads and the return path on the test fixture foil. To obtain the resistor inductance, subtract the estimated loop inductance. The loop inductance is very sensitive to the wire and resistor diameter as well as the precise dimensions of the loop and the return path. My estimated 10 nH value is a combination of theoretical computation and measurement of various diameter wires, and should be regarded as only an estimate. The data is taken at 200 MHz as the measured data has stabilized by this frequency. (Lower frequencies, particularly with the CC parts, result in small ωL values and hence less accurate measurements.)

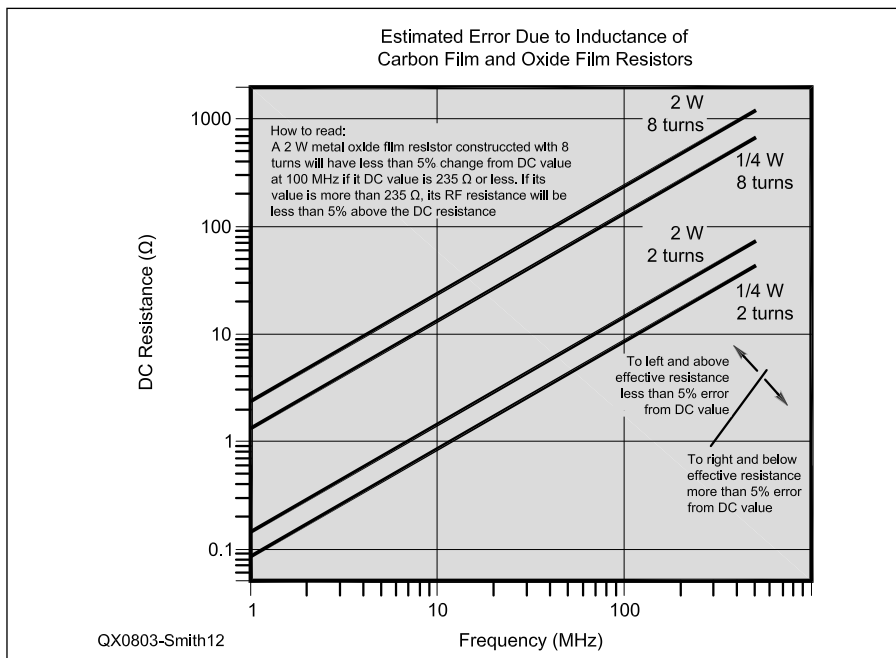


Figure 12 — This graph illustrates the 5% value change for film resistors, based on maximum and minimum inductance values.

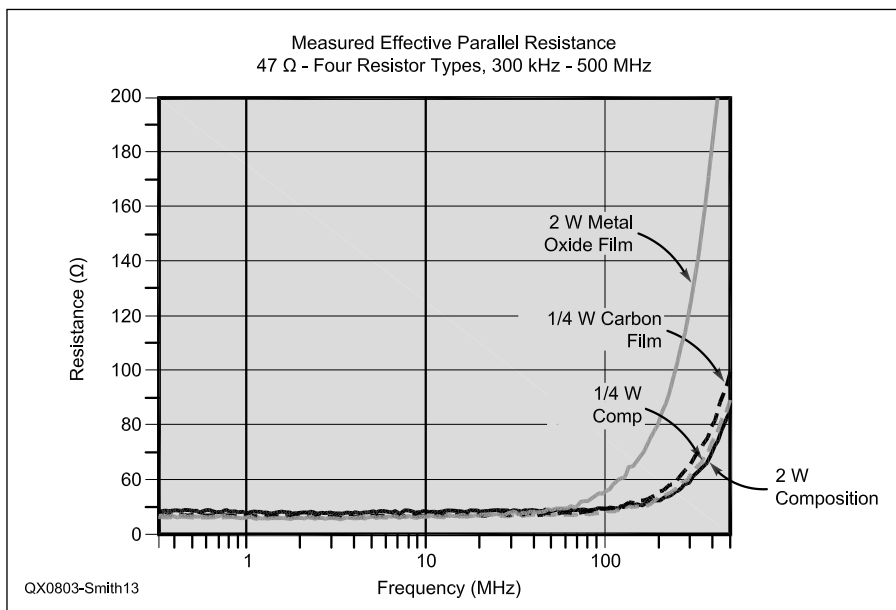


Figure 13 — The effective resistance values for four different resistor construction types are shown on this graph.

Table 4
Resistor Parameters

Type	Diameter	Length	Minimum Expected Turns Inductance (nH)	Maximum Expected Turns Inductance (nH)
2 W metal film form	0.155 in.			
3.94 mm	0.390 in.			
9.90 mm	2	5.2	8	83.6
¼ W carbon film form	0.0645 in.			
1.63 mm	0.116 in.			
2.95 mm	2	3.0	8	47.8

4700 Ω

Figure 10 shows the true (parallel) resistance of the six 4700 Ω resistors over the range 300 kHz to 300 MHz. (See the Sidebar — “Parallel or Series” for the difference between series and parallel resistance.) Below about 10 MHz, except for the 2 W CC part, there is not much difference between the low frequency and high frequency resistance. Above 10 MHz, however, there’s a pronounced drop in the measured resistance, with the 2 W CC resistor dropping to about 1250 Ω at 300 MHz. The ¼ W CF and ¼ W thick film surface mount resistors are relatively unchanged over the 300 kHz to 300 MHz range. Likewise, the 2 W metal oxide film part holds up reasonably well. All CC parts show decreasing resistance with increasing frequency, proportional to their power ratings.

Why is this? In particular, we’ve seen that the carbon film and metal oxide film resistors are constructed like inductors and hence sidebar Equation 13 says we should observe an increase in measured resistance with frequency, not a decrease.

4700 Ω Carbon Composition

First, the drop in resistance of CC parts is primarily a result of their distributed capacitance, as mentioned before. Different manufacturers of CC parts use different construction techniques which cause some differences in performance, but a CC resistor’s HF resistance generally varies as illustrated at Figure 11.⁸ Note the horizontal scale on Figure 11 is the product of the dc resistance in MΩ and the frequency in MHz. My measured data for the 2 W part fits the IRC 2 W curve well, although I do not know if this junkbox resistor is in fact an IRC part. My measured data for ¼ and ½ W Xicon CC parts is about half way between IRC’s and Allen Bradley’s ½ W data. These $f \times R$ curves, or similar curves supplied by some resistor manufacturers, can be used to estimate RF performance of medium to high value resistors.⁹ But, as seen with the 47 Ω measurements, lower value CC resistors are dominated by inductance.

Carbon Film, Metal Film and Thick Film Parts

As Figure 10 illustrates, film resistors hold their dc resistance much better than the CC parts, even though the carbon film and metal oxide film parts are clearly inductive. Why is this? If we recast sidebar Equation 13, the answer to this question becomes clearer:

$$\frac{1}{G} = R_{\text{measured}} = \frac{R_{\text{true}}^2 + \omega^2 L^2}{R_{\text{true}}} \quad [\text{Eq C}]$$

R_{measured} is the observed resistance, calculated from $1/G$.

R_{true} is the resistor’s resistance, as it would be without the series inductance.

If $\omega^2 L^2$ is small compared with R_{true}^2 , then the series inductance will not cause the measured resistance to increase significantly. What is the inductance of these film parts? To determine that, I’ve calculated the inductance based on the winding diameter and length and also measured the inductance of sample parts, as discussed earlier. Table 4 provides the physical dimensions of sample resistors measured with Mitutoyo Digamatic digital calipers, and the expected maximum and minimum number of turns, based on my disassembly of these parts, together with the calculated inductance.¹⁰

Figure 12 plots the “5% change” resistance values for these four maximum and minimum inductance cases based on sidebar Equation 15. Areas to the right and below each line represent combinations of dc resistance and frequency for which the effective RF resistance is more than 5% above the dc resistance. Areas to the left and above the line, conversely, are combinations of frequency and dc resistance for which the effective RF resistance is within 5% of the dc resistance. Of course, this plot excludes other circuit strays but still will be useful as a guide to determine when specific measurements are required.

Figure 12 predicts that a 4700 Ω resistor will not show more than 5% change in effective value through 300 MHz, even if it happens to be a 2 W metal film part with

eight spiral turns. (The 4700 Ω resistors I disassembled had only about four spiral turns.) Figure 10 bears this prediction out.

47 Ω

Figure 12 also predicts that a 47 Ω ¼ W carbon film or 2 W metal oxide film resistor may show resistance increase due to series inductance. Depending on how many spiral turns are cut into the 47 Ω parts, we may see a 5% increase in effective resistance as low as 20 MHz, or as high as 500 MHz. Removing the epoxy coating from the parts shows the sample 47 Ω ¼ W CF resistor to have 2.5 turns and the 2 W metal oxide film resistor to have 4.25 turns. The calculated inductances are 4.7 nH and 23.6 nH, respectively. Interpolating the curves of Figure 12 causes us to expect both parts to diverge from dc resistance over the upper portion of the 300 kHz to 500 MHz frequency sweep.

Figure 13, showing the effective resistance of four 47 Ω resistors over this frequency range, bears out the information in Figure 12.

The two CC parts, in contrast, better maintain their effective resistance for frequencies over 50 MHz.

Sensitivity to Inductance

It should be apparent from Equation C that at radio frequencies, a resistor’s effective resistance is highly dependent upon the series inductance, including the leads in my test setup. Even if a low inductance part is used, lead inductance can be appreciable and cannot be ignored for VHF and UHF work.

In certain circumstances, it’s possible to offset some of the resistor’s inductance. To illustrate this, I inserted a 47 Ω ¼ W carbon film resistor into a male BNC connector and measured its value with an HP872B VNA. In this case, however, the open/short/load calibration standards were BNC-type with low error. The particular BNC connector I used is intended for RG-174 coaxial cable and is a tight fit for a ¼ W resistor; in fact I had to shave some of the epoxy coating off to make the resistor fit into the connector’s sleeve. Sliding the resistor into the sleeve effectively adds capacitance to ground from each turn of the carbon film’s spiral turns, turning the inductor/sleeve combination into a low pass filter. Figure 14 shows the equivalent circuit, whilst Figure 15 compares the measured resistance and the SPICE predicted response. I determined the low pass filter capacitance values in Figure 14 to provide the best fit to my measured response data. Measuring the resistor’s total shunting capacitance to ground when inside the connector provides values in the 2.5 to 3 pF range, consistent with the values used in the simulation. This particular almost perfectly flat frequency response, however, seems to have a large

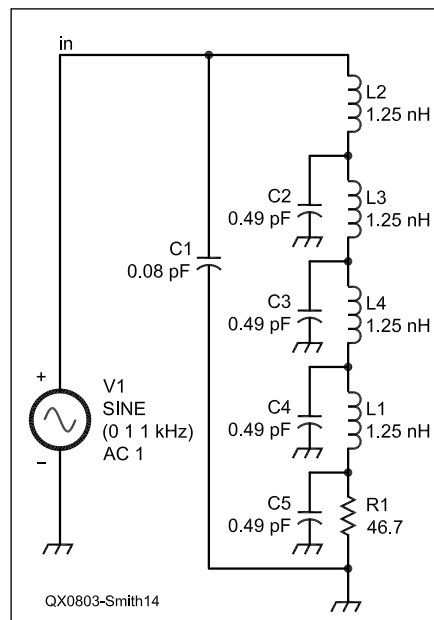


Figure 14 — This equivalent circuit represents a film resistor inside a metal sleeve, so that each turn of the spiral-cut resistance material has capacitance to the grounded metal sleeve.

degree of happenstance associated with it, as very small changes in the turn-to-ground capacitance causes a large change in frequency response in *SPICE* studies.

Conclusions

1) Don't be afraid of metal film or carbon film parts for RF work. Used intelligently, these parts will provide superior performance compared with carbon composition resistors. However, low value (under roughly 100 Ω) 2 W (and, I believe the 1 W versions as well) metal film resistors may be troublesome much above 50 MHz.

2) In repairing equipment, particularly VHF or UHF, keep in mind that the characteristics of carbon composition resistors may have entered into the design. Consequently, it is necessary to evaluate whether the original resistor type is required to assure performance.

3) With a program such as *LTspice* you can accurately model a carbon film or metal oxide film resistor's radio frequency performance by determining its inductance (based on the number of spiral-cut turns) and its capacitance.¹¹ The data in this paper can be used for a capacitance estimate and the number of spiral-cut turns can be found by removing the epoxy coating from a sacrificial part. Figure 16 shows a simple *SPICE* model of 1/4 W carbon film resistor mounted in my home-made test fixture, while Figure 17 shows excellent agreement between *SPICE* simulation data and my VNA measurements.

4) Surface mount components are preferred over through-hole parts for superior accuracy and performance at radio frequencies.

5) There are a wide variety of specialty resistors manufactured, and their use may be called for rather than trying to make a stock part do a job it was not intended to perform.

Notes

¹See, for example, A. Karty, KD4BYW, "Unexpected Long-Term Resistance Increases in Resistors," *QST*, Apr 2002, pp 70-71; A. Weller, WD8KBW, "Composition Resistors — Trimmed and Otherwise," *QEX*, Jul 1985, pp 9-10; D. Andrus, WB6VYN, "Composition Resistors — A Dying Breed?" *QEX*, Oct 1985, pp. 2-5 (Correspondence); Correspondence, "Composition Resistor Gains Wide Recognition," *QEX*, Nov 1985, pp 2-3; H. Balyoz, W6YBP, "Remembering the Carbon Composition Resistor," *QEX*, March 1986, p 3.

²Carbon composition resistors tolerate short-term overload (pulse-type operation, for example) better than carbon film resistors. See, for example, Vishay Dale Co., "Selection Guide for Conversion of Carbon Composition Resistors," Document Number 31049, Revision 20-Jul-01, <http://www.vishay.com/docs/31049/ccxref.pdf>.

³Ohmite Mfg. Co., "Little Demon Carbon Composition Molded Resistors," http://www.ohmite.com/cgi-bin/showpage.cgi?product=little_demon, accessed at 23 July 2007.

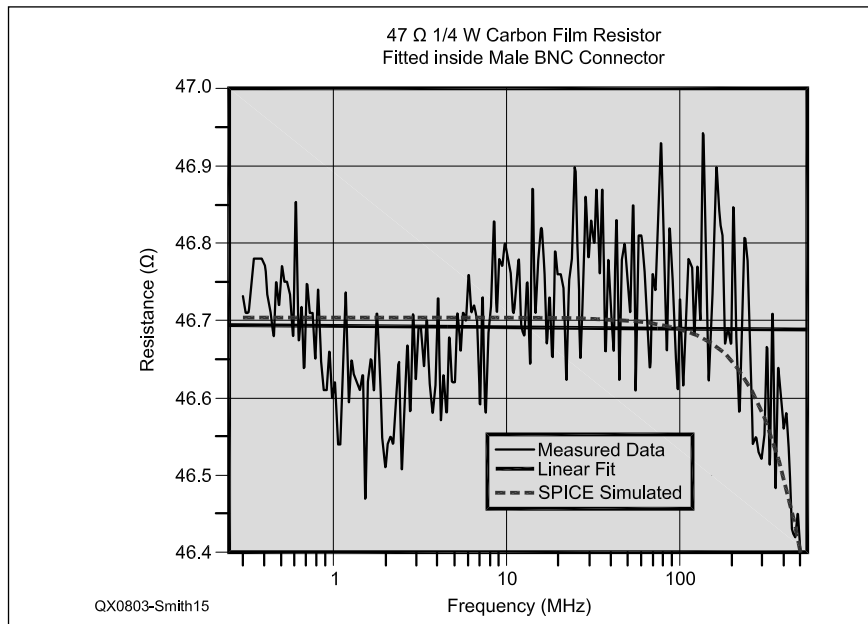


Figure 15 — A comparison of the measured carbon film resistor values and a *SPICE* circuit simulation.

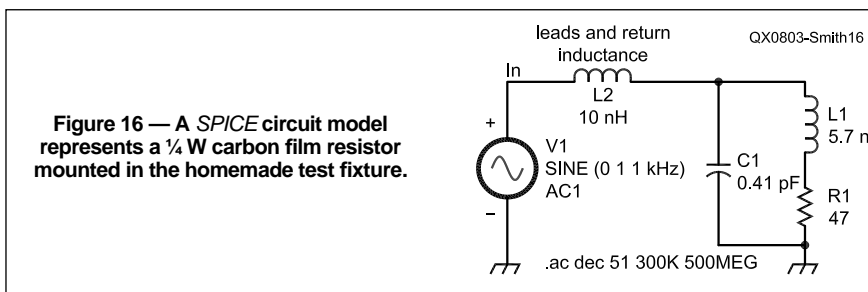


Figure 16 — A *SPICE* circuit model represents a 1/4 W carbon film resistor mounted in the homemade test fixture.

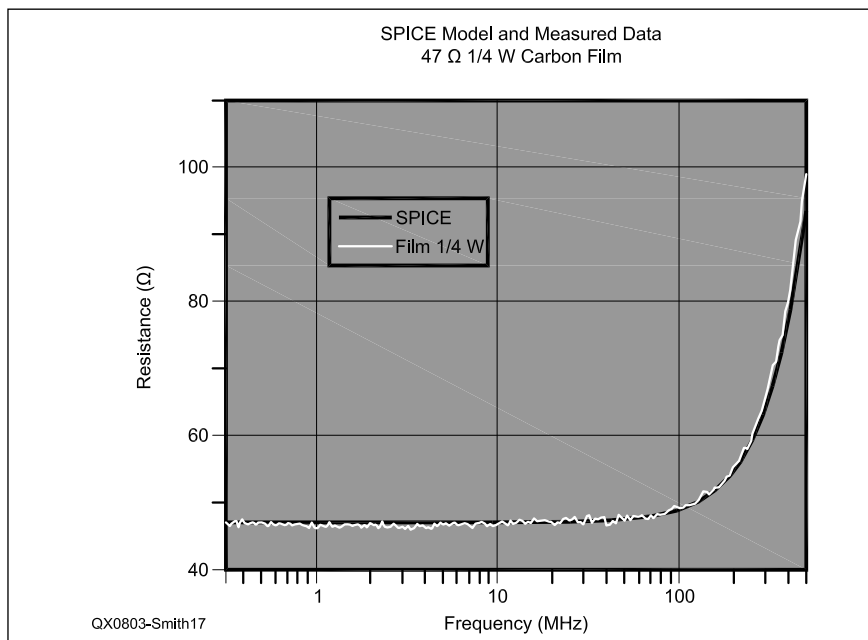


Figure 17 — This graph compares the measured data with the *SPICE* simulation data.

⁴Bowick, C., RF Circuit Design, 1982, Howard W. Sams & Co., Indianapolis, IN., p. 10.

⁵See, for example, Agilent Technologies, "Agilent Advanced impedance measurement capability of the RF I-V method compared to the network analysis methods, Application Note 1369-2" Document No. 5988-0728EN, July 26, 2001. This Application Note may be downloaded from Agilent's Web site at <http://cp.literature.agilent.com/litweb/pdf/5988-0728EN.pdf>.

⁶The combination of nanohenry inductance and resistance makes it very difficult to measure inductance via resonance, as normally used in a Q-meter. I've tried measuring metal oxide film resistor inductance with both an HP4342A Q-meter at 70 MHz and a Boonton 160A Q-meter over the range 40 MHz – 260 MHz, without success. Agilent's Application Note 1369-2, op. cit., provides a good review of techniques for measuring very low Q inductors. Of the equipment in my shop, the most practical tool, other than the VNA, is a Boonton 250A RX meter, which directly measures parallel resistance and capacitance over the range 500 KHz – 250 MHz. As a manual bridge instrument, however, it requires balancing at each test frequency.

⁷I've found only limited data on expected carbon composition resistor capacitance. Anon., "Radio Component Handbook," 1948, Technical Advertising Assoc., Cheltenham, PA, p. 149 suggests 1.0 pF for ½ W CC parts and 0.5 pF for 1 W CC parts. One reference, F. Langford-Smith,

ed., *Radiotron Designer's Handbook*, 4th ed., 1953, Wireless Press, Sydney, Australia, reprinted Electron Tube Division, Radio Corp. of America, p. 189, suggests the RF capacitance of a CC resistor is approximately 1/3rd the low frequency capacitance, noting that the low frequency capacitance is the figure "normally published." My measured data for ½ W CC resistors is about 0.5 pF, broadly consistent with the published data.

⁸*Radiotron Designer's Handbook*, op. cit. p. 189. The figure plots tabular data provided in the RDH, which is described as experimental values.

⁹See, for example, www.ibselectronics.com/ibs/cmpnts/rgaco/catalog/K/K29-35.pdf for similar curves for ¼ and ½ W RGA carbon composition resistors. Essentially identical curves are provided by SPC Technology at www.spctechnology.com/prodinfo/specs/TA-84.pdf.

¹⁰Inductance calculations use Wheeler's equation:

$$L = \frac{r^2 N^2}{9r + 10l}$$

where:

L is the inductance in µH

r is the coil radius in inches

l is the coil length in inches.

F. Terman, *Radio Engineer's Handbook*, 1943, McGraw-Hill, New York, NY, p. 55. Terman says Wheeler's equation is accurate "within one percent for $l > 0.8r$, i.e., if the coil is not too short." The two

film resistor forms meet the criterion of not being "too short."

¹¹Evans, Randy, KJ6PO, "Pspice for the Masses," QEX, Jan/Feb 2006; LTspice/SwitcherCAD is available for free download via www.linear.com/company/software.jsp.

Jack Smith, K8ZOA, has been licensed since 1961, first as KN8ZOA, and has held the Amateur Extra Class license since 1963. He received the BSEE degree from Wayne State University in Detroit in 1968 and a JD degree magna cum laude from Wayne State University School of Law in 1976. Presently retired, he has enjoyed a career involving both engineering and telecommunications law. He is a co-founder of the telecommunications consulting firm TeleworX and is the author of Programming the PIC Microcontroller with MBasic (Newnes Publishing, 2005), as well as articles published in QEX, and 73 Amateur Radio magazine. His web site is www.cliftonlaboratories.com.

Parallel or Series Resistance?

We have a choice in modeling a two terminal network, the "series" or "parallel" model. The example illustrated at Figure A may clarify these choices. Suppose you are given a sealed box with a resistor connected to an inductor, and told that its impedance is $Z = 1 + j1$, measured at 1 Hz. Is it possible to determine how the resistor and inductor are connected and their individual values? (We'll assume both the resistor and inductor are perfect parts, with no parasitic components.)

One answer is the obvious *series* connection of a 1 Ω resistor and a 0.159 H inductor (1 Ω reactance at 1 Hz), as shown at Figure B. A different set of component values, however, produce the identical $Z = 1 + j1$ impedance at 1 Hz. The alternative circuit, shown at Figure C, consists of a 2 Ω resistor in *parallel* with a 0.3183 H inductor. If we are limited to the 1 Hz impedance data, there's no way to distinguish between the series and parallel configurations. Of course, a dc measurement would distinguish the two configurations, as would data at different frequencies, as illustrated by Figure D.

Over the range from 0.5 Hz to 1.5 Hz, the networks of Figures B and C have identical resistance and reactance — and hence identical impedance — only at 1 Hz; at higher or lower frequencies, the two

network differences may thus be easily distinguished. At any single frequency, however, any impedance value can be represented by two networks, one series and the other parallel. We must apply external information to determine which network represents the best model for the problem at hand.

The relationships between series and parallel values are given by Equations 1 through 4.¹

$$R_s = R_p \frac{X_p^2}{R_p^2 + X_p^2} \quad [\text{Eq 1}]$$

$$X_s = X_p \frac{R_p^2}{R_p^2 + X_p^2} \quad [\text{Eq 2}]$$

$$R_p = \frac{R_s^2 + X_s^2}{R_s} \quad [\text{Eq 3}]$$

$$X_p = \frac{R_s^2 + X_s^2}{X_s} \quad [\text{Eq 4}]$$

where subscript S and P indicate series and parallel, respectively.

R is the resistive element.

X is the reactance of the reactive element, or more generally, the net reactance of the combination of multiple reactive elements.

In our sealed box example, the measured impedance $Z = 1 + j1$ ($Z = R + jX$) can be taken as the series configuration with $R_s = 1$ and $X_s = 1$, but R_p and X_p are easily calculated.

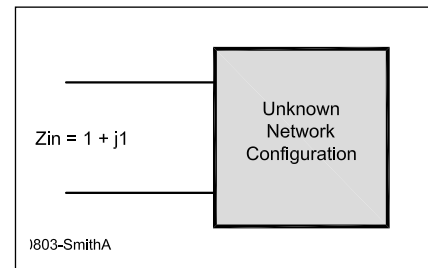


Figure A — There are several possible circuit configurations for the unknown network that will result in the $1 + j1$ Ω impedance. Measurements at different frequencies will help identify the specific circuit inside the box.

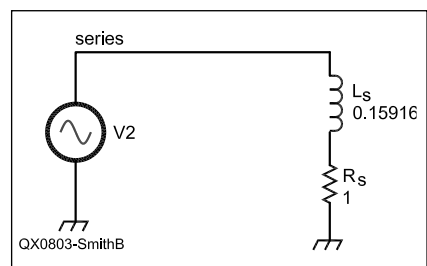


Figure B — The series connected inductor and resistor provide one solution to the question of what circuit is inside the unknown network shown in Figure A.

Continued on next page

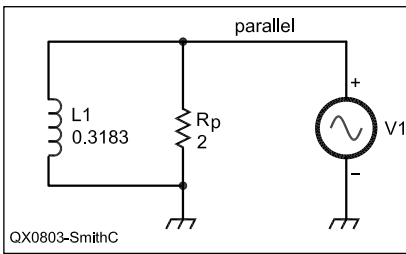


Figure C — A parallel connected inductor and resistor provide an alternate solution for the circuit inside the unknown network of Figure A.

$$R_p = \frac{R_s^2 + X_s^2}{R_s} = \frac{1^2 + 1^2}{1} = \frac{2}{1} = 2$$

$$X_p = \frac{R_s^2 + X_s^2}{X_s} = \frac{1^2 + 1^2}{1} = 2$$

To determine the parallel inductance value of L_p in henrys, we use the relationship:

$$X_L = \omega L = 2\pi f L \quad [\text{Eq. 5}]$$

Solving for L and inserting numerical values for 2 Ω and 1 Hz:

$$L = \frac{X_L}{2\pi f} = \frac{2}{2\pi \times 1} = 0.3138 H$$

So, why is this important when we measure the frequency response of a resistor? The answer is that a resistor's model is best defined in terms of a parallel structure, as reflected at Figure 7 in the main article; a resistor (perhaps with series inductance) shunted by capacitance. In many cases, the series inductance is small enough that it can be neglected, making the resistor model a pure parallel RC combination.

Let's suppose the resistor in this model is almost perfect; it has no frequency dependent effects other than a shunting capacitance. That is, it has no inductance, there is no granule-to-granule capacitance in the CC case or turn-to-turn stray capacitance in a CF or metal oxide film part. R_p is constant with changes in frequency. If we measure the circuit in Figure 7 with a device that reports series impedance, however, we will find that the shunting capacitance reduces the measured resistance. Figure E is an *LTspice* simulator schematic for a perfect 4700 Ω resistor, shunted by 1 pF capacitance, swept over the range 300 kHz to 1 GHz. Figure F shows the series resistance R_s and the reactance X_s (magnitude only; sign ignored for simplicity) of the circuit over this frequency range.

In this case, therefore, a theoretically perfect resistor, save for a small

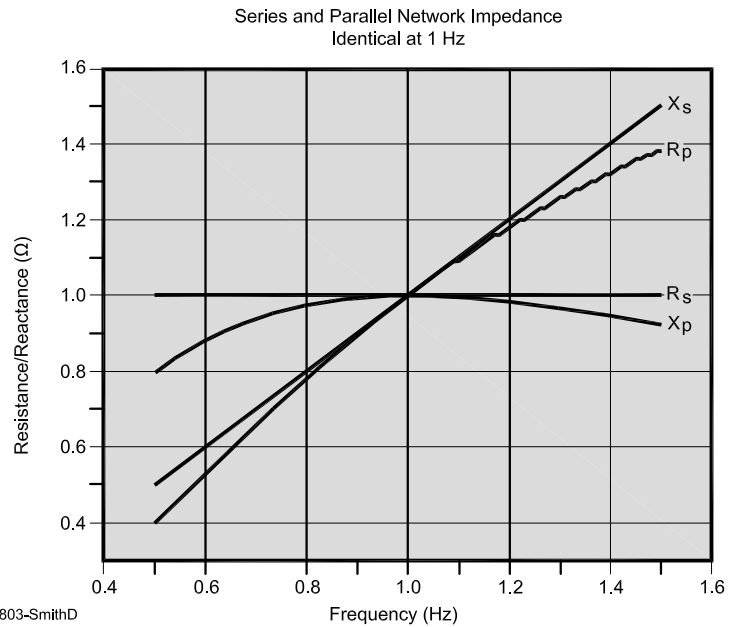


Figure D — Impedance measurements at slightly different frequencies or at dc will help determine the actual unknown circuit. This graph illustrates the variation in resistance and inductance for both the series and parallel circuits.

Figure E — An *LTspice* simulator schematic shows a perfect 4700 Ω resistor, shunted by 1 pF capacitance. The circuit was swept over the range 300 kHz to 1 GHz in the *LTspice* model.

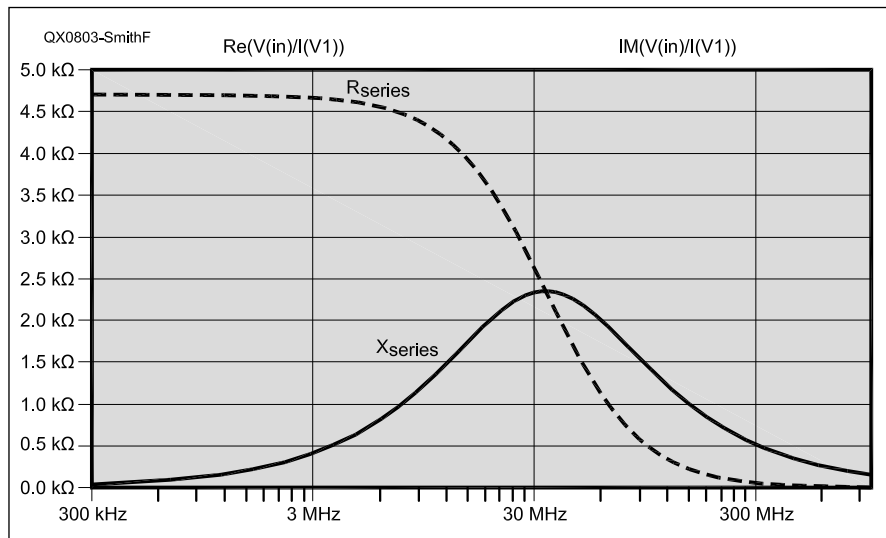
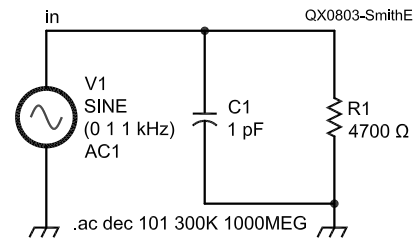


Figure F — This graph is the *LTspice* simulation output, showing the series resistance and inductive reactance over the simulated frequency range.

shunting capacitance, shows a marked reduction in series resistance. The reason for this can be seen by examining Equation 1.

At low frequencies, the shunting impedance, X_p , is large compared with R_p — at 100 kHz, the 1 pF shunting parallel capacitance has a reactance of 1.6 M Ω , some 30 times larger than the 4.7 k Ω of R_p . When $X_p \gg R_p$, Equation 1 says $R_s \approx R_p$ since $X_p^2 / (R_p^2 + X_p^2) \approx 1$. At 50 MHz, however, X_p is about 3.2 k Ω , which may not be ignored when compared with the 4.7 k Ω of R_p , and reduces R_s to about 1.5 k Ω . If the frequency increases to, say, 1 GHz, X_p is about 159 Ω , so that $X_p \ll R_p$ and Equation 1 is approximately $R_s \approx X_p^2 / R_p$ and $R_s \approx 5.4 \Omega$. So, depending on the measurement frequency, our perfect resistor — except for a small shunting capacitance — demonstrates a series resistance ranging from 4.7 k Ω to 5.4 Ω .

Since our purpose is to understand how resistor construction influences its RF properties, it makes far more sense to measure R_p , not R_s , particularly if our measurement technique can separately identify the shunting capacitance value. If the resistor's series inductance is not too large, its main imperfection can be considered to be parallel capacitance.

I collected the RF performance data in this study with an HP 8752B vector network analyzer, operating in reflection mode, with the homemade test fixture shown at Figure G.ⁱ The test fixture is modeled after one shown in Agilent's Application Note AN 1287-9, with four short identical 50 Ω microstrip sections.

ⁱⁱ Three sections are configured as: an open; a short (two parallel "zero ohm" 1206 jumpers); and a 50 Ω standard load (a pair of 100 Ω , 1% 1206 resistors in parallel) used in the VNA's open/short/load calibration. The fourth section holds the device under test. The test fixture also has a "through" section, not used in the measurements made for this article. I believe this test fixture provides reasonable results up through at least 300 MHz. I have not modeled the errors, however. To reduce source match reflections, I use approximately 16 dB attenuation on the 8752B source port.ⁱⁱⁱ

Operating the 8752B with "Y" conversion enabled directly measures the admittance, $Y = G + jB$, of the device under test. By applying the 8752B's real and imaginary modifiers to the display, G and B are separately determined.

If the device under test consists of a pure resistive element in parallel with a pure reactive element, then R_p and X_p

are easily obtained. In general, admittance is the reciprocal of impedance:

$$Y = G + jB = \frac{1}{Z} = \frac{1}{R + jX} \quad [\text{Eq 6}]$$

where:

Y is the admittance

G is the conductance

B is the susceptance

In a network with only parallel R and X elements R_p and X_p are simply related to Y :^{iv}

$$R_p = \frac{1}{G} \quad [\text{Eq 7}]$$

$$X_p = -\frac{1}{B} \quad [\text{Eq 8}]$$

The parallel capacitance can also found directly from the 8752B's susceptance (B) data:

$$C = \frac{B}{\omega} = \frac{B}{2\pi f} \quad [\text{Eq 9}]$$

where:

C is the capacitance in farads

B is the susceptance in Siemens

(capacitive susceptance has a positive sign)

f is the frequency in Hz.

I export the 8752B data over its GPIB interface to a Microsoft *Excel* spreadsheet and post process it with Equations 7 and 9, plotting the data with *Origin 7.5*, a scientific/engineering data analysis and plotting program.

When the resistive element is not a pure resistor and has series inductance as at Figure H, the simple relationship in Equations 7 and 8 is no longer accurate, and is replaced by the following:^v

$$Y = \frac{R - j\omega[L(1 - \omega^2 LC) - CR^2]}{R^2 + \omega^2 L^2} \quad [\text{Eq 10}]$$

The impedance of this configuration is:^{vi}

$$Z = \frac{R + j\omega[L(1 - \omega^2 LC) - CR^2]}{(1 - \omega^2 LC)^2 + \omega^2 C^2 R^2} \quad [\text{Eq 11}]$$

ω is the angular frequency in radians/sec. $\omega = 2\pi f$ where f is the frequency in Hz.

One additional point worth noting is that the reactance vanishes, which is one definition of parallel resonance, when:^{vii}

$$\omega = \frac{1}{\sqrt{LC}} \sqrt{1 - \frac{CR^2}{L}} = \omega_0 \sqrt{1 - \frac{CR^2}{L}} \quad [\text{Eq 12}]$$

Where ω_0 is the resonant frequency when R is zero. Equation 12 shows the parallel resonant frequency as a function of all three elements, R , L and C , not just LC as often stated for the high Q case. (If the inductor Q is even as

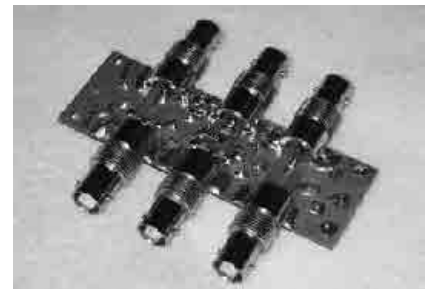


Figure G — This homemade test fixture was used with an HP 8752B vector network analyzer, operating in reflection mode, to collect the data reported in this article.

high as 10, $\omega \approx \omega_0$ for normal working purposes, however.)

The real part of Equation 10 is the conductance (the G term in $Y = G + jB$) measured in the test setup:

$$\text{Re}(Y) = \frac{R}{R^2 + \omega^2 L^2} = G \quad [\text{Eq 13}]$$

R and L are the resistance and inductive values in the series arm.

The net effect of the resistor's series inductance is to increase the effective parallel resistance. As the frequency increases, so does the denominator of G , and since the resistance is $1/G$, a decrease in G corresponds to an increase in resistance.

Equation 13 permits us to estimate the resistor's inductance:

$$L = \sqrt{\frac{R - R^2 \text{Re}(Y)}{\omega^2 \text{Re}(Y)}} \quad [\text{Eq 14}]$$

The accuracy of this relationship depends upon:

- 1) R_p remaining constant with frequency
- 2) The test circuit not having appreciable series inductance from other sources

These two assumptions are only approximately correct, so we will wish to verify L estimates by other methods.

Equation 13 also establishes so long as ωL is small with respect to R , the resistor's inductance will not cause a significant effect on the apparent resistance.

ⁱParallel to series conversion is often considered in the amateur literature in the context of impedance matching. See, for example, W. Hayward, W7ZOI, and others, *Experimental Methods in RF Design*, 2003, ARRL, Newington, CT, at §3.6. In impedance matching, emphasis is often on determining the reactive elements and the full set of equations is not always presented. The four equations presented above can be found in most electronic handbooks, such as ITT Corp. *Reference Data for Radio Engineers*, 4th ed., 1956, ITT, New York, NY, pp 121-122.

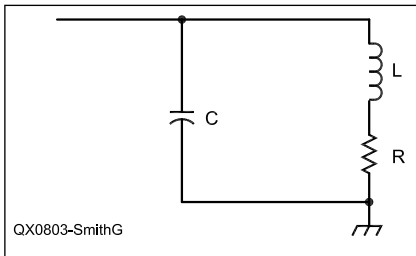


Figure H — When the resistive element is not pure resistance, the circuit model using a series inductance and parallel capacitance must be used to accurately model the circuit element.

ⁱⁱIt is also possible to measure component parameters by placing the device under test in series between the VNA's output and input (receiver) ports, with a suitable test fixture. I found reflection (single port) measurements to be preferable. Newer VNAs are calibrated with more than the simple "through loss" calibration process used in my 8752B, which improves through accuracy.

ⁱⁱⁱAgilent Technologies, "Agilent AN 1287-9, In-Fixture Measurements Using Vector Network Analyzers," Document No.

5968-5392E, dated 8/00. This Application Note may be downloaded from Agilent's Web site at <http://cp.literature.agilent.com/litweb/pdf/5968-5329E.pdf>.

^{iv}The 8752B is the 75 Ω version of HP's 8752A vector network analyzer, and has a built-in reflection bridge. Minicircuits model UNMP-5075 adapters provide 75-50 Ω resistive matching pads (5.7 dB). Additional source attenuation is through a Minicircuits NM-BM-10 "Adaptenuators" a combined 10 dB attenuator and N-male to BNC-male adapter. Source reflection causes ripples in the measured data as signals reflected from the device under test enter the 8752's source generator and are re-reflected back from mismatches in the source impedance. As the phase and amplitude of these reflections change with frequency, errors in the measured impedance are caused. For more details, see Agilent Application Note AN 1287-3, "Applying Error Correction to Network Analyzer Measurements," Document No. 5965-7709E, dated March 27, 2002. I've also post-processed some data to provide smoothed curves.

As with any VNA, data accuracy is ultimately tied to the calibration standards, in this case the quality of the short, open and load in my homebrew fixture, as well as how closely the open, short, load and DUT microstrip lines are identical in impedance characteristics and length.

^vSee, for example, *Reference Data for Radio Engineers*, 4th ed, pp 120-121, op. cit.

^{vi}*Reference Data for Radio Engineers*, 4th ed, p 126, op. cit. This relationship is easily derived using Equations 3 and 4 to convert the series *RL* element into parallel *R* and *L* elements, yielding parallel *R*, *L* and *C* elements.

^{vii}Ibid.

^{viii}F. Langford-Smith, ed., *Radiotron Designer's Handbook*, 4th ed, 1953, Wireless Press, Sydney Australia, reprinted Electron Tube Division, Radio Corp. of America, p 150. Terman provides three definitions of parallel resonance:

Zero net reactance or unity power factor. This is the definition used in the referenced equation.

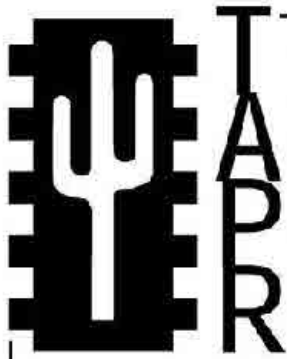
Maximum impedance

The frequency at which $\omega L = 1 / \omega C$, or series resonance.

F. Terman, *Radio Engineer's Handbook*, 1943, McGraw-Hill, New York, NY, pp 143-144.

These three conditions occur at different frequencies where the circuit has loss. Almost all our work as radio amateurs involves high Q tuned circuits, where R is small compared with the inductive reactance, under which condition all three definitions closely converge for practical work. This is not true when dealing with low Q circuits, however, as seen in some measurements in this article.

QEX+



Join the effort in developing Spread Spectrum Communications for the amateur radio service. Join TAPR and become part of the largest packet radio group in the world. TAPR is a non-profit amateur radio organization that develops new communications technology, provides useful/affordable kits, and promotes the advancement of the amateur art through publications, meetings, and standards. Membership includes a subscription to the *TAPR Packet Status Register* quarterly newsletter, which provides up-to-date news and user/technical information. Annual membership \$20 worldwide.



TAPR CD-ROM

Over 600 Megs of Data in ISO 9660 format. TAPR Software Library: 40 megs of software on BBSs, Satellites, Switches, TNCs, Terminals, TCP/IP, and more! 150Megs of APRS Software and Maps. RealAudio Files. Quicktime Movies. Mail Archives from TAPR's SIGs, and much, much more!

Wireless Digital Communications: Design and Theory

Finally a book covering a broad spectrum of wireless digital subjects in one place, written by Tom McDermott, N5EG. Topics include: DSP-based modem filters, forward-error-correcting codes, carrier transmission types, data codes, data slicers, clock recovery, matched filters, carrier recovery, propagation channel models, and much more! Includes a disk!



Tucson Amateur Packet Radio

8987-309 E Tanque Verde Rd #337 • Tucson, Arizona • 85749-9399
Office: (972) 671-8277 • Fax (972) 671-8716 • Internet: tapr@tapr.org www.tapr.org
Non-Profit Research and Development Corporation

Antenna Options

Beam Matching

Most modern HF and VHF beams present the builder with modest matching problems, relative to the antenna impedance and the impedance of the main feed line. Rarely does the impedance difference exceed an SWR of 3:1. Under these conditions, the builder has numerous options among matching systems. These notes provide a very brief overview of the main systems available.

Series Matching

Series matching includes three systems, ranging from the most specific to the most general. All series matching systems presume that the matched element is insulated and isolated from any conductive boom.

1. *The 1/4-Wavelength Transmission-Line Transformer:* The 1/4-wavelength transmission-line transformer is perhaps the best known of the series matching systems. Figure 1 outlines the basic application of the system.

We may insert a 1/4-wavelength section of transmission line between a resonant antenna impedance and a feed line if the transformer section Z_0 is the geometric mean between the antenna and the feed line impedance. For example, if a beam has an impedance of 25 Ω and we have a 50 Ω feed line, then a transformer section of 35.36 Ω will effect the required impedance transformation. We may use RG-83 or parallel sections of RG-59 to create the transformer. We may also step up or step down: the only requirement is that the transformer Z_0 be roughly the geometric mean of the two end values.

$$Z_0 = \sqrt{Z_{Load} Z_{Source}}$$

$$Z_{Source} = \frac{Z_0^2}{Z_{Load}}$$

If the feed point impedance is slightly reactive, or if the available transformer line is not quite the exact geometric mean between the antenna and the cable impedance, the system will still work, although the lowest SWR may not be 1:1. Perhaps the simplest way to determine the optimal line length under these conditions is to use an antenna modeling program and experiment with line lengths, taking SWR sweeps for each trial length of line.

2. *The Bramham System:* The Bramham system of series matching tackles a special problem: matching a resonant an-

tenna impedance to a different feed line Z_0 . The basic problem and solution appear in outline form in Figure 2. In *Electronic Engineering* for Jan 1961 (pp 42-44), B. Bramham published a paper on "A Convenient Transformer for Matching Coaxial Lines," based on work he had done for a CERN report in 1959. Bramham's solution was to develop a means for calculating equal lengths of the two lines, Z_1 and Z_2 , which would effect the impedance transformation for a given frequency. The solution is elegantly simple. First, let's define a special term, M:

$$M = \left(\frac{Z_2}{Z_1} + 1 + \frac{Z_1}{Z_2} \right)$$

Z_1 and Z_2 are the values of the two lines to be joined in the scheme shown in Figure 2. The required lengths (L_1 and L_2) of the two are a function of M:

$$L_1 = L_2 = \arctan \frac{1}{\sqrt{M}}$$

L_1 is the length of the matching line Z_1 and L_2 is the length of the matching line Z_2 . The lengths are in degrees relative to a 360° wavelength for simple translation into electrical line lengths, which then translate into physical line lengths taking the line's Velocity Factor into account.

3. *The Regier General Series Matching Solution:* Three decades ago, Regier developed a general solution for series matching any antenna impedance to a given line with a single line insertion. The details of Regier's solution can be found in the following references:

"Impedance Matching with a Series Transmission Line Section," *Proceedings of the IEEE*, Jul 1971, pp 1133-1134.

"The Series-Section Transformer," *Electronic Engineering*, Aug 1973, pp 33-34.

"Series-Section Transmission-Line Impedance Matching," Jul 1978 QST, pp 14-16.

The general outline of the Regier system appears in Figure 3. Regier's solution is best used in "normalized" form, where the ratios of one impedance to an-

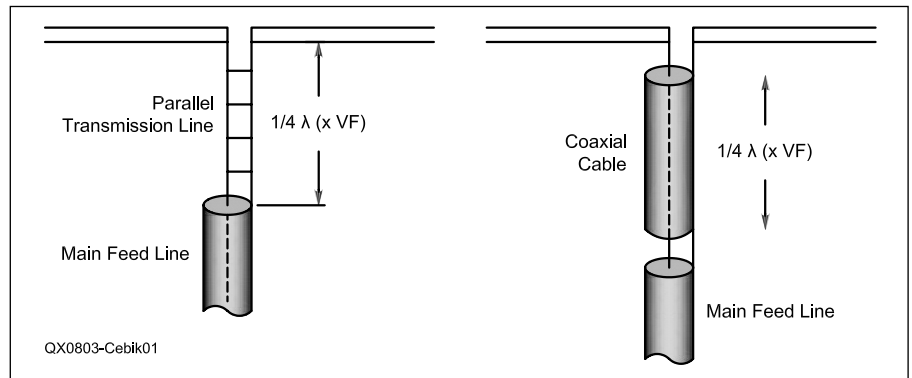


Figure 1 — Two usual arrangements of quarter wavelength matching sections.

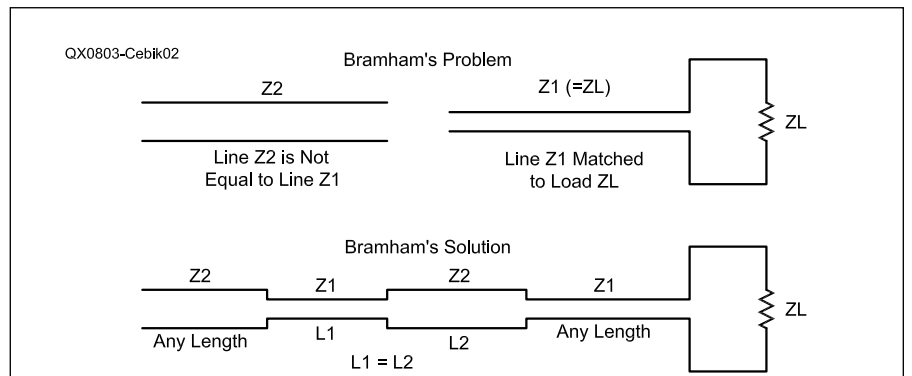


Figure 2 — Bramham's limited series matching problem and solution.

other are first reduced to single values. Otherwise, the calculation equations tend to look terribly opaque. So let's define a few quantities.

$$n = \frac{Z_1}{Z_0}$$

$$r = \frac{R_L}{Z_0}$$

$$x = \frac{X_L}{Z_0}$$

The load impedance is specified as $R_L \pm jX_L$ and Z_1 is the selected impedance of the special matching section. We shall let L_1 be the electrical length in degrees of the line Z_0 between the load and the special matching section, while L_2 is the electrical length in degrees of the special matching section.

Now we can calculate the two lengths, starting with L_2 , since it plays a role in calculating L_1 .

$$L_2 = \arctan \pm \sqrt{\frac{(r-1)^2 + x^2}{r\left(n - \frac{1}{n}\right)^2 - (r-1)^2 - x^2}}$$

Although this equation looks a bit forbidding, it can be handled on a calculator or with a spreadsheet. The equation produces two good results, plus and minus. The positive result gives a shorter length for L_1 and hence is preferred. If the result is an imaginary number, then the value of n must be changed. You can do this by increasing the value of Z_1 , the characteristic impedance of the special matching section. Remember that the series matching technique can use parallel transmission-line sections as well as coaxial cables, so using a length of 300- Ω or 450- Ω line as the special matching section is perfectly appropriate.

$$L_1 = \arctan \frac{\tan L_2 \left(n - \frac{r}{n} \right) + x}{r + xn \tan L_2 - 1}$$

In some cases, a calculator will return a negative value for the electrical length of L_1 . To arrive at the correct positive value, simply add 180° to the calculated result. For example, should L_2 return a value of -62°, the correct result will be 118°.

There are limits to what combinations of Z_0 and Z_1 we may use and still obtain a desired match. In general, the closer the values of Z_0 and Z_1 , the smaller the range of antenna impedance values that we can match.

The Beta or Hairpin Match

Essentially, the beta match is a form of L-network specifically arranged to transform a higher line Z_0 to a lower antenna impedance. In the process, the network usually uses a shortened element that has

capacitive reactance in the feed point impedance as one of the reactive components in the L-network. Figure 4 shows the general evolution of the typical beta or hairpin match.

Let's begin our treatment of the L-network with the designation, δ (Greek lower case delta). The designation appears in Terman's 1943 classic, *Radio Engineers Handbook* (p 213 and elsewhere), but a number of more recent publications have preferred to use terms such as "working Q," "network Q," or "loaded Q" (Q_L , in contrast to the "unloaded Q," or Q_U) in preference to the older term. However, δ will do nicely for our work.

In an L-network, we may express the relationships that define δ in two ways:

$$\delta = \sqrt{\frac{R_{in}}{R_{out}} - 1}$$

$$\frac{R_{in}}{R_{out}} = \delta^2 + 1$$

The ratio of the input or source resistance (R_{in}) to the output or load resistance (R_{out}) defines the value of δ . I have chosen this starting point for our treatment as a tribute to George Grammer, whose classic volume *A Course in Radio Fundamentals* makes use of the concept (pp 69-70). The fact that this starting point simplifies the calculation of the reactance components of the network adds some substance to the reference. In fact, the calculation of the reactive components is very easy.

$$X_s = \delta R_{out}$$

$$X_p = \frac{R_m}{\delta}$$

For our down-converting version of the L-network, the series component is simply the product of δ and the load resistance. The parallel or shunt reactance is the ratio of the source or input resistance to δ . Both results are in Ω , but — as noted

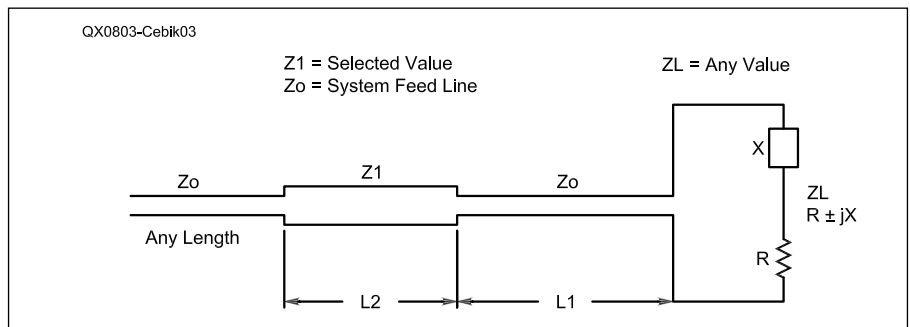


Figure 3 — Regier's series section matching system.

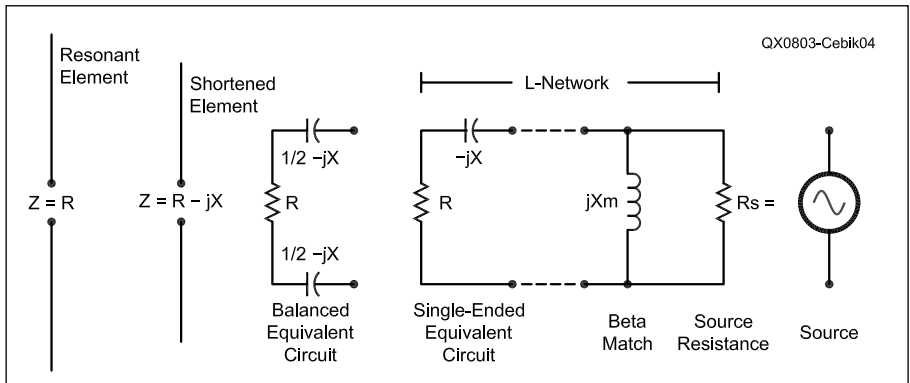


Figure 4 — Basic elements of the most common form of the beta match.

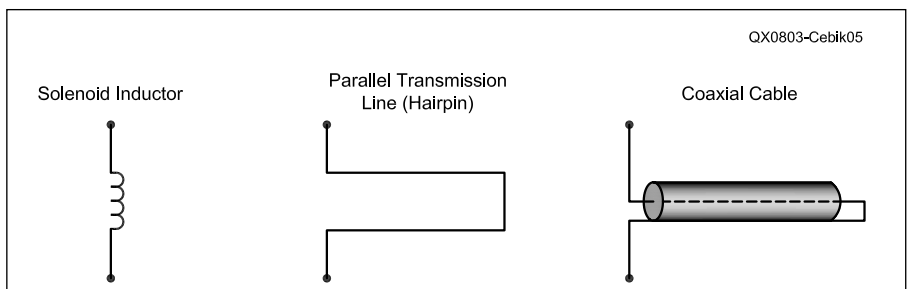


Figure 5 — Alternative beta match inductive reactances.

earlier the reactances are of opposite types. For the highest level of effectiveness for a given resistive component of feed point impedance, the beta match requires a certain series reactance. Other reactance values can be matched but may result in higher values of δ and hence in slightly higher losses.

We obtain the optimal value of δ by adjusting the antenna's element length. The only component that we need to add to the system is the parallel or shunt element. If the element has a capacitive reactance, the shunt element must be inductive (and vice versa).

Some folks distrust the beta match because one form of shunt inductance seems to be a short circuit across the feed point. Figure 5 shows three typical forms for adding inductive reactance across the feed point terminals, which are insulated and isolated from any conductive supporting boom. A solenoid inductor is feasible and generally has little loss, since its reactance will normally be quite low.

Shorted transmission line stubs, however, may generally provide the same inductive reactance with even lower loss. The hairpin or shorted parallel transmission line section is the version that most worries new users. The beta match in any form is as effective as virtually any other system in effecting a low loss match between the element and the feed line — when the element resistive component is less than the feed line Z_0 . In addition, one may also lengthen an element to make it inductively reactive. Then the shunt component becomes a capacitance. Both versions of the beta match have undergone extensive modeling confirmation and physical confirmation. Like the series matching systems, the beta match presumes an element that is insulated and isolated from any conductive boom.

The Gamma Match

The third major system for matching the impedance of beam driven elements to a standard feed line, such as 50- Ω coaxial cable, is called the *gamma match*. H. H. Washburn, W3MTE, introduced the amateur community to the gamma match in his Sep 1949 *QST* article, "The Gamma Match," pp 20-21, 102. D. J. Healey, W3PG, provided the first mathematical analysis of the match in "An Examination of the Gamma Match," *QST*, Apr 1969, pp 11-15, 57. Healey's treatment, however, required the use of nomographs and a Smith chart.

Since these seminal articles, several alternative analyses have appeared in amateur journals. H. F. Tolles, W7ITB, presented a purely mathematical analysis in "How to Design Gamma Matching Networks" in *ham radio* for May 1973, pp 46-55. Because the Tolles equations proved tedious to many gamma designers, R. A. Nelson, WBØIKN, set them into a *BASIC* program in "Basic Gamma Matching," *ham radio*, Jan 1985, pp 29-33.

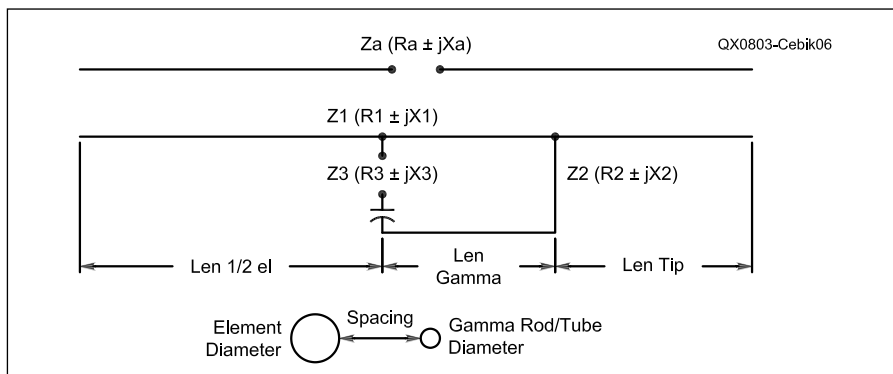


Figure 6 — Key factors in calculating a gamma match.

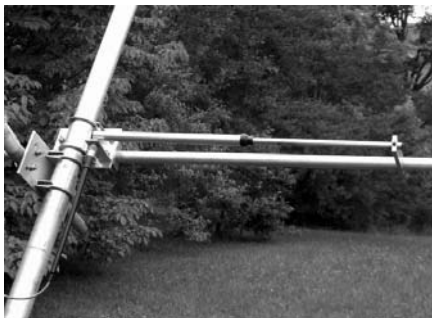


Figure 7 — A typical gamma match using a tubular series capacitor within the gamma rod.

ARRL converted Nelson's *Apple-BASIC* program into a version suitable for IBM computers, and a listing appears in *The ARRL Antenna Book*, 16th Ed, p 26-20.

In 2000, Dave Leeson, W6NL, corrected portions of the program so that it is perhaps the most accurate of the available means to calculate gamma matches. This program is also available within the *Ham-Calc* collection of *BASIC* utilities edited by George Murphy, VE3ERP, and in the 21st edition of *The ARRL Antenna Book*.

Since the work of Tolles and Nelson, two alternative mathematical analyses have appeared. Ron Barker, G4JNH, presented "A New Look at the Gamma Match" in *QEX*, May/June 1999, pp 23-31. Barker changed some of the fundamental assumptions about the key factors in a gamma match to arrive at his results. Unfortunately, his work is less amenable to easy placement in a *BASIC* utility or a spreadsheet, since the calculations require the solution to simultaneous equations.

In contrast, R. Wheeler, G3MGW, returned to the Healey analysis and converted the graphical techniques back into mathematical methods that allow a straightforward spreadsheet set of calculations. Wheeler's two-part "Re-Examination of the Gamma Match" appeared in *RADCOM*, Sep 2004, pp 35-37, and Oct 2004, pp 54-56, with reprints appearing in *antenneX* for Oct and Nov 2006.

Both of these later analyses rely on something that was unavailable to earlier gamma calculations. In most cases, the determination of the initial or pre-match

driver feed-point impedance rested on assumption, guesswork or rudimentary measurement. Measurement became difficult if the builder connected the driver to the boom and did not allow for a feed-point gap, even if it would later be closed. Both Barker and Wheeler require the use of antenna modeling software to determine the pre-match driver impedance.

The gamma match differs from the previous matching systems in that the calculations are not precise. Rather, they produce starter values that will require careful field adjustment (the gentler sounding term for trial and error). Figure 6 shows some of the reasons why the calculations are less than fully precise. The gamma system begins with a larger number of variables, some of which are the physical dimensions of the assembly components. We need to know or decide upon the main element diameter, the gamma rod diameter and the center-to-center spacing between these two parts. Calculations usually proceed (although there have been variations) by treating the gamma assembly as a section of parallel transmission line, shorted at the far end. The end result is a change in the position of the antenna feed point relative to the element without the gamma assembly. Most calculation systems do not take into account the far-end shorting bar structure or the structure that supports the feed-line connector.

Practical gamma matches also include a number of variations on the ideal situation used in calculations. The rod may extend beyond the shorting bar. The required series capacitor may not be at the feed point, but may be somewhere along the gamma rod. This change of placement alters the structure relative to the ideal form used for calculations, but not so much as to prevent you from devising a highly successful match.

Figure 7 provides a photo of a practical gamma match that uses a tubular capacitor within the central part of the rod. The gamma system is the only matching system in this group that permits a direct connection of the main element center to the boom. We cannot easily obtain the initial feed point impedance through modeling, however, when we connect the element to the boom, and the boom itself will have an

effect upon the feed point impedance.

The two major calculation systems have different sources but similar starting points. Both begin by calculating the characteristic impedance of the presumed parallel transmission line formed by the main element and the gamma rod or tube. The next step is to calculate the impedance step-up created by treating the gamma section as a short folded dipole or monopole. The following steps involve calculating the impedance of the gamma section at the outer end. The impedance at the feed point then becomes a parallel combination of the transformed end impedance and the stepped feed-point impedance. The Healey-Wheeler method requires the user to insert trial values of the gamma rod length until the resulting resistive component at the new feed point matches the target line Z_0 . The Tolles-Nelson-Leeson method calculates the gamma rod length.

The two systems do not produce identical results. As well, the results differ from the results of antenna modeling. Because *NEC* cannot effectively handle the gamma match, only a highly corrected version of *MININEC* (such as *Antenna Model*) is adequate to the modeling task. Even *MININEC* cannot show the required variations that emerge from connecting the element to a central boom, however. Since gamma matches receive only spot checks rather than systematic comparison of calculations and/or models with physical antennas, all three methods are tentative guides, useful for beginning the process of designing a gamma match but always needing some field adjustment.

I have omitted the detailed equations used in the progression of gamma calculations because they are too numerous for our short space. For a more systematic look at the two major gamma calculation schemes, see "Notes on the Gamma Match," (parts 1 and 2), *antenneX*, Sep and Oct 2006. The notes also include an extensive but inexhaustive set of comparisons with *MININEC* models of the gamma match.

In many ways, the gamma match is far more flexible than the series or beta matching systems. It works for elements connected to a conductive boom or for isolated driven elements. Within limits, it can handle impedances both higher and lower than the cable impedance. Nevertheless, the system always requires field adjustment (trial and error), since the calculations are only approximations.

Conclusion

We have surveyed a number of options open to the modern beam builder for matching the impedance values at driven elements to the feed line and equipment. Series and beta calculations are both precise, under the condition that we know the actual velocity factor of the lines used in the matching efforts. Both series and beta matching systems, however, require

that we use insulated driven elements relative to any conductive boom that may support the elements. (Of course, the parasitic element center points may be grounded to the boom.)

An additional restriction on the beta match is that the driver impedance must be below the line impedance. The Bramham system requires a resonant feed point impedance that matches one of the two line lengths used.

The gamma match system allows (but does not require) the builder to use what we once called "plumber's delight" construction methods with all elements connected to the boom. It matches a wide range of impedances. The main calculation systems for the gamma match achieve only working approximations that require field adjustment, however.

Other matching methods exist. We may conduct beam matching at the shack-end of the line. As well, we may install more complex networks at the antenna feed point, so long as the assembly will support them easily. Match line and stub methods also exist. These alternatives, plus the ones that we have discussed, still only list some, but certainly not all, of the options.

For most of the items in this series, I have provided models of antennas discussed. Since we did not discuss any specific antennas, there are no models for this episode. I have made available a somewhat primitive spreadsheet, however, which includes all of the systems that I have listed. There are separate pages for the Healey-Wheeler and the Tolles-Nelson-Leeson systems. In addition, the sheet contains a page for the match line and stub system, which is useful for antennas such as the extended double Zepp.¹ The sheets serve only to increase your options for easy calculation of the matching systems, since utility programs are also available from other sources.

¹The spreadsheets are available in both *Excel* and *Quattro Pro* formats at the ARRL Web site. Go to www.arrl.org/qexfiles and look for 3x08_AO.zip.

QEX

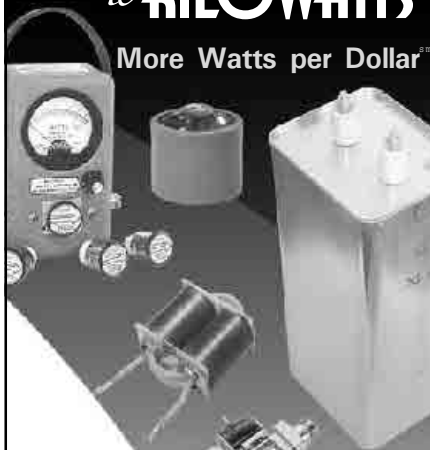
In the Next Issue of QEX

James Ahlstrom, N2ADR, describes his All-Digital SSB Exciter for HF. He explains his use of a field programmable gate array (FPGA) and an Ethernet link to a computer to create a 300 mW SSB exciter signal. A different program changes the FPGA to produce a CW transmitter. James uses this software defined radio (SDR) transmitter along with an SDR receiver. A power amplifier gives his station a 100 W output signal.

Cornell Drentea, KW7CD, completes his series about the design of his Star-10 transceiver. In this part, Cornell describes the product detector and audio DSP. He also introduces the 9 MHz transmitter IF and power amplifier stages. He concludes the article with detailed lab testing results.

From MILLIWATTS to KILOWATTS

More Watts per Dollar



- **Wattmeters**
- **Transformers**
- **TMOS & GASFETS**
- **RF Power Transistors**
- **Doorknob Capacitors**
- **Electrolytic Capacitors**
- **Variable Capacitors**
- **RF Power Modules**
- **Tubes & Sockets**
- **HV Rectifiers**



ORDERS ONLY:

800-RF-PARTS • 800-737-2787

Se Habla Español • We Export

TECH HELP / ORDER / INFO: 760-744-0700

FAX: 760-744-1943 or 888-744-1943



An Address to Remember:
www.rfparts.com

E-mail:

rfp@rfparts.com



Upcoming Conferences

2008 Eastern VHF/UHF Conference

April 18-20, 2008
Enfield, CT

The 34th Annual Eastern VHF/UHF Conference will be held April 18-20, 2008, at the Crowne Plaza Hotel in Enfield, Connecticut.

The aim of the Conference is to share technical achievements in the field of communication and experimentation with our fellow VHF and above operators. You are all invited to participate by presenting a technical paper or submitting one for publication in the *Conference Proceedings* CD. Your attendance is also welcome and we have a full program scheduled once again this year.

For technical presentations, PowerPoint presentations are preferred, but not required. The conference will provide an LCD projector, screen and wireless microphone for use by its participants. If your presentation requires a different format such as a slide projector, please contact me prior to the conference and arrangements will be made. A *Conference Proceedings* will be published on CD. You do not need to be a speaker to have your material included in the proceedings; just be interested in sharing with your fellow radio enthusiasts. If you are interested in presenting a paper at the conference or submitting one for the *Proceedings*, or need general information, please contact: Bruce Wood, N2LIV at n2liv@arrl.net. Deadline for receipt of papers is March 1, 2008.

12th Annual Southeastern VHF Society Conference

April 25-26, 2008
Orlando, Florida

The 12th Annual Southeastern VHF Society Conference will be held April 25-26, 2008 in Orlando, Florida. Papers and presentations will cover both the technical and operational aspects of VHF, UHF and Microwave weak signal Amateur Radio. For further information about the conference please go to www.svhfs.org or www.flwss.net.

42nd Annual Central States VHF Society Conference

July 24-26, 2008
Wichita, KS

The Central States VHF Society is soliciting papers, presentations, and Poster / table-top displays for the 42nd Annual CSVHFS Conference to be held in Wichita, Kansas on

July 24-26, 2008. Papers, presentations, and posters on all aspects of weak-signal VHF and above amateur radio are requested. You do not need to attend the conference, nor present your paper to have it published in the proceedings. Posters will be displayed during the conference.

Submission Deadlines:

Proceedings and for presentations to be delivered at the conference: May 15, 2008.

Poster for display: July 1, 2008, for notifying us you will have a poster to be displayed at the conference. (Bring your poster with you on July 24!)

Please see the Web site at www.csvhfs.org for more information.

Microwave Update 2008

October 17-18, 2008
Bloomington, MN

Call for Papers

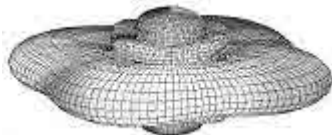
Microwave Update 2008 will be held on Friday, October 17 through Saturday, October 18 in Bloomington, Minnesota.

Technical papers are currently being solicited for publication in the ARRL's *Microwave Update 2008 Conference Proceedings*. You do not need to attend the conference nor present your paper to have it published. Strong preference will be given to original work and to those papers that are written and formatted specifically for publication rather than as a presentation visual aid.

This is a microwave conference, so papers must be on topics for frequencies above 900 MHz. Examples of such topics include microwave theory, construction, communication, deployment, propagation, antennas, activity, transmitters, receivers, components, amplifiers, communication modes, LASER, software design tools, and practical experiences. Authors retain the basic copyright, and by submission, consent to publication in the *Proceedings* and possible publication of the *Proceedings* in CD/DVD format. If you are interested in submitting a paper please contact Jon Platt, W0ZQ, at w0zq@aol.com for additional information. The deadline for papers is Sunday, August 31, 2008. If you are interested in presenting at Microwave Update please contact Barry Malowanchuk, VE4MA, at ve4ma@shaw.ca.



A picture is worth a thousand words...



With the

ANTENNA MODEL™

wire antenna analysis program for Windows you get true 3D far field patterns that are far more informative than conventional 2D patterns or wire-frame pseudo-3D patterns.

Describe the antenna to the program in an easy-to-use spreadsheet-style format, and then with one mouse-click the program shows you the antenna pattern, front/back ratio, front/rear ratio, input impedance, efficiency, SWR, and more.

An optional **Symbols** window with formula evaluation capability can do your computations for you. A **Match Wizard** designs Gamma, T, or Hairpin matches for Yagi antennas. A **Clamp Wizard** calculates the equivalent diameter of Yagi element clamps. **Yagi Optimization** finds Yagi dimensions that satisfy performance objectives you specify. Major antenna properties can be graphed as a function of frequency.

There is **no built-in segment limit**. Your models can be as large and complicated as your system permits.

ANTENNA MODEL is only \$90US. This includes a Web site download and a permanent backup copy on CD-ROM. Visit our Web site for more information about ANTENNA MODEL.

Teri Software
P.O. Box 277
Lincoln, TX 78948

www.antennamodel.com

e-mail sales@antennamodel.com
phone 979-542-7952

We Design And Manufacture To Meet Your Requirements

*Prototype or Production Quantities

800-522-2253

This Number May Not Save Your Life...

But it could make it a lot easier!
Especially when it comes to ordering non-standard connectors.

RF/MICROWAVE CONNECTORS, CABLES AND ASSEMBLIES

- Specials our specialty. Virtually any SMA, N, TNC, HN, LC, RP, BNC, SMB, or SMC delivered in 2-4 weeks.
- Cross reference library to all major manufacturers.
- Experts in supplying "hard to get" RF connectors.
- Our adapters can satisfy virtually any combination of requirements between series.
- Extensive inventory of passive RF/Microwave components including attenuators, terminations and dividers.
- No minimum order.

NEMAL

Cable & Connectors
for the Electronics Industry

NEMAL ELECTRONICS INTERNATIONAL, INC.

12240 N.E. 14TH AVENUE
NORTH MIAMI, FL 33161

TEL: 305-899-0900 • FAX: 305-895-8178

E-MAIL: INFO@NEMAL.COM

BRASIL: (011) 5535-2368

URL: WWW.NEMAL.COM

Letters to the Editor

A Low-Cost Atomic Frequency Standard (Nov/Dec 2007)

Hi Larry,

I am building John Raydo's frequency standard. The little rubidium locked oscillator is working just fine on the bench and I'm busy installing it into a suitable Ten-Tec enclosure. Nifty! I think I'll add a little LCD panel meter to monitor the operating parameters of the frequency standard unit.

Thanks for the very nice article in *QEX*, and keep up the good work.

— Best regards, Bob McCulla, K7HBG, 5025 E Pacific Coast Hwy 340, Long Beach, CA 90804; k7hbg@dslextreme.com

Hi Bob,

Thanks for your kind words, and the note about this project. It's nice to know that readers find some of our projects helpful.

— 73, Larry Wolfgang, WR1B, *QEX* Editor, lwolfgang@arri.org

A New Subscriber

Larry,

I just subscribed to *QEX* and received my first issue (Nov/Dec 07).

Great job! The publication is awesome! How much for ALL the back issues? Well... I likely can't afford that...

Thank for your hard work. I can't wait to get the next issue.

— 73, Steve Niles, N5EN, 11215 Monique Dr, Houston, TX 77065; n5en@arri.net

Hi Steve,

Thanks for letting us know you enjoyed your first issue! We do have some back issues available, although not all of them. Back issues are \$5 each, if there are a few particular articles of interest. Another solution for having a more complete collection of back issues would be to purchase the 1981-1998 *QEX* Collection CD-ROM (\$39.95) and the annual ARRL Periodicals on CD-ROM from 1999 to the present (\$19.95 each). The annual Periodicals CD-ROM includes all issues of *QST*, *QEX* and *NCJ* for that year. Back issues are available from ARRL and the CD-ROM products are available directly from ARRL or from your local ARRL Dealer. Call 888-277-5289 or go to www.arri.org/shop to order.

— 73, Larry, WR1B; lwolfgang@arri.org

Empirical Outlook (Nov/Dec 2007)

Hi OM,

I saw your comment in *QEX* (Nov/Dec 2007, p 2) on experiencing the BASIC Stamp. I used to use that product but then came upon what seems a far easier one to use and at less cost, too — the PICAXE units. This is also a PIC microcontroller with an on board BASIC interpreter. For \$4.00 or so you can get an 8 or 14 pin unit that has PWM, ADC (10 bit 3 pins), ASCII, Servo and other functions, and a very good technical support forum. The parent company Web site in the UK is www.picaxe.co.uk. Peter H. Anderson, KZ3K, (www.phanderson.com) extols their virtues and sells them. SparkFun Electronics (www.sparkfun.com) also stocks the product. The best deal to start with I know of is from www.world-educational-services.com; \$15.95 for a PICAXE 14M unit with circuit board, download cable and CD ROM.

The PICAXE was conceived as an educational product in the UK and funded by the petroleum industry to encourage young engineers — it's mainly been known and used in the UK, New Zealand and Australia, and only recently discovered by USA folks like me — through Professor Peter Anderson's enthusiasm for it. *Nuts & Volts* published a few articles and more are reported to be in the works. Many articles have appeared in *Silicon Chip* magazine (by Stan Swan, a New Zealand ham) but unfortunately not much else in USA magazines.

The programming is done with a free editor and three wire interface from a serial port (or USB adaptor) with two resistors as the PC to PICAXE interface. Many BASIC Stamp programs have been adapted to run on the PICAXE units, which as I've mentioned are less than \$4.00. They also have up to 40 pin units, which I haven't tried. I did run some 18 pin [18X] units, which have more capability and on board flash memory for about \$9.

Google PICAXE, and you will find the Rev-Ed site for manuals, free program editor and plenty more information. You can buy a starter kit for less than \$20, if I remember correctly (I started several years ago). It's quite amazing what these cheap little units can do (an early version with much more limited memory than the current 8M unit could be programmed to send Morse strings for instance).

I don't in any way want to detract from what Parallax has done since they are great — there are also many other micro controller products that are faster and with more memory and speed. The PICAXEs are, in my opinion, simpler and cheaper for beginners, which at 71 years old, I still am! These are used by the hundreds in schools by 8 year olds and up.

— 73, S. Premena, AJØJ, PO Box 1038, Boulder, CO 80306; premzee@juno.com

From MILLIWATTS to KILOWATTS™
More Watts per Dollar™



Quality
Transmitting
& Audio Tubes

Taylor
TUBES



- COMMUNICATIONS
- BROADCAST
- INDUSTRY
- AMATEUR

Immediate Shipment from Stock

3CPX800A7	3CX15000A7	4CX5000A	813
3CPX5000A7	3CX20000A7	4CX7500A	833A
3CW20000A7	4CX250B	4CX10000A	833C
3CX100A5	4CX250B8	4CX10000D	845
3CX400A7	4CX250B7	4CX15000A	866-SS
3CX400U7	4CX250F6	4X150A	872A-SS
3CX800A7	4CX250R	YC-130	5867A
3CX1200A7	4CX350A	YU-106	5868
3CX1200D7	4CX350F	YU-108	6146B
3CX1200Z7	4CX400A	YU-148	7092
3CX1500A7	4CX800A	YU-157	3-500ZG
3CX2500A3	4CX1000A	572B	4-400A
3CX2500F3	4CX1500A	807	M328/TH328
3CX3000A7	4CX1500B	810	M338/TH338
3CX6000A7	4CX3000A	811A	M347/TH347
3CX10000A7	4CX3500A	812A	M382

— TOO MANY TO LIST ALL —



ORDERS ONLY:

800-RF-PARTS • 800-737-2787

Se Habla Español • We Export

TECH HELP / ORDER / INFO: 760-744-0700

FAX: 760-744-1943 or 888-744-1943



An Address to Remember:
www.rfparts.com

E-mail:

rfp@rfparts.com



Mr. Premena,

Wow! Thanks for all of that information. We would certainly welcome some PICAXE projects for QEX from you or any of our readers.

— 73, Larry, WR1B; lwwolfgang@arrl.org

Transmission Line Paradigm (Jul/Aug 2007)

Dear Editor,

There is an error in my article "Transmission Line Paradigm," QEX, Jul/Aug 2007, pp 40-44. The Voltage Equation and Current Equation given on page 41 do not jointly satisfy the Telegrapher's Equations because the distance-time parameters are incorrect in those two equations. The correct equations are:

Voltage Equation:

$$V(d, t) = f(ct - d) + g(ct + d) \quad [\text{Eq 5}]$$

Current Equation:

$$I(d, t) = [f(ct - d) - g(ct + d)] / Z_0 \quad [\text{Eq 6}]$$

Beyond this glaring failure to satisfy the Telegrapher's Equations, I do not see any heavy damage done to the article by the error. Although the distance-time parameters determine directions traveled by the wave functions *f* and *g*, the directions of the mathematical waves are extraneous to the salient ideas developed in the article. In particular, the presentation of the **Two-Function Rule** on page 41 is still valid. The trigonometry for **Standing Waves** on page 42 can be reworked for the parameters given above, and it remains true that **The Rule Unravels the Riddle** on page 43.

I apologize for the error, and thank Michael McCullough, KA6QJU, for spotting it.

— 73, Richard Thompson, W3ODJ, 3755 Leonardtown Rd, Waldorf, MD 20601; rthompson@earthlink.net

A Large Aperture, Resonant, Regenerative Frame Antenna (LARRFA) (Jan/Feb 2007)

Dear Larry,

Here is a brief follow-up to the Large Aperture Resonant Regenerative Frame Antenna article published in QEX, Jan/Feb, 2007:

• I have built and am operating a new version, 12.5 inches square with a 2-turn signal winding and an 8-turn tickler winding, which performs well from below 6 MHz to almost 6.2 MHz (49 m Broadcast Band). When noise inside my house is low enough, I can hear Chinese language from CRI emanating from well inside China. I can copy Radio Australia and Radio New Zealand regularly.

(The central air conditioning and heating system in our new home blankets my listening area with "hash" when it is running. I don't want to open up this new system to install suppression, and moving the antenna

and receiver is not an option. I just wait for a nighttime listening opportunity, when the AC/heating is not running and conditions are good for DX. Otherwise strong stations for news and other programs can sometimes be heard over the hash. I suspect that some of the signal I hear is being picked up by house wiring and coupled to the frame antenna. The antenna is not directional.)

• If this antenna does not oscillate, reverse not only the tickler winding but the leads to the signal winding. I don't know why, but it works.

• Leave the frame antenna winding disconnected from the electronics when not using the antenna. I lost a 2N3819 because of a nearby lightning strike. Maxwell was right. An intense electric current produces an intense magnetic field, which transfers enough energy to my windings to kill a JFET. Replacement of the 2N3819 wasn't too hard, and LARRFA/2 is working well again.

• Relative humidity of the air around LARRFA/2 seems to have an effect on antenna gain, lowering it somewhat when humidity is high.

• My observation of gain variation with humidity is subjective only. I have no data to back it up. I have noticed that on humid days I can't push the gain as high as on dry days. On a good day, when the receiver and antenna are "peaked" on a weak signal, there is a persistent "buzzing" noise on the signal, which can be eliminated by backing the antenna gain off slightly. I can then "re-peak" and try to hear the signal. I have read

an evaluation for a high gain UK manufactured active shortwave loop antenna. Apparently the same "buzzing" noise is a characteristic of that antenna. I have a lot of reserve audio gain, which helps, but the system is never completely quiet. There is always some background manmade or impulse noise.

• I may get around to building new antenna windings to work with the existing electronics with as little solid material in the field of the windings as possible. A single, self supporting signal winding with a multi turn tickler somehow suspended inside the signal winding would be good. This configuration should have a larger aperture for the same inductance. I have maybe two more feet of clear space above the surface holding the antenna to expand into.

• Go to the Internet and enter "regenerative loop antenna" on Google. You should see a reference to a Sony regenerative loop and an early regenerative loop built and operated by Vladimir Zworykin and his business partner. He dropped that idea and went on to TV.

— 73, Bill Young, WD5HOH, 4907 Grand Chateau Ln, Houston, TX 77084; bilaquieta@yahoo.com

Hi Bill,

Thanks for the updates on your antenna. I hope others will find this information useful.

— 73, Larry, WR1B; lwwolfgang@arrl.org

QEX

1010 Jorie Blvd. #332
Oak Brook, IL 60523
1-800-985-8463
www.atomictime.com

ATOMIC TIME

 <p>14" LaCrosse Black Wall WT-3143A \$21.45</p> <p>This wall clock is great for an office, school, or home. It has a professional look, along with professional reliability. Features easy time zone buttons, just set the zone and go! Runs on 1 AA battery and has a safe plastic lens.</p> <p>WT-3143A - \$21.45</p>	 <p>Digital Chronograph Watch ADWA 101 \$49.95</p> <p>Our feature packed Chrono-Alarm watch is now available for under \$50! It has date and time alarms, stopwatch backlight, UTC time, and much more!</p> <p>ADWA 101 - \$49.95</p>
 <p>LaCrosse Digital Alarm WS-8248U-A \$49.95</p> <p>This deluxe wall/desk clock features 4" tall easy to read digits. It also shows temperature, humidity, moon phase, month, day, and date. Also included is a remote thermometer for reading the outside temperature on the main unit, approx. 12" x 12" x 1.5"</p> <p>WS-8248 - \$49.95</p>	 <p>LaCrosse WT-5720U Clock \$24.95</p> <p>This digital projection clock is great for travel and fits in a small space. Shows 12 or 24 hour time, time zone, and alarm time. Size 5.25" x 1.25" x 4"</p> <p>WT-5720U - \$24.95</p>

Tell time by the U.S. Atomic Clock - The official U.S. time that governs ship movements, radio stations, space flights, and warplanes. With small radio receivers hidden inside our timepieces, they automatically synchronize to the U.S. Atomic Clock (which measures each second of time as 9,192,631,770 vibrations of a cesium 133 atom in a vacuum) and give time which is accurate to approx. 1 second every million years. Our timepieces even account automatically for daylight saving time, leap years, and leap seconds. \$7.95 Shipping & Handling via UPS. (Rush available at additional cost) Call M-F 9-5 CST for our free catalog.

The Theme of Dayton Hamvention® is Amateur Radio + People = Fellowship

Dayton Hamvention®
Sponsored by Dayton Amateur Radio Association
Since 1952

2008

May 16 – 18, 2008 at Hara Arena in Dayton, Ohio
Forums – 500 Inside Exhibit Spaces – 2,300 Flea Market Spaces
Over \$50,000 in Prizes!



Buy Tickets and Flea Market Spaces on-line!

www.hamvention.org

Ticket prices: \$20 in advance, \$25 at the door.

No Internet access? Send SASE with your check (made out to Dayton Hamvention) to Hamvention Tickets, P.O. Box 1446, Dayton, OH 45401

For hotel info, see our web site or contact the
Dayton Convention and Visitors Bureau at (800) 221-8235

Dayton Hamvention®
tel. (937) 276-6930
PO Box 964,
Dayton, OH, 45401

Don't Miss Ham Radio's Greatest Show!

And Featuring...

ARRL EXPO

Your Hamvention admission includes access to ARRL EXPO
(located in the Hara Ballarena, near the 400-numbered booths).

- Visit special ARRL exhibits and booths, including the huge ARRL bookstore!
- See live presentations on the ARRL Stage
- Meet ARRL staff and volunteers
- DXCC Card Checking
- ARRL Youth Exhibit – friends, fun and food!
- Join or renew with ARRL – and receive a FREE GIFT



ARRL The national association for
AMATEUR RADIO

Visit www.arrl.org/expo for the latest ARRL EXPO news!

KENWOOD

Listen to the Future

Kenwood & AvMap The Ultimate APRS[®] Combination

TM-D710A

AvMap G5



Two Great Companies...Providing One Outstanding Solution!

KENWOOD U.S.A. CORPORATION
Communications Sector Headquarters
3970 Johns Creek Court, Suite 100, Suwanee, GA 30024

Customer Support/Distribution
P.O. Box 22745, 2201 East Dominguez St., Long Beach, CA 90801-5745
Customer Support: (310) 639-4200 Fax: (310) 537-8235



www.kenwoodusa.com
ADS#01308



ISO 9001 Registered
Communications Equipment Division
Kenwood Corporation
ISO 9001 certification



AVMAP
SATELLITE NAVIGATION



www.avmap.us • e-mail: info@avmap.us
1.800.363.2627